MECHANICS OF CONSOLIDATION WITH REFERENCE TO EXPERIMENTALLY SEDIMENTED CLAYS

Thesis by

Dennis Vernon Long

In Partial Fulfillment of the Requirements
For the Degree of
Doctor of Philosophy

California Institute of Technology
Pasadena, California

1961

To my wife

Mary

for her enduring patience,

love, and assistance.

ACKNOWLEDGMENTS

The author wishes to express his sincere appreciation to his advisor, Professor R. F. Scott, for his suggestion of the thesis problem and for his constant assistance and advice throughout the entire period of this study.

Acknowledgment is also made to the Ford Foundation for the financial assistance of a Ford Foundation Fellowship during the final year of graduate residence.

ABSTRACT

The problem of large strain consolidation in soils is investigated by analysis and experiment. A mathematical model is formulated to include the effects of large strains. Analytic and numerical solutions are discussed.

The design, fabrication and operation of apparatus to study consolidation and other phenomena in sedimented clays is described. Results of experiments on two types of clay are presented. Finally, the consolidation characteristics of one of these clays are shown to be in close agreement with a particular solution of the large strain consolidation equation.

TABLE OF CONTENTS

TABLE OF CONTENTS (Continued)

TABLE OF CONTENTS (Continued)

CHAPTER I

MECHANICS OF SOIL CONSOLIDATION AND CONSOLIDATION OF SEDIMENTED FINE-GRAINED SOILS

A. INTRODUCTION

In developing his consolidation theory, Karl Terzaghi (1,1)* proposed some basic concepts which permit a rational explanation of the process of soil consolidation. In order to formulate a mathematical model for the process, a series of assumptions concerning some soil parameters and the magnitude of strains were introduced. With these assumptions a linear mathematical model was obtained. Subsequently, Terzaghi and many others have found solutions to this equation for a variety of loading and boundary conditions. Experience with various types of engineering structures has shown that the Terzaghi equation, when properly applied, adequately describes the consolidation process for many practical problems and thus is a most useful tool for the practicing engineer.

The usefulness of the Terzaghi equation is greatly enhanced by the fact that the equation is exactly analogous to the classical linear heat conduction and diffusion equation. Thus, when faced with the problem of finding a solution for a particular case, the engineer has available a large body of literature** on the mathematics of the problem.

---

*References are numbered consecutively by chapters and are listed at the end of the text.

**See, for example, reference 1,2 and reference 1,3.

There are some soil consolidation problems for which the assumptions used to obtain the linear mathematical model are not reasonable. Using only the basic concepts of the Terzaghi consolidation theory a consolidation equation is developed here which, although difficult to apply, is a more accurate model for such problems.

The assumptions necessary to obtain the Terzaghi equation from this more general equation are considered.

Finally the more general equation is applied to a consolidation problem for which the linearizing assumptions are clearly not reasonable.

B. MECHANICS OF CONSOLIDATION

When a saturated fine-grained soil is subjected to a load, it is observed to slowly decrease in volume by expulsion of some of its pore fluid at drained boundaries. The problem is to describe the mechanics of this process. The assumptions required to do this may be divided into two groups: assumptions concerning the properties of the soil constituents and assumptions concerning the mechanics of the consolidation process.

The pore fluid (water) and the soil grains are assumed incompressible, or, stated differently, the range of stress is limited such that the compressibility of the soil constituents is negligible compared to changes in pore volume. The pore spaces are assumed completely filled with water.

In discussing the mechanics of consolidation, the concepts of pore fluid pressure and intergranular stress are required. Figure 1-1a is a section through a soil with a horizontal surface. At some distance beneath the soil surface there is a horizontal water table, below which there is a hydrostatic water pressure profile, so there is no flow of pore water anywhere. At any level below the water table the total vertical stress must equal the weight of the column of water and soil particles above that level. This total stress is divided into two parts. The pore fluid pressure is simply the hydrostatic pressure. In addition, there are a large number of small forces in the grain structure of the soil. That portion of the stress due to pore fluid pressure is defined as acting over the whole unit area and is given the name, "neutral stress." The difference between total stress and neutral stress must be provided by all the small intergranular forces. The intergranular stress is defined as the sum of all these forces acting over the whole unit area. Defined in this way, these three stresses are simply related*:

$$\sigma_t = \gamma_w \xi + \overline{\sigma}$$

where σ_t = total stress

$\gamma_w \xi$ = neutral stress

γ_w = unit weight of water

---

*Symbols are defined as they appear and are listed alphabetically in the appendix.

ζ = depth below water table

$\overline{\sigma}$ = intergranular stress.

The distribution of total volume between pore volume and soil particle volume is commonly expressed by a dimensionless volume ratio. The ratio most used in soil mechanics is the void ratio, e, which is given by:

$$e = \frac{V_v}{V_s}$$

where V_v = percentage of total volume occupied by pores

V_s = percentage of total volume occupied by soil particles.

For a given soil formed in a given way in a given environment, the void ratio is a continuous single valued function of $\overline{\sigma}$. This is assumed to be true for any soil when $\overline{\sigma}$ is increased from lower to higher values once only. Upon unloading and reloading, different curves of $\overline{\sigma}$ vs. e are traced out.

If a uniform load is placed on the surface of the soil in figure 1-1a, σ_t is increased everywhere by the load per unit area. The intergranular stress, $\overline{\sigma}$, may not increase until the void ratio decreases. In the soil below the water table, the void ratio may decrease only as pore water is removed. Thus, at the moment of application, the increased load must be supported entirely by an appropriate increase in neutral stress. If the free water

table remains fixed, the neutral stress profile is no longer hydrostatic and water starts to flow through the soil. That portion of pore water pressure above hydrostatic is called the "hydrostatic excess pressure" and given the symbol, u.

As pore water is removed by this flow process, the pore volume decreases and some of the load is transferred to the soil structure. This is the concept of the consolidation process proposed by Terzaghi. When the hydrostatic excess pressure is completely dissipated everywhere, all the increased load has been transferred to the soil structure, and the consolidation process is complete with the soil structure in equilibrium at the appropriate lower void ratio for the increased load.

This discussion is limited to one-dimensional consolidation only. This means all aspects of the consolidation are one-dimensional. Neutral pressure, intergranular pressure, void ratio, and the movement of pore water and soil particles are all functions of time and one (vertical) dimension.

The final assumption concerning the mechanics of consolidation is that the flow of pore fluid takes place in accordance with Darcy's Law (1,4) and that the permeability of a given soil in a given environment is a single-valued continuous function of the void ratio. Since only one-dimensional consolidation and thus only one-dimensional pore fluid flow is considered here, the problem of anisotropy

in soil permeability does not appear, and no assumptions on this matter are required.

The relationships governing the consolidation process will now be considered.

The domain of the problem is indicated in figure 1-1b. The symbols used are defined below:

z = vertical distance from fixed base, cm

$\bar{z}$ = z at the soil surface or upper boundary of the soil under consideration = $\bar{z}(t)$, cm

t = time, minutes

$\overline{\sigma}$ = intergranular stress = $\overline{\sigma}(z,t)$, gms/cm^2

u = hydrostatic excess pressure = $u(z,t)$, gms/cm^2

$\sigma = \overline{\sigma} + u$, gms/cm^2

γ_s = unit weight of soil solids, gms/cm^3

γ_w = unit weight of pore fluid (water), gms/cm^3

$\gamma = \gamma_s - \gamma_w$, gms/cm^3

V = total volume, cm^3

V_v = pore (or void) volume, cm^3

V_s = volume of soil grains, cm^3

$n = \frac{V_v}{V}$ = porosity, dimensionless

$e = \frac{V_v}{V_s}$ = void ratio, dimensionless

$E = \frac{V}{V_s}$ = volume ratio = e + 1, dimensionless

k = permeability = $k(y,t)$, cm/min

i = velocity of soil particles = $i(y,t)$, cm/min

j = superficial velocity of pore fluid such that j multiplied by the total cross-sectional area equals the quantity of fluid passing a given horizon per unit time, cm/min

A fixed elemental layer at z has both soil particles and fluid passing through both faces so that the porosity changes with time (Fig. 1-2a). The volume flow rates are indicated in the figure. (Assume unit cross-sectional area.)

Since the total volume of the layer remains unchanged, the outflow volume must equal the inflow volume or

$$(1-n)i + \frac{\partial}{\partial z}[(1-n)i]\Delta z + j + \frac{\partial j}{\partial z}\Delta z - (1-n)i - j = 0$$

or

$$\frac{\partial}{\partial z}[(1-n)i] + \frac{\partial j}{\partial z} = 0 \qquad (1:1)$$

In the special case of an impermeable base, there is no net flow of soil and water through any surface and equation 1:1 reduces to

$$(1-n)i + j = 0 \qquad (1:1a)$$

The rate of pore volume increase is equal to the net inflow rate of pore fluid i.e.,

$$\frac{\partial}{\partial t}(n\Delta z) = j - (j + \frac{\partial j}{\partial z}\Delta z)$$

or

$$\frac{\partial n}{\partial t} = -\frac{\partial j}{\partial z} \qquad (1:2)$$

The pore fluid flow velocity is in accordance with Darcy's Law, that is, the velocity is proportional to the gradient of total fluid head. The only head causing flow is that due to hydrostatic excess pressure. The velocity, here, is that relative to the soil grains. As indicated in figure 1-2b for consideration of Darcy's Law, the soil may be considered as an assemblage of small vertical tubes. If the total cross-sectional area is unity, then the fluid flow area is n.

At time, t, the reference tube section and reference fluid section are at 1. At time, $t + \Delta t$, the reference tube section has moved to 2, and the reference fluid section to 3.

The quantity of fluid passing the reference tube section in the time increment, Δt, is

$$\left(\frac{i}{n}\,\Delta t - i\,\Delta t\right) n$$

In this time, the fluid reference level has moved relative to the tube as indicated, so the applicable head gradient is

$$\frac{1}{\gamma_w}\left\{\frac{u + \frac{\partial u}{\partial t}\Delta t + \frac{\partial u}{\partial z}\left(\frac{i}{n}\,\Delta t\right) - \left[u + \frac{\partial u}{\partial t}\,\Delta t + \frac{\partial u}{\partial z}\,(i\,\Delta t)\right]}{\frac{i}{n}\Delta t - i\,\Delta t}\right\}$$

which, when multiplied by the permeability and total area, gives the quantity flow rate according to Darcy's Law.

$$\left(\frac{1}{n} - 1\right) n \Delta t = - \frac{k}{u} \frac{\left(\frac{1}{n} - 1\right) \frac{\partial u}{\partial z} \Delta t}{\left(\frac{1}{n} - 1\right) \Delta t} \Delta t$$

$$j - i\, n = - \frac{k}{u} \frac{\partial u}{\partial z} \qquad (1:3)$$

The sum of intergranular stress and hydrostatic excess pressure at any point is this sum at z = 0 reduced by the buoyant weight of soil grains between z = 0 and z.

$$\sigma = \sigma_o - \int_o^z (1 - n)\, \gamma' dz$$

where $\sigma_o = \sigma$ at $z = 0$

σ_o may be a function of time.

$$\overline{\sigma} + u = \sigma_o - \int_o^z (1 - n)\, \gamma dz \qquad (1:4)$$

Summarizing, there are four equations in the four variables u, i, j, and n:

$$\frac{\partial}{\partial z} [(1 - n)\, i] + \frac{\partial i}{\partial z} = 0 \qquad (1:1)$$

$$\frac{\partial n}{\partial t} = - \frac{\partial i}{\partial t} \qquad (1:2)$$

$$j - i\, n = - \frac{k}{\gamma_w} \frac{\partial u}{\partial z} \qquad (1:3)$$

$$\overline{\sigma} + u = \sigma_o - \int_o^z (1 - n)\, \gamma dz \qquad (1:4)$$

As noted before, $\overline{\sigma}$ is assumed to be a function of n (or of e or E since n, e, E are all simply related).

It has been convenient to use n in setting up these equations. For subsequent developments it is more convenient to use E. The volume ratio, E, may be substituted for n in equations 1:1 through 1:4 by means of the following relationships:

$$n = \frac{V_v}{V} = \frac{V - V_s}{V} = \frac{E - 1}{E} = 1 - \frac{1}{E} \quad ; \quad 1 - n = \frac{1}{E}$$

$$\frac{\partial n}{\partial t} = \frac{dn}{dE}\frac{\partial E}{\partial t} = \frac{1}{E^2}\frac{\partial E}{\partial t} \tag{1:5}$$

With appropriate substitutions of E for n, equations 1:1 through 1:4 become:

$$\frac{\partial}{\partial z}\left(\frac{1}{E}\right) + \frac{\partial J}{\partial z} = 0 \tag{1:6}$$

$$\frac{1}{E} + J = 0 \tag{1:6a}$$

$$\frac{1}{E^2}\frac{\partial E}{\partial t} = -\frac{\partial J}{\partial z} \tag{1:7}$$

$$J - i\left(\frac{E - 1}{E}\right) = -\frac{k}{\tau_w}\frac{\partial u}{\partial z} \tag{1:8}$$

$$\overline{\sigma} + u = \sigma_o - \int_0^z \frac{\gamma}{E}\, dz \tag{1:9}$$

Subsequent treatment of this set of equations including simplifying assumptions, which might be appropriate, depends on the particular problem under consideration.

As noted above, if there is no flow through the base surface at z = o, equation 1:6 reduces to equation 1:6a. In this form, it is possible to obtain a second order equation in a single dependent variable (n, e, or E) with quite general applicability subject to this one restriction.

Combining equations 1:6a, 1:7, and 1:8 gives:

$$\frac{1}{E^2} \cdot \frac{\partial E}{\partial t} = \frac{\partial}{\partial z} \left[\frac{k}{E \gamma_w} \cdot \frac{\partial u}{\partial z} \right] \qquad (1:10)$$

Taking $\frac{\partial}{\partial z}$ of equation 1:9 yields a simple equilibrium equation, which is valid under any condition.

$$\frac{\partial \overline{\sigma}}{\partial z} + \frac{\partial u}{\partial z} + \frac{\gamma}{E} = 0$$

It was assumed, above, that $\overline{\sigma}$ is a continuous single valued function of E. In this case the term $\frac{\partial \overline{\sigma}}{\partial z}$ may be replaced by:

$$\frac{\partial \overline{\sigma}}{\partial z} = \frac{d\overline{\sigma}}{dE} \frac{\partial E}{\partial z}$$

In soil mechanics literature, the standard term used to describe the slope of the E - $\overline{\sigma}$ curve is a_v, the "coefficient of compressibility":

$$a_v = - \frac{dE}{d\overline{\sigma}}$$

In terms of a_v the equilibrium relationship, above, becomes

$$\frac{\partial u}{\partial z} = \frac{1}{a_v} \frac{\partial E}{\partial z} - \frac{\gamma}{E} \qquad (1:11)$$

Combining equations 1:10 and 1:11 gives

$$\frac{1}{E^2}\frac{\partial E}{\partial t} = \frac{\partial}{\partial z}\left[\frac{k}{\gamma_w E}\left(\frac{1}{a_v}\frac{\partial E}{\partial z} - \frac{\gamma}{E}\right)\right] \qquad (1:12)$$

This, then, is the equation describing the distribution of E with depth and time during the consolidation process. The term $(\frac{1}{a_v}\frac{\partial E}{\partial z} - \frac{\gamma}{E})$ is the excess pore pressure gradient. When the excess pore pressure is completely dissipated, this term is zero and the consolidation process is complete.

Before considering possible application of equation 1:12 and comparing it to Terzaghi's consolidation equation, it should be normalized.

In any soil, E decreases with increasing $\overline{\sigma}$. In order to make a_v a positive quantity, it is defined as the negative value of the rate of change of E with increasing $\overline{\sigma}$. Since E is dimensionless, a_v has the units of the reciprocal of a stress or pressure. Thus, $/a_v/ = cm^2/gm$, where the notation $//$ means the units of the enclosed quantity. Now, if as assumed above, a_v is a function of E only, then no matter what the form of this function may be, a_v may be written as

$$a_v = a\,F(E) \qquad (1:13)$$

where a is a constant and F (E) is a function of E only. Since F (E) is dimensionless,

$$/a/ = /a_v/ \qquad (1:14)$$

When a soil is at equilibrium so that the hydrostatic excess pressure is zero everywhere,

$$-\frac{d\bar{\sigma}}{dz} = \frac{1}{a_v}\frac{dE}{dz} = \frac{\gamma}{E}$$

or
$$\frac{E}{F}\frac{dE}{dz} = a\gamma \qquad (1:15)$$

Equation 1:15 may be integrated to give E as a function of depth:

$$\int_{(E)_{z=0}}^{E} \frac{E}{F}\, dE = \int_{0}^{z} a\gamma\, dz$$

or
$$\int_{(E)_{z=0}}^{E} \frac{E}{F}\, dE = a\gamma z \qquad (1:16)$$

The constants a and γ and their product have the dimensions of length^{-1}. It is natural, therefore, to choose $a\gamma z$ as a dimensionless length variable in normalizing equation 1:12. Therefore, define

$$x = a\gamma z, \text{ dimensionless} \qquad (1:17)$$

The permeability, k, is also assumed to be a function of E only. Thus, by the same reasoning as used for a_v, k may be written as

$$k = K\, G\,(E) \qquad (1:18)$$

where G (E) is a function of E, and K is a constant with the dimensions of k, i.e.,

$$|K| = |k| = \text{cm/min} \qquad (1:19)$$

Using equations 1:13, 1:17, and 1:18, equation 1:12 becomes

$$\frac{1}{E^2}\frac{\partial E}{\partial t} = a\gamma \frac{\partial}{\partial x}\left[\frac{K}{\gamma_w}\frac{G}{E}\left(\frac{a\gamma}{aF}\frac{\partial E}{\partial x} - \frac{\gamma}{E}\right)\right]$$

or

$$\frac{1}{E^2}\frac{\partial E}{\partial t} = \frac{a\gamma^2 K}{\gamma_w}\frac{\partial}{\partial x}\left[\frac{G}{E^2}\left(\frac{E}{F}\frac{\partial E}{\partial x} - 1\right)\right] \qquad (1:20)$$

The term $\frac{a\gamma^2 K}{\gamma_w}$ has the units of one over time, so a dimensionless time variable may be defined as

$$\tau = \frac{a\gamma^2 K}{\gamma_w} t \qquad (1:21)$$

Substituting equation 1:21 into equation 1:20 gives the normalized form of equation 1:12,

$$\frac{1}{E^2}\frac{\partial E}{\partial \tau} = \frac{\partial}{\partial x}\left[\frac{G}{E^2}\left(\frac{E}{F}\frac{\partial E}{\partial x} - 1\right)\right] \qquad (1:22)$$

Before considering ways of obtaining solutions to equation 1:22 or equation 1:12, their relation to the Terzaghi consolidation equation will be investigated.

C. THE TERZAGHI CONSOLIDATION EQUATION

Equations 1:6a, 1:7, and 1:8 are combined, as before, to obtain equation 1:10, i.e.,

$$\frac{1}{E^2}\frac{\partial E}{\partial t} = \frac{\partial}{\partial z}\left(\frac{k}{E\gamma_w}\frac{\partial u}{\partial z}\right) \qquad (1:10)$$

However, equations 1:10 and 1:9 are combined so as to eliminate E as the dependent variable to obtain an equation in u. To do this, a time derivative is taken of the equilibrium equation 1:9, i.e.,

$$\frac{\partial \bar{\sigma}}{\partial t} + \frac{\partial u}{\partial t} = \frac{d}{dt}\,\sigma_o - \frac{\partial}{\partial t}\left[\int_o^z \frac{\gamma}{E}\,dz\right] \qquad (1:23)$$

Introducing a_v, as before, equation 1:23 becomes

$$\frac{\partial u}{\partial t} = \frac{1}{a_v}\frac{\partial E}{\partial t} + \frac{d}{dt}(\sigma_o) - \frac{\partial}{\partial t}\left[\int_o^z \frac{\gamma}{E}\,dz\right] \qquad (1:24)$$

To combine equations 1:10 and 1:24 in a single equation with u as the dependent variable, some assumption must be made concerning the last term of equation 1:24. This term is the time rate of change of the volume of soil particles between a fixed base and the fixed co-ordinate horizon, z, expressed in terms of buoyant weight. To obtain the Terzaghi equation, this term must be assumed to be zero. Making this assumption and combining equations 1:10 and 1:24:

$$\frac{a_v}{E^2}\left(\frac{\partial u}{\partial t} - \frac{d\sigma_o}{dt}\right) = \frac{\partial}{\partial z}\left(\frac{k}{E\gamma_w}\frac{\partial u}{\partial z}\right) \qquad (1:25)$$

The factor $\frac{k}{E\ \gamma_w}$ is a function of E, except in the special case where k varies linearly with E. The next assumption that must be made is that $\frac{k}{E\ \gamma_w}$ is independent of z, or, in general, that E is independent of z. Equation 1:25 then becomes

$$\frac{\partial u}{\partial t} = \frac{k\,E}{a_v \gamma_w} \frac{\partial^2 u}{\partial z^2} + \frac{d\,\sigma_o}{dt} \qquad (1:26)$$

If σ_o is a constant, i.e., if the externally applied load does not vary in time, then equation 1:26 reduces to

$$\frac{\partial u}{\partial t} = \frac{k\,E}{a_v \gamma_w} \frac{\partial^2 u}{\partial z^2} \qquad (1:27)$$

which is the Terzaghi consolidation equation as it is usually presented.

When applied to the standard laboratory consolidation test, the many assumptions used to derive equation 1:27 are at least qualitatively reasonable. In the standard laboratory consolidation test*, a cylindrical sample of soil, whose diameter is approximately twice its thickness, is placed in a consolidometer with load applied to the top surface through a porous stone. The applied load is normally much larger than the weight of the sample itself. Thus, a close approximation to equation 1:9 is

---

*For a detailed description, see for example reference 2,1; pp. (74-87).

$$\overline{\sigma} + u = P = \text{the applied load} = \text{a constant} \quad (1:28)$$

(per unit area)

Taking the time derivative of equation 1:28 then gives

$$\frac{\partial u}{\partial t} = \frac{1}{a_v} \frac{\partial E}{\partial t} \quad (1:29)$$

In solving equation 1:27, the boundaries are normally assumed fixed. This assumption produces an error which, in sense, tends to cancel the error arising from the assumption of E being independent of z. The initial and final values of E in the standard test are probably nearly constant over the depth of the sample. However, during the test, E certainly is not independent of depth. Immediately after the load is applied, the soil at the drained surface assumes the ultimate E value corresponding to the applied $\overline{\sigma}$, whereas E in the interior of the sample will not change much until some time has elapsed. The reduced E, and therefore k value, in the surface layer has the effect of restraining the dissipation of the interior excess pore pressure, for, however permeability may vary with E, it always decreases with decreasing E. On the other hand, because consolidation is taking place, the drainage surface is progressively moving down providing higher gradients of pore pressure than those which would exist if the boundary surface remained fixed. The two effects of lower permeability and higher gradient tend to cancel each other.

In solving equation 1:27, the group, $\frac{k\,E}{a_v \gamma_w}$, which is given the symbol, c_v, and called the "coefficient of consolidation," is taken as constant. This is not an independent assumption but follows from the assumptions of E independent of depth and fixed boundaries. These two assumptions taken together make E independent of both depth and time and, since c_v is a function of E only, it is also independent of depth and time.

In summary, the assumptions required to obtain the Terzaghi equation (Eqn. 1:27) over and above those required to obtain equation 1:12 are

1. $\frac{\partial}{\partial t}\left[\int_0^{\infty} \frac{\gamma}{E}\, d\,x\right] = 0$

2. E is independent of depth

In addition, solutions to equation 1:26 are usually found assuming fixed boundaries

3. Fixed boundaries

Assumptions 2 and 3 taken together amount to assuming E independent of both depth and time, from which assumption 1. follows immediately.

From this and the foregoing discussion, the following observations may be made:

1. Solutions of the Terzaghi equation give the dissipation of excess pore-pressure as a function of time from

which the consolidation-time relationship may be obtained as a second step.[2] In practice, agreement between observed consolidation and that obtained from the mathematical solution is probably always improved by making the seemingly contradictory assumption of fixed boundaries.

As noted in the introduction to this chapter, the Terzaghi equation has been found through experience to be a good mathematical model for consolidation and settlement calculations in many engineering problems, and none of the above remarks are to be construed to imply otherwise. However, in formulating the equation, there seems to be some advantage in making the minimum number of assumptions at first and then to examine what sort of additional assumptions are required to put the equation in a form for which solutions may be obtained without difficulty. In textbooks and technical papers on the subject, the universal practice is to make a series of assumptions in the first instance which will yield the linear Terzaghi equation. This practice tends to obscure the real assumptions that are, in fact, made; for, in all the considerable literature on the subject, the author is not aware of any mention of assumption 1, above. Furthermore, considerable stress is often placed on assuming a_v and c_v to be constants,* while, in fact, this follows automatically from the more fundamental assumptions 2 and 3, above.

---

*See, for example, reference 1,5; pp. (220-226).

D. APPLICATION OF GENERAL CONSOLIDATION EQUATION

The general equation 1:12 or 1:22 is non-linear and, in application, would usually be associated with moving boundaries. For such problems, analytic solutions may be expected only in special limited cases. However, it should be possible to obtain solutions numerically.

To utilize some established principles for solving initial-value problems by finite differences, it is helpful to change the dependent variable, E, in equation 1:27 to another volume distribution parameter concentration. If c is the concentration of soil particles in grams per cm^3, then c and E are related by

$$c = \frac{\gamma_s}{E} \qquad (1:30)$$

To keep things in dimensionless form, c_o may be defined as the value of c when E = 1, i.e., the value of c when the pore volume is zero. Then C, a dimensionless concentration, may be defined,

$$C = \frac{c}{c_o} = \frac{\gamma_s/E}{\gamma_s} = \frac{1}{E} \qquad (1:31)$$

Equation 1:22, in terms of C, becomes

$$\frac{\partial C}{\partial \tau} = \frac{\partial}{\partial x}\left[\frac{G}{CF}\frac{\partial c}{\partial x} + GC^2\right] \qquad (1:32)$$

where $G = G(E) = G\left(\frac{1}{c}\right)$

$F = F(E) = F\left(\frac{1}{c}\right)$.

With a suitable change in co-ordinates, equation 1:32 may be expressed in terms of fixed boundaries with the effect of moving boundaries thrown into the coefficients.

$$\text{Let } T = \tau$$

$$y = \frac{x}{\bar{x}} \tag{1:33}$$

where $\bar{x}$ (T) is the co-ordinate of the moving upper boundary. The lower boundary is assumed fixed. In this new co-ordinate system equation 1:32 becomes

$$\frac{\partial C}{\partial T} = \frac{1}{\bar{x}} \frac{\partial}{\partial y}\left[\frac{G}{CF} \frac{1}{\bar{x}} \frac{\partial C}{\partial y} + G C^2\right] + \frac{d\bar{x}}{dT} \frac{y}{\bar{x}} \frac{\partial c}{\partial y}$$

or

$$\frac{\partial C}{\partial T} = \frac{1}{\bar{x}^2}\left[\frac{G}{CF} \frac{\partial^2 C}{\partial y^2} + \frac{d}{dc}\left(\frac{G}{CF}\right)\left(\frac{\partial C}{\partial y}\right)^2\right]$$

$$+ \frac{1}{\bar{x}} \frac{d}{dc}(G C^2) \frac{\partial C}{\partial y} + \frac{d\bar{x}}{dT} \frac{y}{\bar{x}} \frac{\partial c}{\partial y}$$

The problems in finding solutions to equation 1:34 by finite difference methods are, perhaps, more easily approached by considering a specific example.

Consider the following situation. A portion of a harbor or bay is to be filled in by dredging in coarse sand from another part of the bay. Assume the sand will be placed in a short time over the whole area. The bottom of the harbor is covered with a layer of fine sediments, which have accumulated slowly and are assumed to be in equilibrium under their own weight. Prior

to the dredging operation, samples are taken at intervals in the sediments. Laboratory data from these samples give the initial steady state distribution of C with depth and, assuming the sediments to be in equilibrium, the C-$\bar{\sigma}$ curve up to the maximum value of C, at x = 0, prior to loading. Using the laboratory apparatus described in Chapter II, the C-$\bar{\sigma}$ curve may be extended to the maximum $\bar{\sigma}$ which will prevail after loading is complete. This apparatus also provides the k-C (or k-E) curve over the required range of C. The laboratory data provide, then, the distribution of C with x or y at T = 0 and the form of the coefficients, $\frac{G}{CF}, \frac{d}{dC}\left(\frac{G}{CF}\right)$ and $\frac{d}{dC}\left(G\,C^{2}\right)$ for all values of C which will occur during the consolidation process. It remains to establish the boundary conditions.

The material, on which the sediments rest, is assumed impermeable. In the original co-ordinate system, this condition requires:

$$\text{at } z = 0, \frac{\partial u}{\partial z} = 0$$

From equation 1:11

$$\frac{\partial u}{\partial z} = \frac{1}{a_v}\frac{\partial E}{\partial z} - \frac{\gamma}{E} = 0$$

or $$\frac{1}{a_v}\frac{\partial E}{\partial z} = \frac{\gamma}{E}$$

or $$\frac{E}{F}\frac{\partial E}{\partial z} = a\gamma \quad \text{at } z = 0$$

(1:35)

recalling $x = a\nu z$

and $C_v = \frac{1}{E}$

equation 1:35 becomes

$$\frac{1}{C^3 F} \frac{\partial C}{\partial x} = -1$$

or in terms of y $$\frac{1}{C^3 F} \frac{\partial C}{\partial y} = -\gamma \qquad (1:36)$$

At the upper boundary, $x = \bar{x}$, $y = 1$, hydrostatic excess pressure is assumed to be zero for all T, that is, the permeability of the dredged sand fill is assumed to be so high that any excess pressures in it are dissipated immediately. Then at $x = \bar{x}$, $y = 1$, C_o (t) is prescribed for all T from the $\bar{\sigma}$ -C curve and the known rate of loading.

The total amount of soil solids between the two boundaries remains constant. This condition is used to determine the moving boundary,

$$\int_0^{\bar{x}} C \, dx = A = \text{a constant for all T} \qquad (1:37)$$

The finite difference calculations must be set up to meet stability criteria. That is, a small error introduced at any point in the calculations must damp out as the calculations proceed. Two aspects of equation 1:34

present problems in establishing a stability criterion: the C- dependent coefficients and the presence of the first-order term on the right hand side of the equation. Disregarding, for the moment, the first-order terms, equation 1:34 is in the form of a diffusion equation with a concentration dependent diffusion coefficient. For such equations Courant, Friedrichs, and Lewy (ref. 1,6) have shown that the stability criterion depends on the solution as it progresses, but that an absolute stability criterion may be established if the maximum value of the variable coefficient is known *. This coefficient, for the problem here, is $\frac{1}{\bar{x}^2}\frac{G}{CF}$. The functions G and F are known from the laboratory data for the range of C values that will occur. The initial and final values of $\bar{x}$ are known. This coefficient can be computed for all values of x at T = o and when consolidation is complete, $T \to \infty$. The maximum of these values may be used to establish the stability criterion to start the calculations. If, as the calculations proceed, larger values of the coefficient occur, the stability criterion and calculation procedure would be adjusted accordingly.

With the stability criterion established, a choice of Δy fixes the maximum ΔT which may be used. The $\Delta y - \Delta T$ grid remains constant as the solution progresses, unless the solution requires a revision of the stability

---

*For a recent application see reference 1,7.

criterion.

Richtmyer (ref. 1,8) demonstrates that for linear problems, the presence of lower order terms has little or no effect on stability. The problem here is, of course, non-linear. In a given case, it may be possible to assess the effect of the first-order terms of equation 1:34; however it does not seem to be possible to make any general statements in non-linear problems. Still, the effect of this term hopefully will be small.

To write equation 1:34 in finite difference form, the following notation is defined:

C = C evaluated at y, T

${}_{+}C$ = C evaluated at $y, T + \Delta T$

C_{+} = C evaluated at $y + \Delta y, T$

C_{-} = C evaluated at $y - \Delta y, T$

In this notation,

$$ {}_{+}C = C + \frac{\partial C}{\partial T} \Delta T \qquad (1:38) $$

that is, the values of C at $T + \Delta T$ are computed from the known values of C at T and equation 1:34. Equation 1:34, in finite difference form, is substituted into equation 1:38 to obtain:

$$ {}_{+}C = C + \frac{1}{\bar{x}^2}\frac{\Delta T}{(\Delta y)^2}\left[\frac{G}{CF}(C_+ - 2C + C_-) + \frac{d}{dC}\left(\frac{G}{CF}\right)\left(\frac{C_+ - C_-}{4}\right)^2\right] $$

$$ + \frac{1}{\bar{x}}\frac{d}{dC}(GC^2)\frac{\Delta T}{\Delta y}\left(\frac{C_+ - C_-}{2}\right) + \frac{d\bar{x}}{dT}\frac{y}{\bar{x}}\frac{\Delta T}{\Delta y}\left(\frac{C_+ - C_-}{2}\right) \qquad (1:39) $$

The "y" derivatives in equation 1:34 are approximated by central differences in equation 1:39. Central differences cannot be used to find ${}_{+}C$ at the boundaries. At y = 1, there is no difficulty since ${}_{+}C$ is a prescribed boundary condition. At y = o, ${}_{+}C$ must be calculated to conform to the boundary condition, equation 1:36. But equation 1:36 involves $\bar{x}$ which in turn, involves equation 1:37. Thus the new values of C at y = o and of $\bar{x}$ are found by simultaneously applying equations 1:36 and 1:37. This must be done with care, since equation 1:39 is clearly sensitive to errors in $\bar{x}$.

Knowing the values of $\bar{x}, \frac{d\bar{x}}{dT}$, and C at time, T, all the C values at time $T+\Delta T$ are calculated directly from equation 1:39 except ${}_{+}C_o$, the value at y = o. Equation 1:36 may be written in finite difference form as

$$ \left(\frac{1}{C^3F}\right)_{\substack{y=o \\ T+\Delta T}} \frac{{}_{+}C_1 - {}_{+}C_o}{\Delta y} = -\bar{x} \qquad (1:40) $$

by using a forward difference to approximate $\left(\frac{\partial C}{\partial y}\right)_{y=o}$.

In view of the above comments, it may be worthwhile to use a better approximation.

Expanding $\frac{\partial C}{\partial Y}$ in a Taylor's series, gives

$$\left(\frac{\partial C}{\partial Y}\right)_{Y=0} = \left(\frac{\partial C}{\partial Y}\right)_{Y=1} - \Delta Y \frac{\partial}{\partial Y}\left(\frac{\partial C}{\partial Y}\right)_{Y=1} + \cdots$$

or

$$\left(\frac{\partial C}{\partial Y}\right)_{Y=0} = \left(\frac{\partial C}{\partial Y}\right)_{Y=1} - \Delta Y \left(\frac{\partial^2 C}{\partial Y^2}\right)_{Y=1} + \cdots$$

Using central differences for the derivatives at $y = \Delta y$, this becomes (note: ${}_+C_m \equiv C$ at $T+\Delta T$, $m\Delta y$)

$$\left(\frac{\partial C}{\partial y}\right)_{y=0} \doteq \frac{{}_+C_2 - {}_+C_0}{2\Delta y} - \Delta y \frac{{}_+C_2 - 2{}_+C_1 + {}_+C_0}{(\Delta y)^2} \qquad (1:41)$$

or

$$\left(\frac{\partial C}{\partial y}\right)_{y=0} \doteq \frac{-{}_+C_2 + 4{}_+C_1 - 3{}_+C_0}{2\Delta y}$$

Using this expression, the approximate form of equation 1:36 is

$$\left(\frac{1}{C^3 F}\right)_{\substack{y=0 \\ T+\Delta T}} \left(\frac{-{}_+C_2 + 4{}_+C_1 - 3{}_+C_0}{2\Delta y}\right) \doteq -\bar{x} \qquad (1:42)$$

where ${}_+C_0$ and $\bar{x}$ are unknown.

The simplest approximation to the integral in equation 1:37 is

$$\left(\int_0^{\bar{x}} C\,dx\right)_{T+\Delta T} \doteq \frac{{}_+C_0 + {}_+C_1}{2}\Delta x + \frac{{}_+C_1 + {}_+C_2}{2}\Delta x + \cdots + \frac{{}_+C_{n-1} + {}_+C_n}{2}\Delta x + \frac{{}_+C_n + {}_+C_{n+1}}{2}\Delta y$$

(If y is divided into n increments, there are n+1 values of C.) Since $\Delta x = \bar{x}\,\Delta y$, this may be written as

$$\left(\int_0^{\bar{x}} C\,dx\right)_{T+\Delta T} \doteq \left(\frac{{}_+C_0}{2} + {}_+C_1 + {}_+C_2 + \cdots + {}_+C_n + \frac{{}_+C_{n+1}}{2}\right)\bar{x}\,\Delta y$$

This approximation assumes that the value of C, at an interior point, is the average value for the interval from $\frac{\Delta y}{2}$ below the point to $\frac{\Delta y}{2}$ above the point. However, the C values at the end points are taken as the average for the increments, $\frac{\Delta y}{2}$ next to the boundaries. A better approximation to the integral would be to use the values of C at the midpoints of the boundary half-increments. These are

$$(C)_{y=\frac{\Delta y}{4}} = (C)_{y=0} + \frac{1}{4}\left[(C)_{y=\Delta y} - (C)_{y=0}\right]$$

and

$$(C)_{y=1-\frac{\Delta y}{4}} = (C)_{y=1} + \frac{1}{4}\left[(C)_{y=1} - (C)_{y=1-\Delta y}\right]$$

Using these relations, the approximate form of equation 1:37 is

$$\Delta y\, \bar{x}\left(\tfrac{3}{8}\,{}_{+}C_0 + \tfrac{9}{8}\,{}_{+}C_1 + {}_{+}C_2 + \cdots + {}_{+}C_{n-1} + \tfrac{9}{8}\,{}_{+}C_n + \tfrac{3}{8}\,{}_{+}C_{n+1}\right) = A \qquad (1:43)$$

Combining equations 1:42 and 1:43 yields an equation from which ${}_{+}C_0$ is found

$$\frac{{}_{+}C_2 - 4\,{}_{+}C_1 + 3\,{}_{+}C_0}{2(C^3F)_{y=0}} = \frac{A}{\frac{3}{8}\,{}_{+}C_0 + \frac{9}{8}\,{}_{+}C_1 + C_2 + \cdots + {}_{+}C_{n-1} + \frac{9}{8}\,{}_{+}C_n + \frac{3}{8}\,{}_{+}C_{n+1}} \qquad (1:44)$$

After finding ${}_{+}C_0$ from equation 1:44, $\bar{x}$ is obtained from either equation 1:42 or 1:43.

As with $\bar{x}$, a good approximation for $\frac{d\bar{x}}{dT}$ is required. Obviously, some sort of backward difference must be used. The simplest one is

$$\left(\frac{d\bar{x}}{dt}\right)_T = \frac{(\bar{X})_T - (\bar{X})_{T-\Delta T}}{\Delta T} \qquad (1:45)$$

A better approximation comes from a Taylor's series expansion

$$\left(\frac{d\bar{x}}{dT}\right)_T = \left(\frac{d\bar{x}}{dT}\right)_{T-\Delta T} - \Delta T \frac{d}{dT}\left(\frac{d\bar{x}}{dT}\right)_{T-\Delta T} + \cdots$$

or

$$\left(\frac{d\bar{x}}{dT}\right)_T = \left(\frac{d\bar{x}}{dT}\right)_{T-\Delta T} - \Delta T\left(\frac{d^2\bar{x}}{dT^2}\right)_{T-\Delta T} + \cdots$$

Using central differences for the derivates at $T-\Delta T$, this becomes

$$\left(\frac{d\bar{x}}{dT}\right)_T \doteq \frac{(\bar{x})_T - (\bar{x})_{T-2\Delta T}}{2\Delta T} - \Delta T \frac{(\bar{x})_T - 2(\bar{x})_{T-\Delta T} + (\bar{x})_{T-2\Delta T}}{(\Delta T)^2}$$

or

$$\left(\frac{d\bar{x}}{dT}\right)_T \doteq \frac{-(\bar{x})_T + 4(\bar{x})_{T-\Delta T} - 3(\bar{x})_{T-2\Delta T}}{2\Delta T} \qquad (1:46)$$

For the first time step, equation 1:45 must be used, since there is no $(x)_{T-2\,T}$ to use at $T = T$ in equation 1:46. After the first time step, equation 1:46 may be used.

Although the numerical techniques, outlined above, have not been tested by application in this study, the discussion indicates that numerical solutions are feasible.

E. CONSOLIDATION IN SEDIMENTED FINE-GRAINED SOILS

Natural streams transport a wide range of sizes of sediments. When a stream discharges into a body of relatively still water, these sediments are deposited with greater or lesser degrees of sorting. Differences in settling velocity are sufficient to provide considerable degrees of sorting. Classification is further enhanced by development of density currents which can transport the fine materials distances of many miles from the stream outlet*. Whatever the mode of deposition, observations of recent sediments in artificial lakes yield abundant evidence of well developed size sorting. Sedimentary rocks also show marked effects of size sorting from sandstones through siltstones and shales.

This study is concerned with only certain phases of the consolidation of clay-size sediments after suspended transport has ceased. The consolidation problem is certainly not independent of the transport problem, since the mode of transport defines the addition of sediment to the top of the bed and thus gives loading as a function of time in nature. Here the investigation is confined to certain simple initial and loading conditions in order to learn something of the consolidation mechanism per se. It is recognized that this is only one part of the much larger problem.

Laboratory investigations and field observations indicate a considerable list of factors which bear on the consolidation problem.

---

*See, for example, reference 1, 9 (pp. VIII 289-VIII 299)

The following list is not necessarily complete.

Physico-Chemical factors

Type of clay mineral

Dissolved salts in the water

Presence and decay of organic matter

Degree of flocculation

Size distribution of individual particles

Mechanics factors

Rate of deposition at the surface

Nature of lower boundary

Temperature

Topography

The available data on the densities and consolidation characteristics of sedimented fine-grained soils cast doubt on any analysis which would assume the rate of surface movement and a constant coefficient of consolidation. Samples of sub-aqueous fine sediments* show that initial dry weight of the material may be of the order of 5 or 6 pounds per cubic foot and that the same soil will consolidate to a dry weight of 90 pounds per cubic foot as the overburden builds up. For common values of grain specific gravity, this change means a porosity change from about 97% to about 45%. Expressed differently,

---

*For some published data see reference 1, 9 (figure 103 facing p. VIII 296); reference 1, 10 ch. 12 by C. B. Brown who reports some unpublished data from experiments by J. L Hough (pp. 784-786); reference 1,11, reference 1, 12, and reference 1, 13.

the quantity of soil required to make one cubic foot, as laid down at the surface, compresses to a volume 0.055 cubic feet.

The mathematical difficulties of large strain consolidation problems are of two types: moving boundaries and changes in physical characteristics of the soil which govern its consolidation characteristics. Obviously these two effects are coupled. Moving boundaries mean changing void ratios, and the pertinent physical properties of the soil are functions of void ratio.

The literature on the subject tends to treat the effects separately, and, to the author's knowledge, without exception, the governing equations are written in terms of excess pore pressure.

There is a large body of literature in the fields of heat conduction and diffusion concerned with non-linearities in equations analogous to the Terzaghi consolidation equation. These studies are pertinent to the consolidation problem when the study is directed towards hydrostatic excess pressure. When the approach is to study volume changes directly, as was done in formulating equation 1:12, the analogy no longer exists, except in special cases.

Schiffman (1, 14) analyzes the effects of varying permeability on consolidation. Permeability is assumed to vary linearly with porosity, and porosity is permitted to change as excess pore pressure dissipates and intergranular pressure increases. Even with this rather restrictive assumption concerning permeability, the equations in general must be solved numerically.

Abbott (1, 15) has made a useful contribution in formulating the problem of one-dimensional consolidation of multi-layered soils. The linear equation is assumed to hold in each layer, but the layers have different coefficients of consolidation. The theory is applied to an engineering problem and the theoretical and measured settlements are in close agreement.

Gibson (1, 16) studies the problem of consolidation in a soil layer increasing in thickness by the addition of soil at the surface, The soil is added at a uniform rate and its initial void ratio is assumed constant. Analytic solutions are obtained for two rates of thickness increase, and the numerical solution is outlined for arbitrary rates. The method is applied with interesting and useful results to the analysis of pore pressures in an earth dam during construction. The results were used to establish the earth fill placement schedules. Gibson suggests the use of his analysis to study consolidation in a soil forming by sedimentation under water.

These studies may all be grouped together under the classification of studies of variations of the Terzaghi equation. In analyzing sedimented clays, which exhibit such large volume changes, it would seem more reasonable to investigate the consolidation as such, avoiding the intermediate step of hydrostatic excess pressure.

The following chapters describe some experiments on sedimented clays and the correlation of the data from these experiments with the consolidation equation, 1:12, developed in this chapter.

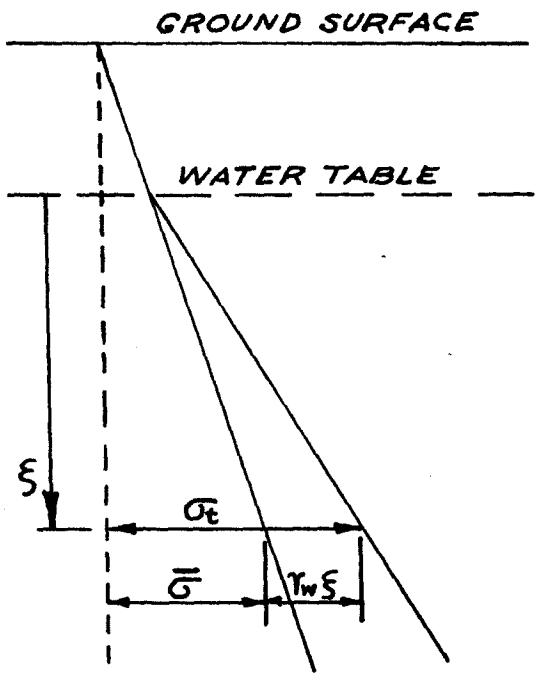

FIG. 1-1a
EQUILIBRIUM SOIL STRESSES

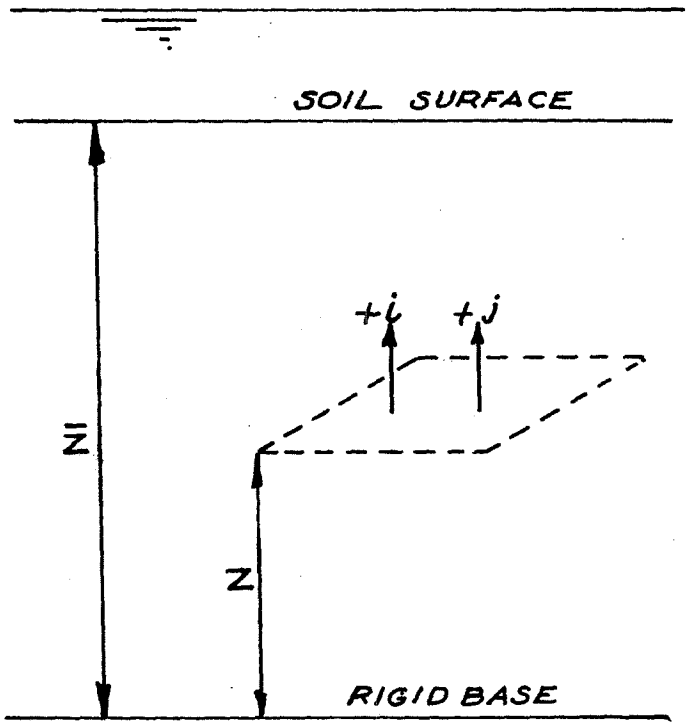

FIG. 1-1b
DOMAIN OF
CONSOLIDATION PROBLEM

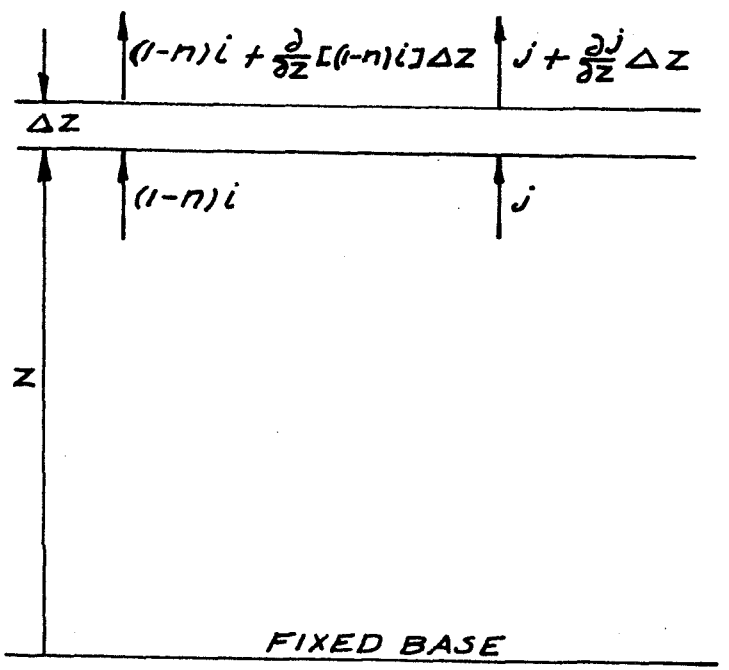

FIG. 1-2a
EQUATION 1:1

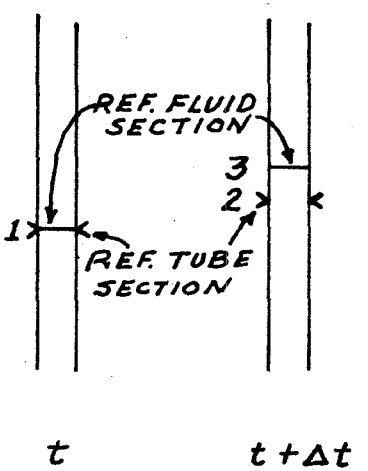

FIG 1-2b
EQUATION 1:3

CHAPTER II

APPARATUS DESIGN AND OPERATION

A. INTRODUCTION

This chapter describes the design and operation of the various types of laboratory equipment which were built to study the properties of sedimented clays.

The several formulae used in Chapter III for reducing data to useable form are developed in this chapter.

The chapter concludes with some comments on other possible uses for the general types of apparatus developed for this study and with some suggestions for improvements that might be made in the design.

In discussing apparatus design and fabrication, the English system of units is used. Metric units are used for all data and calculations.

B. LABORATORY APPARATUS--DESIGN AND FABRICATION

1. Design Criteria

a. The general purpose of the experiments is to obtain data on the consolidation, permeability, and strength characteristics of clays formed by settling of clay floc under water at controlled rates and in a prescribed environment.

b. A transparent column is required in which the clay bed may be formed and observed.

c. A source of clay floc is required, and the rate of clay input must be subject to close control and measurement.

d. Provision should be made for pore pressure measurement at various levels within the column.

e. The column base should be equipped with a filter and outlet valve and provision should be made to pressurize the top of the column. Such an arrangement provides a means of imposing a hydraulic gradient on the clay bed in the column.

f. The column should be so designed as to permit removal of clay bed sections for other tests.

g. Apparatus is required to perform consolidation, permeability and shear tests on individual column sections.

2. Design and Fabrication

The assembled settling column is shown in (fig. 2-1). It consists of a base plate and base column section (fig. 2-2), any desired number of cinch-ring sections (fig. 2-3), a coupling section identical to the base column section, a settling section, and a cap plate (fig. 2-4).

The base plate (fig. 2-2) is machined from brass and is provided with a center outlet and valve. Eight pore pressure tap holes are arranged at even spacing halfway between the plate center and the inside wall of the column. The pore pressure tap holes are machined to provide "O"

ring gland seats and threaded for gland bolts on each side. One pore pressure tap is shown inserted through the base plate. The tap is made from $\frac{1}{4}$ inch O.D. Monel tubing. The tube is swaged $\frac{3}{8}$ inch from the upper end, the end packed with a nylon thread filter, and the tip of the tube swaged to hold the filter in place. The seal between the plate and base column section is made with an "O" ring which fits into a groove in the base plate as shown.

The base column section is made from 4 $\frac{1}{4}$ inch I.D. by $\frac{1}{4}$ inch wall lucite tubing. A lucite flange is threaded and cemented onto the lower end of the section. The top face is rough finished on a lathe and then fine finished by hand against a flat surface to make it smooth, plane, and square to the column axis.

The cinch-ring sections (fig. 2-3) are made from the same 4 $\frac{1}{4}$ inch I.D. by $\frac{1}{4}$ inch wall lucite tubing. They are first cut slightly over length. The steel cinch rings are then located at the section mid-height and tightened. A threaded hole is made in the tubing wall halfway between the cinch-ring and one end of the section. A nylon tubing fitting is screwed into this hole and a piece of 200 mesh brass screen is cemented over the inside end of the fitting. The section is then set up in a lathe so that its axis coincides as nearly as possible with that of the lathe. This is a matter of compromise since lucite tubing of this large diameter is commonly not uniform in diameter or

wall thickness. The outer end surface is then faced off. This newly faced surface is used as the reference surface for the final cut on the other end of the section. All cinch-ring sections are cut to length in this manner, after which the end surfaces are finished by hand as with the base column section. At this point the cinch-ring sections have finished end faces, square with the column axis, and are all of the same length. All that remains is to finish the inside diameter of the sections. Besides the diameter variations in the tubing as received, the pressure of the cinch-ring produces a small, but measurable reduction in diameter at the mid-point of each section. To correct this condition, the sections are bored out on the lathe with the boring tool locked in its traverse position. Thus all sections are finished to the same inside diameter. As a final step, the outside edge of all end faces are given a slight chamfer.

Indicated in figure 2-1, above the sectionalized portion of the column, is the settling section. It is made from a 30 inch section of the lucite tubing with lucite flanges threaded and cemented onto each end.

The cap plate (fig. 2-4) is machined from brass and provided with an "O" ring groove in the same way as with the base plate. The other main features are a center inlet hole fitted with a pipe-nipple and an outlet hole fitted with a needle valve.

The clay slurry agitator tank (fig. 2-5) is an aluminum drum coated on the inside with coal tar enamel to inhibit corrosion by the chemical constituents of the slurry. The cross frame across the top of the drum supports an electric motor with a built in speed reduction and output shaft speed of 12 r.p.m. The motor drives the vertical paddle shaft through one to one ratio bevel gears. The shaft is fitted with two paddles and is supported so the paddles just clear the bottom of the tank. An outlet with valve is provided through the side of the tank. The end of the valve is connected by a horizontal piece of plastic tubing to the glass slurry inlet tube. The glass tube passes through a gland nut and the center of the column cap plate.

Figure 2-6 shows the inlet pressurizing system. It is made from a boiler gage glass modified for this purpose. The gage glass is mounted on a piece of aluminum bar stock which has a scale mounted behind the glass. The gage glass volume is calibrated against the scale. The lower valve is connected to pipe which, in turn, is connected to a piece of flexible hose. In operation, the other end of the hose is connected to a fitting screwed onto the column cap place center hole nipple. The upper gage valve is connected to an air line. A water line is connected to a hole through the upper gage valve body.

Figure 2-7 shows a column cinch-ring section set up for a consolidation test. The filter housing is machined from brass and a sintered bronze filter disc is pressed into the space provided. A threaded hole is located at the center of the housing to accommodate a tubing fitting. The cinch-ring column section is held against the "O" ring seal by tightening the four cinch-ring nuts on the bolts passing through the four cinch-ring holes. The bolts are machined from brass hex-stock with long heads to provide space for the tubing fitting in the housing.

The loading disc consists of another sintered bronze filter disc pressed into a bronze ring which has an "O" ring groove on its O.D. for a wiper ring.

Figure 2-8 shows a column cinch-ring section set up for a vane shear test. The cinch-ring section is secured into a filter housing as for a consolidation test. Two vanes of $\frac{1}{64}$ inch thick stainless steel fit into cross cuts at right angles in the end of the loading shaft. The loading shaft passes through a low friction ball thrust bearing and is attached to a pulley with a set screw. The shaft bearing is pressed into an aluminum spider which fits into a lucite tubing spacer section which, in turn, is bolted onto the cinch-ring section below. The circumference of the shaft pulley is marked for each degree of rotation so that the strain angle can be measured and a reference pointer is attached to the spacer section. Load

is applied through a nylon thread which is connected to the shaft pulley, proceeds horizontally to a side pulley, under the apparatus up and over a second side pulley and thence horizontally back to the shaft pulley. Spacer screws are provided to hold the shaft pulley up so that the shear vanes are above the top of the cinch-ring section when not in use.

C. COLUMN-ASSEMBLY, OPERATION, AND DISASSEMBLY

1. Introduction

This section contains a detailed description of a typical experiment from beginning to end including derivations of formulas used in reducing data.

2. Column Assembly

The base lucite section is forced over the "O" ring on the brass base plate (fig. 2-2). The base plate is placed on a support table with the base plate outlet valve and gland bolts projecting into the opening provided in the support table. Long threaded studs are passed through the four matching holes in the base column section flange, base plate, and support table. These studs are located in elevation with nuts resting on the base column section flange so that the upper ends of the studs will project $\frac{1}{4}$ inch above the cinch-ring of the next column section above. The studs are then secured with nuts and lock

washers on the under side of the support table.

If the pore pressure tubes are to be used, they are installed through the base plate at this time. The tubes run through gland bolts on both sides of the base plate and are positioned so their upper ends are at the desired elevations. The upper gland bolts are tightened slightly so the tubes may be lowered by a firm pull from below. The lower gland bolts are then drawn up tight. The tight lower gland bolts prevent leakage during the experiment, and the upper glands are sufficiently tight to prevent leakage while lowering the tubes prior to disassembly. Plastic tubes are connected to the copper tubing at the lower ends of the pore pressure tubes. The other ends of the plastic tubes are fitted with valves which are, for the moment, left closed.

If the pore pressure tubes are not to be used, the gland bolts are replaced with solid bolts which are drawn up tight against the "O" ring packings to make the base plate water tight.

The base plate outlet valve is closed and a 2 inch diameter by $\frac{1}{4}$ inch thick porous stone is placed over the outlet. The base lucite section is now filled with a 28 to 200 mesh graded Ottawa sand filter. The filter surface is leveled off at the top of the base column section.

A thin layer of vacuum grease is spread on the top face of the base section and on the end faces of all column

sections to be used. The grease provides some insurance against leaks. A cinch-ring section (fig. 2-3) is now placed on the base section and four cinch-ring nuts screwed onto the projecting studs. The studs are $\frac{3}{8}$ inch while the cinch-ring holes are $\frac{7}{16}$ inch. This difference permits the cinch-ring section to be located over the base section so there are no projecting edges at the joint. The four cinch-ring nuts are now tightened so there is enough pressure between the column section faces to prevent leaks. "Enough" pressure is a matter of feel and experience since too much pressure will displace the cinch-rings. Prior to assembly, each cinch-ring section is fitted with a length of plastic tubing connected to the tubing fitting in the cinch-ring wall. The other ends of the tubes are connected to needle valves which are closed.

The cinch-ring nuts are $\frac{5}{8}$ inch long, the cinch-rings are $\frac{1}{2}$ inch thick, and the cinch-ring sections are 2 inches long. Studs 1 $\frac{7}{8}$ inches long are screwed $\frac{1}{4}$ inch into the four cinch-ring nuts holding the first column section. They will then project $\frac{1}{4}$ inch above the cinch-ring of the next section. Any number of cinch-ring sections may now be added. As each section is added, it is tightened securely to the one below and positioned so there are no projecting edges on the inside surface of the column.

After the first cinch-ring section is in place, deaired water is admitted through the base plate valve slowly so

as not to disturb the sand filter. More water is added as each cinch-ring is installed.

After the desired number of cinch-rings are in place, four long studs are screwed into the last set of cinch-ring nuts. These project through the mating lucite flanges of the coupling section and settling section. A rubber gasket is placed between the flanges, and nuts are turned onto the studs to secure the settling section to the column.

The cap plate is now pressed into the top of the settling section with the "O" ring in place to make a seal. The cap plate is secured to the settling section with four bolts through the matching holes in the upper settling section flange and cap plate.

During assembly, deaired water is added periodically to keep the water surface near the top of the column. In this way any major leaks may be detected and corrected before assembling the whole column. As each side wall pressure tap becomes submerged, its valve is opened and water allowed to pass through the tube and valve until all air is removed. The pore pressure tubes are best deaired by forcing water up through the tubes and thus expelling the air through the filters at the ends of the tubes. The base plate valve is opened several times to make sure no sand can escape. This also has the effect of seating the filter.

After the cap plate is installed, the column is filled with water including enough electrolyte to produce the same concentration in the column as will be used in the slurry tank. The glass slurry inlet tube is now installed with its gland nut screwed onto the cap plate center hole nipple (fig. 2-9). The gland nut is tightened with the horizontal section of the glass tube at the same level as the slurry tank valve. The glass tube and slurry tank valve are then connected with a piece of plastic tubing. A piece of plastic tubing is connected to the inclined branch section of the glass tube. The other end of the tubing is connected to a funnel which is supported at a level above the top of the slurry tank. The slurry tank is partially filled with deaired water. The tank valve is opened, filling the glass tube with water.

A piece of plastic tubing is connected to the cap plate outlet valve and inserted into the top of a burette (fig. 2-9). An auxiliary slurry agitator is mounted above the main slurry tank. This is a 10 liter aspirator bottle placed on a magnetic stirrer. The base outlet of the bottle is fitted with a rubber stopper from which tubing passes horizontally over the rim of the main slurry tank and down into the tank. A rubber stopper is inserted in the top outlet of the flask. Tubing passes from here into the main slurry tank with its end fixed at the desired

slurry level in the main tank.

A scale is attached to the side of the column. This completes the column assembly. Slurry may now be prepared for an experiment.

3. Experimental Procedure and Data Taking

a. Slurry preparation.--Clay slurry is made up of a mixture of clay, water, and common salt. The Pasadena tap water, used in the experiments, contains approximately 0.7 grams of dissolved solids per liter, of which an unknown but considerable percentage is bivalent metals such as magnesium and calcium. The slurry concentrations varied somewhat but are of the order of 10 grams of dry clay and 2 grams of salt to one liter of tap water.

Reference 2,1 discusses the effect of electrolyte concentration on flocculation in clay-water systems. The presence of electrolyte is shown to have a marked effect on the net attractive (or repulsive) force between particles as a function of particle separation distance. Further, bivalent and trivalent positive ions are shown to influence the net particle-to-particle force more strongly than monovalent ions. The concentration and types of electrolyte used here are in the range at which the net force between particles would be repulsive, if ever, to only a small degree and over a short span of interparticle distances. This is borne out by the good floc formation in the slurries used here.

The slurry concentration used is governed more by the mechanics of the flow system than anything else. In a given experiment some fixed flow rate of grams of dry clay per minute is desired. (See Chapter I-Section B.) The more concentrated the slurry, the lower the slurry flow rate will be to attain the desired result of flow of clay solid. At very low slurry flow rates, the horizontal portion of the slurry flow line nearly fills with clay leaving only a small flow passage along the top of the tube. This raises the question as to whether or not the slurry flowing through the line is of the same concentration as that in the tank. On the other hand, if the slurry is very dilute requiring a high flow rate, eddy formation in the column at the end of the slurry flow line can be sufficient to lift some clay floc up to the cap plate and allow it to escape through the cap plate outlet valve. By trial and error a suitable compromise in flow rate is used.

The slurry concentration has no effect on the size of floc reaching the clay bed in the column. Within the range of concentrations allowable from the mechanics of the system, the clay floc leaves the slurry flow line at a uniformly small size visually estimated at approximately $\frac{1}{3}$ mm. In the process of settling in the column, these small floc occasionally will collide to form larger floc. The frequency of collisions is a statistical problem depending on the initial distribution of floc sizes (or

settling velocities) and the floc concentration. As the flocs grow in size, their settling velocities increase. Visual observation indicates a terminal floc size for a given set of conditions. Floc, larger than this terminal size, tend to break up from the higher viscous drag forces incident to their increased settling velocities. In the apparatus used here, this terminal size was attained at some 40 to 50 cms below the slurry inlet tube and was of the order of 3 times the initial size.

After choosing a slurry concentration, two batches of dry clay and proportional amounts of salt are weighed; one batch for the volume of slurry in the main agitator at the control level and one batch for 10 liters of slurry in the auxiliary agitator. These batches are mixed with one to two liters of water in a dispersion cup to make dense slurries. The mixing process fills the dense slurries with small air bubbles so they are deaired by application of vacuum for several hours.

The dense slurry batches are then added to the two agitators along with the required amounts of deaired water. To obtain good dispersion the slurries are mixed in the agitators for at least one hour. The slurry tank outlet valve is open during this period but no slurry may enter the column until the cap plate outlet valve is opened. The tube between the two agitators is open but no flow can occur here until the surface in the main tank drops enough

to allow air to pass through the tube connected to the top of the auxiliary agitator.

b. Clay bed formation.--The cap plate outlet valve is now opened. The outflow rate of clear effluent was measured periodically by closing the burette valve (fig. 2-9) and noting the time required for some quantity of flow. The cap plate valve is a needle valve. A few flow measurements and valve adjustments are sufficient to bring the flow rate to the desired value. This flow rate will not change so long as the pressure drop across the valve remains constant. This is one reason for maintaining a constant level in the main slurry tank with the secondary agitator system. During the period of clay input, the flow rate is periodically checked.

Additional batches of clay for 10 liters of slurry are prepared as required. The auxiliary slurry agitator is allowed to empty completely before being refilled. The outlet from this flask is at the base, and thus the slurry flowing into the main agitator is of a higher concentration than the average in the flask. By allowing the flask to empty before refilling, the consequent change in concentration in the main tank is cyclical around the desired mean and does not steadily drift upward. Since the main tank contains some 40 liters of slurry, the variation from the mean is small. The main tank outlet valve is at an appro-

priate location to remove slurry at the mean concentration. This is checked by measuring the mean concentration in the tank at the conclusion of the clay input period. This measurement is made by pipetting samples from five equally spaced levels in the tank, mixing the samples together and measuring the concentration by drying the slurry and recording the dry weight.

There is, however, another effect tending to steadily increase concentration in the main tank and that is surface evaporation. An evaporation pan is placed alongside the main tank and evaporation rate is measured. The slurry surface in the main tank rotates smoothly, but even this mild motion would be expected to produce a higher evaporation rate than that from a still surface. To compensate for this, the water surface in the evaporation pan is within a few cms of the top while the slurry surface in the main tank is kept at some 15 cms below the top of the tank. Assuming, for the moment, that this procedure gives the correct evaporation rate, the change in main tank concentration may be computed. Two cases must be considered. In the early experiments, the auxiliary agitator was not used so that the main tank surface moved down with time and was raised periodically by adding a batch of slurry. In these cases the flow rate was maintained constant by periodic valve adjustments. The second case is for a fixed level in the slurry tank.

Case 1. Moving slurry surface

With reference to figure 2-11a, the following symbols are defined:

t = time, minutes

A = cross-sectional area of tank, cm^2

H_o = slurry depth at $t = 0$, cm

H = slurry depth at t, cm

q = outflow rate, cm^3/min, a constant

v = evaporation rate, cm/min, a constant

c_o = slurry concentration at $t = 0$, gms/cm^3

c = slurry concentration at t, gms/cm^3

W_o = total weight of clay in tank at $t = 0 = c_o A H_o$ gms

W = total weight of clay in tank at $t = cAH$ gms

v and q are taken as constants over a given time interval.

By definition:

$$c = \frac{W}{AH} \text{ or } \frac{dc}{dt} = \frac{1}{A}\left[\frac{1}{H}\frac{dW}{dt} - \frac{W}{H^2}\frac{dH}{dt}\right] \qquad (2:1)$$

Fluid is removed through the outlet and by evaporation:

$$H = H_o - \frac{q}{A}t - v\,t \qquad (2:2)$$

from which

$$\frac{dH}{dt} = -\frac{q}{A} - v \qquad (2:3)$$

Clay is removed through the outlet valve at the rate qc:

$$\frac{dW}{dt} = -q\,c \qquad (2:4)$$

Substituting equations 2:3 and 2:4 into equation 2:1:

$$\frac{dc}{dt} = \frac{1}{A}\left[\frac{1}{H}(-qc) - \frac{AHc}{H^2}\left(-\frac{q}{A} - v\right)\right]$$

or

$$\frac{dc}{dt} = v\,\frac{c}{H}$$

which may be integrated to give c as a function of t

$$\int_{c_o}^{c} \frac{dc}{c} = v\int_{0}^{t} \frac{dt}{H_o - \frac{q}{A}t - vt}$$

or

$$c = c_o\left[\frac{H_o}{H_o - (\frac{q}{A} + v)t}\right]\left(\frac{1}{1 + \frac{q}{Av}}\right) \qquad (2:5)$$

At some later time, t_1, a batch of slurry of known concentration is added. A new c_o and H_o are then known for computing c after t_1. This process is repeated for each time a slurry batch is added.

Case 2. Fixed slurry surface

With reference to figure 2-11b, the following symbols are defined

t = time, minutes

A = cross-sectional

H = slurry depth, cm, a constant

q_1 = slurry inflow rate, cm^3/min, a constant

q_2 = slurry outflow rate, cm^3/min, a constant

v = evaporation rate cm/min, a constant

c_1 = concentration of slurry flowing into the tank gms/cm^3, a constant

c = c(t) slurry concentration in tank, gms/cm^3

W_o = total weight of clay in tank at t = 0, $c_o AH$ gms

W = total weight of clay in tank at t = cAH gms

Since the tank level remains constant, continuity requires

$$q_1 = q_2 \quad v\,A \tag{2:6}$$

The total weight of clay in the tank is the original weight plus the input less the output:

$$W = W_o + q_1\ c_1\ t - \int_o^t q_2\ c\ dt \tag{2:7}$$

or,

$$\frac{dW}{dt} = q_1\ c_1 - q_2\ c \tag{2:8}$$

also,

$$\frac{dW}{dt} = AH\,\frac{dc}{dt} \tag{2:9}$$

Combining equations 2:8 and 2:9

$$\frac{dc}{dt} = \frac{1}{AH}\,(q_1\ c_1 - q_2\ c) \tag{2:10}$$

Equation 2:10 may be integrated to give c as a function of t:

$$\int \frac{dc}{(q_1\ c_1 - q_2\ c)} = \int \frac{dt}{AH}$$

or

$$q_1 c_1 - q_2 c = B\epsilon^{-\frac{q_2}{AH} t} \qquad (2:11)$$

where B is a constant of integration and is the Naperian base. At $t = 0$, $c = c_1$ so the constant, B, must satisfy the relation:

$$B = q_1 c_1 - q_2 c_1$$

or

$$B = vAc_1 \qquad (2:12)$$

Combining equations 2:11 and 2:12:

$$c = \left[\frac{q_2 + vA}{q_2} - \frac{vA}{q_2}\epsilon^{-\frac{q_2}{AH} t}\right] c_1 \qquad (2:13)$$

In either case there is a check on the procedure. By integrating the flow rates and concentrations computed from equation 2-8 or equation 2-15, whichever applies, the total weight of clay passed into the column may be computed. This total may be compared with the total weight made into slurry less the weight left in the slurry tank at the conclusion of the clay input period. As shown in the following Chapter these two totals checked closely.

The slurry flow line must project horizontally from the tank before turning down into the column. If inclined upwards, the slurry reaching the column is of a lower concentration than that in the tank. The reverse is true if the line inclines downward. This results from the fact that the floc settling velocities are not insignificant compared to the flow velocity in the line. There is no accurate method extant for correcting this effect. In particular,

siphoning, which requires slurry flow up out of the tank, must be rejected as a means of a slurry transfer.

As noted above, the clay floc grow considerably while settling in the column. The slurry flow rates are kept low enough so that the individual floc are clearly seen settling until they strike the clay bed surface If clay slurry is added to the column in batches, there are no simple means of distinguishing between a dense suspension and a clay bed in which the flocs are in contact, so that the bed height cannot be measured.

As the surface of the clay bed rises in the column, its level is noted, periodically, from the scale mounted on the side of the column. The reading is made through a hand level to eliminate parallax. In this way the elevation may be read to $\pm \frac{1}{2}$ mm.

At intervals during the clay input period, 25 cc of red clay slurry, at a concentration of 15 gms of dry clay per liter, are injected into the funnel connected to the inclined side section of the glass slurry inlet tube. Since the clays used in the experiments are white in color, this small amount of red clay forms a visible reference line in

the clay bed. These lines permit observation of consolidation of sections of the clay bed by noting the differential movements of adjacent reference lines.

In the experiments with bentonite clay, these red reference lines remain intact and clearly visible as they move down in the column. Besides providing useful data, the lines are good evidence that the column walls have little or no influence on the consolidation process and that it is truly one dimensional. With kaolin, however, the lines are erased soon after being formed due, apparently, to an affinity between kaolin and lucite. The significance of this is discussed in Chapters III and IV.

The time at which clay input should cease is determined by consideration of how close the bed surface should be allowed to approach the end of the slurry inlet tube. Observations indicate that, by the time clay floc have settled some 40 cm below the end of the slurry line, they have grown to nearly their terminal size. Moreover, if the bed surface is permitted to get much closer than this, it will begin to feel the effects of the flow pattern around the end of the inlet tube.

c. Clay bed consolidation in settling column.--After clay input is stopped, the bed surface subsides as the clay continues to consolidate under its own weight. Readings are continued on the surface elevation and the elevations of red reference lines when possible.

When the clay approaches equilibrium under its own weight, it may be further consolidated by imposing a hydraulic gradient across the bed. To do this, the slurry inlet tube is removed and the inlet pressurizing system is connected to the column cap plate (fig. 2-6). The inlet line is filled with water with a visible surface in the gage glass. The desired air pressure is imposed through the upper gage valve. The water surface in the glass drops a little when pressure is applied because of the elastic enlargement of the inlet lines and column. The column base plate valve and a constant level free surface reservoir are connected with a piece of tubing. The base plate valve is now opened. The total head drop across the bed is the gage pressure head of the air above the gage glass water surface plus the gage glass water surface elevation less the outlet water surface elevation. The rate of flow through the column outlet is given directly by the water surface movement in the calibrated gage glass. When the gage glass water surface nears the bottom of the glass, it is raised by admitting water through the upper gage valve. The flow rates are typically low. Under these conditions, it is easier to obtain accurate data by measuring flow at the inlet side rather than attempting to catch the outflow with the attendant evaporation problems. The fluctuating water surface in the gage

glass means the total head drop across the bed is not constant. However, these variations are small compared to the total head drop.

d. Pore pressure measurements. -- During the three stages: Bed formation, consolidation under gravity, and consolidation under hydraulic gradient, pore pressures may be read from the pore pressure tubes through the base plate or from the connections through the cinch-ring section walls or from both. During the first two stages, pressures are read with water manometers. The pore pressure taps are connected to flexible transparent tubes which are mounted on vertical boards fitted with scales. The scales are related to reference elevations on the column. Water manometers are, of course, quite sensitive. Their main drawback, here, is that pressure changes are necessarily accompanied by flow into or out of the manometer tubes. During the period of clay input, this problem is minimized by keeping the main slurry tank level constant so that the only inflow or outflow in the manometers is that due to changes in hydrostatic excess pressure. This is the principal reason for using the double slurry tank scheme.

For the higher pressures during the period of consolidation under hydraulic gradient, water manometers cannot be used. Replacing the water with mercury is also not suitable because of head room restrictions. In any case, as the clay becomes more dense, the flow problem inherent in

the use of manometers becomes more serious. A pressure transducer was selected as a more suitable means of pressure measurement under these conditions.

The instrument used is a Statham Instrument Company Pressure Transducer; Model No. P6-50D-350; Serial No. 2765; input resistance, 369.0 ohms; output resistance, 369.0 ohms; calibration factor, 28.69 microvolts (open circuit) per volt excitation per psi. The transducer is calibrated against a mercury column using a 12 volt wet cell battery for excitation. The calibration curve and the wiring diagram are shown in figure 2-10. The sensing element in the transducer is an unbonded strain gage connected in a Wheatstone Bridge. Two legs of the bridge are for temperature compensation so that the calibration curve does not change with temperature. The "zero-adjust" circuit provides a means of balancing the bridge at any desired pressure. Then as the pressure is increased above this "zero," the bridge becomes unbalanced and the output voltage is measured with a potentiometer. As shown by the calibration curve, the output voltage varies linearly with pressure. For tests, here, the "zero" is set at atmospheric pressure. Perhaps the most desirable feature of the transducer is that the quantity of water required to actuate the device is negligible. In use, the transducer is connected in turn to the needle valves at the ends of the pore pressure tubes.

Care is taken that no air bubbles are trapped in making the connection. The needle valve is then barely "cracked" open and the pressure recorded. Connecting the transducer directly to the valves is a slow procedure but preferable to any sort of manifold system since the direct connection requires only the very small flow volume necessary to activate the instrument. The valves need to be opened only a small amount to sense the pressure. Opening the valves further than necessary is avoided since the volume of water in the line is changed as the valve stem retracts. Cock-valves have the advantage of producing no line volume changes from full closed to full open. However, needle valves give much more positive insurance against leaks.

After the clay bed has reached equilibrium under the hydraulic gradient, the bed surface stops subsiding and flow through the bed settles down to a steady rate. Pore pressure data give the gradient of total head for each segment of the clay bed. With the flow rate known, the permeability of each segment of the bed may be calculated. Seepage forces are calculated from the gradients also. After the contents of the column sections are dried (see disassembly procedure, below), the volume ratios (eqn. 1:5) may be calculated.

A curve of permeability as a function of volume ratio (or porosity or void ratio) may now be constructed for the material under consideration. By summing the buoyant

weights and seepage forces from the clay surface down, a curve of volume ratio as a function of intergranular pressure may also be constructed.

To obtain solutions of equation 1:22 , in a given case, k and a, must be known as functions of E. Data from the apparatus and methods described above provide this information.

In some experiments the column of clay was disassembled after coming to equilibrium under its own weight. The $\overline{\sigma}$-E curve for the upper range of E is obtained in this way, but no information on permeability is obtained.

4. Column Disassembly

At the time of column disassembly the clay surface is, in all experiments, below the coupling section (fig. 2-1).

The column cap plate is removed and the clear water above the clay surface is withdrawn, care being taken not to remove any clay in the process. The column sections above the clay surface are then removed. Two finger clamps are applied to the cinch-rings of the top section and the next one below. These serve the purpose of maintaining pressure between the section faces while the cinch-ring nuts and studs are removed from the top section. If further tests are to be run on the top section, a brass filter housing (fig. 2-7) is placed over the top of the cinch-ring section. Four of the long head bolts are passed through

the base section and cinch-ring and secured with four cinch-ring nuts. Water is admitted slowly through the center hole of the base section until the porous disc and the space above it are filled. This is the reason for the taper in the space above the porous disc. A piece of flexible tubing is connected to the base section with a valve at the other end. The tube is filled with water and the valve closed. The assembly is held down by hand while the two finger clamps are removed. A thin sheet of stainless steel is now passed quickly through the bed at the interface between the column sections. The chamfer on the outside edges of the sections is provided to facilitate this operation. The top section and stainless steel sheet are now slid horizontally off the column below. They may not be lifted off the column, since this would pull some clay out of the next section below due to its tendency to adhere to the steel slicing sheet. The section and steel sheet are now turned over and placed on the bench so that the column section with its brass filter housing rests on the four long-head bolts. The steel slicing sheet is slid horizontally off the column section. This whole process is repeated until the column is completely disassembled.

If no additional tests are to be made on some of the sections, the section removal process is the same except that the brass filter housing is not attached. After removing the section from the column, its contents are

emptied into a previously weighed drying pan. The contents of all sections are ultimately placed in drying pans and dried in an oven at 105° C until weight loss is complete. The dry clay weights for each section are obtained in this way.

D. TESTS ON COLUMN SECTIONS

The column sections mounted in the filter housing may now be subjected to permeability, consolidation and vane shear tests.

1. Permeability Tests

For permeability tests, a second filter housing is placed on top of the section. It is filled with water and fitted with a piece of tubing. The falling head permeability test (ref. 2,2) is used with the water passing through the clay from bottom to top. In principle, it would be desirable to keep the head drop through the sample below that which would lift the sample up were it not enclosed. In practice this is not feasible. The densities of the sections are typically so low that the maximum head drop under this criterion would be a fraction of a centimeter of water. The best that can be done is to use low head drops of a few centimeters and take a reading after only a small amount of water has passed through the sample. With the fluid pressure force difference across

the sample greater than the weight of the sample, either the sample must rupture forming a passage through which the water may flow unrestrained, or the whole sample must be lifted against the top porous disc forming a relatively impermeable layer against the disc. The experience here indicates the latter effect in all cases, for the permeability dropped sharply as flow continued through the sample. If the flow system is reversed so that water flows down through the section, the clay is subjected to a consolidating force in the same way as the clay in the assembled column is consolidated by a hydraulic gradient across the bed.

It must be noted that the permeameter assembly provides some resistance to flow without any clay in it. This is measured and a correction made to the reading for the combined system to obtain the permeability of the clay alone. In both tests, with and without the clay, the same initial and final head drops are used. The cross-sectional areas of the supply column and test section are the same in both cases.

With reference to figure II-12a, the following symbols are defined:

t = time

a = cross-sectional area of supply column, cm^2

A = cross-sectional area of test section, cm^2

L = length of test specimen, cm

h_o = initial head drop, cm

H = head drop through clay, cm

h_1 = final head drop, cm

h = head drop at some intermediate time, cm

R_a = apparatus conductivity, min^{-1}

R_c = clay conductivity, min^{-1}

V_a = superficial flow velocity through apparatus only, cm/min

V_T = superficial flow velocity through apparatus plus clay, cm/min

t_a = total time for test with apparatus only, mins

t_T = total time for test with apparatus plus clay, mins

k = permeability of clay, cm/min

With no clay in the apparatus, the quantity flow rate is

$$V_a A = R_a h A \qquad (2:14)$$

This equals the flow out of the supply column

$$R_a h A = -a \frac{dh}{dt} \qquad (2:15)$$

The minus sign is required because $\frac{dh}{dt}$ is always negative.

Integrating equation 2:15 gives

$$R_a = \frac{a}{A t_a} \log \left(\frac{h_o}{h_1} \right) \qquad (2:16)$$

With clay in the apparatus, the quantity flow rate is

$$V_T A = R_c HA = R_a (h - H)A \qquad (2:17)$$

or

$$V_T A = \frac{R_c R_a}{R_a + R_c} hA \qquad (2:18)$$

As before, this equals the flow out of the supply column,

$$\frac{R_c R_a h A}{R_c + R_a} = - a \frac{dh}{dt} \qquad (2:19)$$

Integrating equation 2:19 gives

$$\frac{R_c R_a}{R_c + R_a} = \frac{a}{A t_T} \log \left(\frac{h_o}{h_1} \right) \qquad (2:20)$$

Combining equations 2:16 and 2:20 gives an expression for R_c

$$R_c = \frac{a}{A(t_T - t_a)} \log \left(\frac{h_o}{h_1} \right) \qquad (2:21)$$

The conductivity, as defined here, is, for a homogeneous medium, the permeability divided by the length of the sample. Thus, from equation 2:21

$$k = R_c L = \frac{aL}{A (t_T - t_a)} \log \left(\frac{h_o}{h_1} \right) \qquad (2:22)$$

2. Consolidation Tests

For consolidation tests, a porous loading disc is placed on the surface of the clay (fig. 2-7). Load is applied through a rigid loading frame which bears on the bronze ring surrounding the porous disc. Weights are added to the under side of the frame as required. If the anticipated settlement of the loading disc is greater than the thickness of the loading disc ring, additional rings must

be placed between the disc and the loading frame. Otherwise the loading frame will come to rest on the end face of the lucite section. Care must be taken to center the loading disc and spacer rings over the column section and to place the loading frame symmetrically over the section. If this is not done correctly, the loading disc will impinge on the inside surface of the lucite.

Settlement measurements are made with a dial gage resting on a steel ball which in turn rests in a tapered depression in the top of the loading frame.

Load is added in increments, and the clay permitted to consolidate to near equilibrium for each load. The time at which the next load increment may be added is discussed in Chapter III. Most tests are carried out with drainage from the top surface only although the apparatus is also suitable for double drainage tests.

The consolidation apparatus also permits permeability tests to be conducted in conjunction with the consolidation test. After the sample is at equilibrium at a particular load, the tube from the center hole of the filter housing is connected to a burette filled with water. When the valve is opened in this line, a falling head permeability test is run. The initial fluid pressure force at the base of the sample must be less than the sum of the load on the sample and the sample weight or the whole sample will be lifted out of the column section.

3. Vane Shear Tests

In considering possible tests to conduct on sections of a clay column, various methods of measuring shear strength were studied. The anticipated high void ratios and low shear strengths seemed to rule out any strength testing system which required removing the clay from its column section. Even if this could be accomplished, it would, inevitably, result in appreciable disturbance of the sample. The clays and environments used here suggest the possibility of the resulting clay beds exhibiting thixotropy to a high degree. In such materials any appreciable disturbances result in sharply decreased shear strengths (2, 3).

Under these circumstances a vane test seemed to be the only reasonable solution. The vane shear test apparatus is shown in figure 2-8. The apparatus is assembled with the shaft pulley supported on the spacer screws. The shaft pulley is turned so its spokes clear the spacer screw and then it is lowered forcing the shear vanes straight down into the clay. The position of the reference pointer on the shaft pulley scale is noted and the spacer screws removed. The length and weight of the loading thread is chosen earlier such that it is just sufficient to overcome the static friction of the shaft and side pulley bearings. Load is added at the center of the thread loop which hangs freely below the apparatus.

The tension in the thread is calculated from the angle it makes with the vertical. Load is added in steps and the shaft pulley scale noted when it comes to rest. When the failure load is reached, the shaft pulley does not come to rest but continues turning.

At failure, the cylinder of clay prescribed by the geometry of the vanes rotates while the clay outside the vanes remains fixed. The shear stress on this cylindrical surface is assumed to be a measure of the shear strength of the soil. Reference 2,4 describes the use of vane shear tests in engineering practice and suggests the results of such tests correlate well with more rational laboratory tests such as the triaxial shear test. It is the author's impression that the vane test has not gained wide acceptance amongst soil mechanics engineers apparently because of much experience to the contrary.

The shear stress developed by the device is computed as follows. With reference to figure II-12b the following notation is defined:

D = diameter of cylinder generated by vanes, cm

h = depth of penetration of vanes into clay, cm

T = torque applied to vane shaft gm-cm

s_1 = shear stress on surface of soil cylinder of diameter D, gms/cm^2

s_2 = shear stress on base of soil cylinder, gms/cm^2

The resisting torque from the clay is equal to the applied torque and is the sum of resisting torques from the vertical surface and base surface of the cylinder.

Resisting torque from vertical cylindrical surface

$$= \pi D h s_1$$

Along the base surface, the shear stress is assumed to vary linearly from zero at the center to s_1 at the edge of the vane.

$$\text{Resisting torque from base} = \int_0^{\frac{D}{2}} s_2 \, (2\pi r \, dr)$$

$$\text{but} \quad s_2 = \frac{r}{\frac{D}{2}} s_1$$

$$\text{thus} \int_0^{\frac{D}{2}} s_2 \, (2\pi r dr) = \frac{4\pi}{D} s_1 \int_0^{\frac{D}{2}} r^2 \, dr$$

$$= \frac{\pi D^2}{6} s_1$$

so that $$T = \pi D h s_1 + \frac{\pi D^2}{6} s_1$$

or $$s_1 = \frac{T}{\pi D \left(h + \frac{D}{6}\right)}$$ 2:23

E. EVALUATION OF APPARATUS

1. Pore Pressure Measuring Systems.

Of the two methods of obtaining pore pressures, the tubes through the base plate have the decided advantage of sensing pressures in the column interior, thus avoiding any wall effects. The cross-sectional area taken by the tubes can hardly have any serious effects. The combined area of eight tubes is 0.63 cm^2 while the column has an area of 91.5 cm^2. Unfortunately, despite repeated attempts, no reliable data could be obtained from these tubes. This appeared to be caused by plugging of the filter ends of the tubes.

After the end of a tube is buried by the rising clay surface, the fluid pressure at that level must start to rise above the hydrostatic level at that point. For the water manometers to detect this rise, water must flow into the pressure tubes. This is one mechanism by which the filter ends may be plugged with clay. In addition, as the clay consolidates, it moves down in the column, tending to force clay into the stationary ends of pressure tubes.

The clay forced into the tube ends combined with the filter material to form a plug which resisted flow in either direction. This was evidenced by attempts to clear the tubes. Water was poured into the open ends of the manometer tubes and in some cases the free water surface

in these tubes stood one to two feet above the maximum possible level that could exist at the ends of the tubes without any apparent movement of the water surface. In some cases, the tube ends could be cleared in this manner but they soon plugged up again.

Despite these problems, the advantages of this system seem to justify further attempts to make the tubes usable.

As noted in section C of this chapter, pressure transducers have the desirable feature of requiring almost no flow to sense a pressure. Unfortunately, the instrument described in that section was obtained after most of the experiments were finished; also, its range is much too great for the purpose of detecting the small pressure differences between the several tubes. Possibly, a low-range, high-sensitivity instrument would solve much of the problem caused by flow through tube filters.

The problem of clay being forced into the tube ends as the bed consolidates could, perhaps, be eliminated by drilling small holes in the walls of the tubes near the ends and sealing of the ends. Then the movement of the clay would not impinge directly on the hole.

That this scheme might work was suggested by the fact that some measure of success was attained with the pore pressure measurements through the walls of the cinch-ring sections.

The base plate tubes were finally abandoned after the montmorillonite experiments were completed. At this time, the cinch-ring sections were fitted with pressure tubes in the hope of obtaining some data in the kaolinite experiments. As discussed in section C, Chapter III, this action met with a qualified success. That the tube remained free was shown by prompt movements of the manometer free water surfaces when these were raised or lowered. Unfortunately, the characteristics of the clay were such that pore pressure measurements had little meaning, at least during the periods of bed formation and settlement under gravity.

One of the kaolin beds was consolidated in the column with the pressure gradient system. This was the one time during all the experiments when some meaningful pore pressure data were obtained.

The fact that the holes through the cinch-ring section walls did not plug when pressures were measured with a transducer suggests that a more appropriate transducer used with base plate tubes having closed ends and holes through their sides may produce some useful data.

2. Consolidation By Pressure Gradient.

The principle of consolidating a soil by means of a pressure gradient would seem to be a useful soil-testing technique, presuming, of course, the apparatus problems could be solved. The possibility of obtaining data on permeability, void ratio-intergranular pressure relationships, and time-consolidation characteristics, all over a range of void ratios, in one laboratory test, would seem to warrant further study of the apparatus problem. Conceivably, such a test could be made on an undisturbed soil sample. This, however, would complicate the problem.

To develop the intergranular pressures commonly required for engineering purposes would necessitate high fluid pressures. Lucite may not be a suitable material for a high pressure column. If the column were made of metal, lucite windows could be installed so as to retain some of the advantages of visual observation.

In common with many soil testing problems, pore pressure measurements probably would present the most difficult problems in both design and operation.

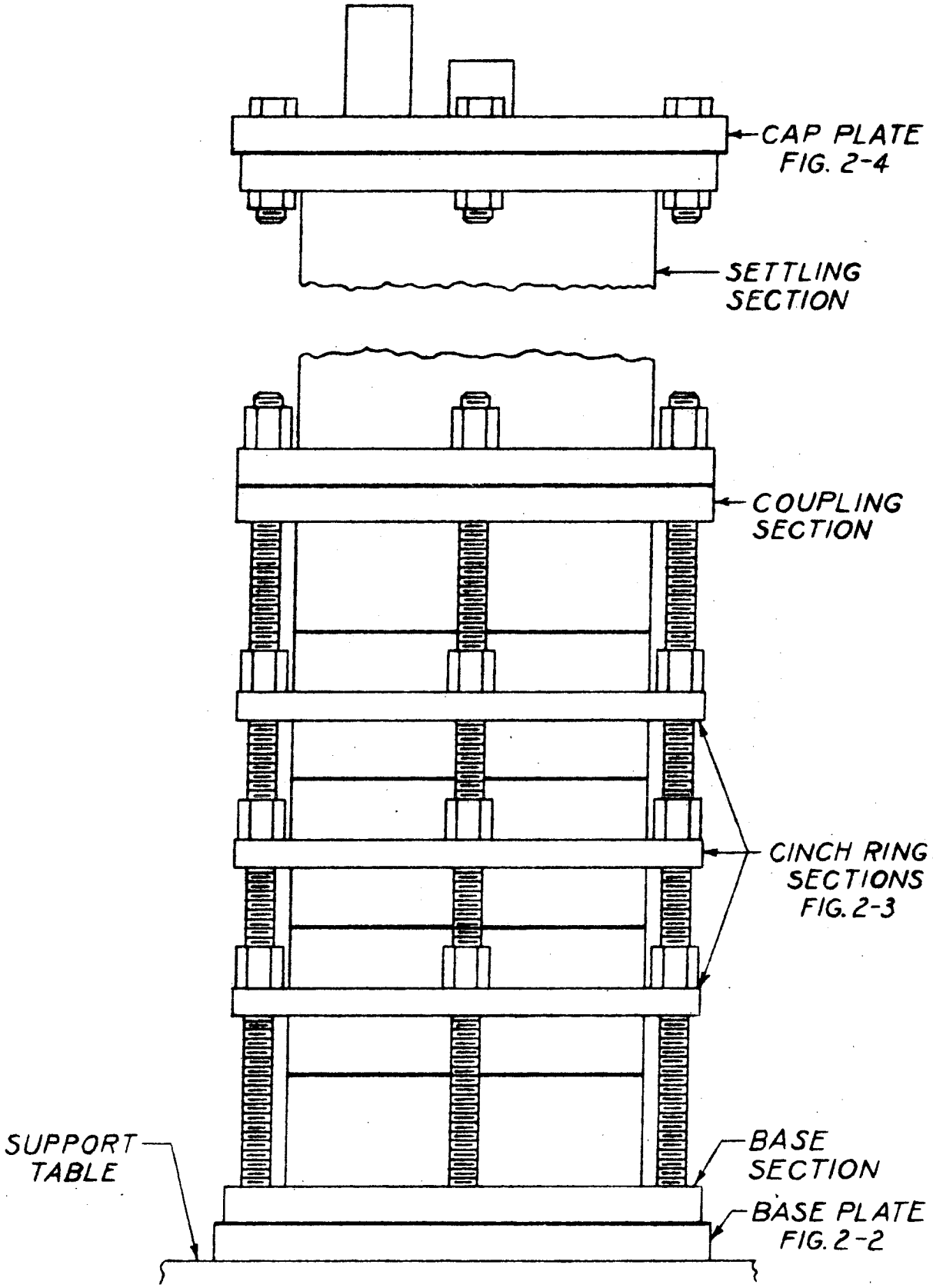

FIG. 2-1
ASSEMBLED SETTLING COLUMN

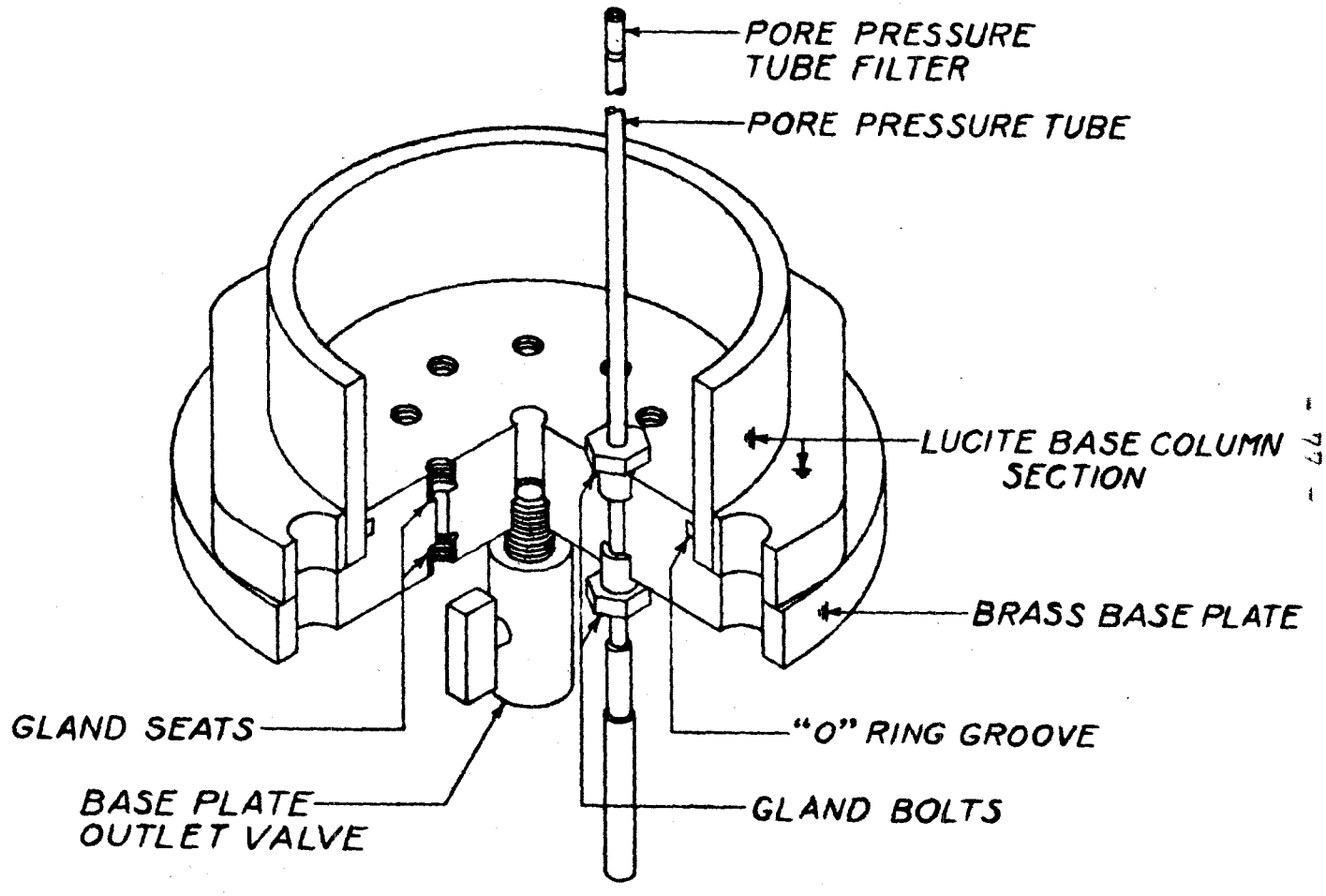

FIG. 2-2
SETTLING COLUMN
BASE PLATE AND BASE COLUMN SECTION

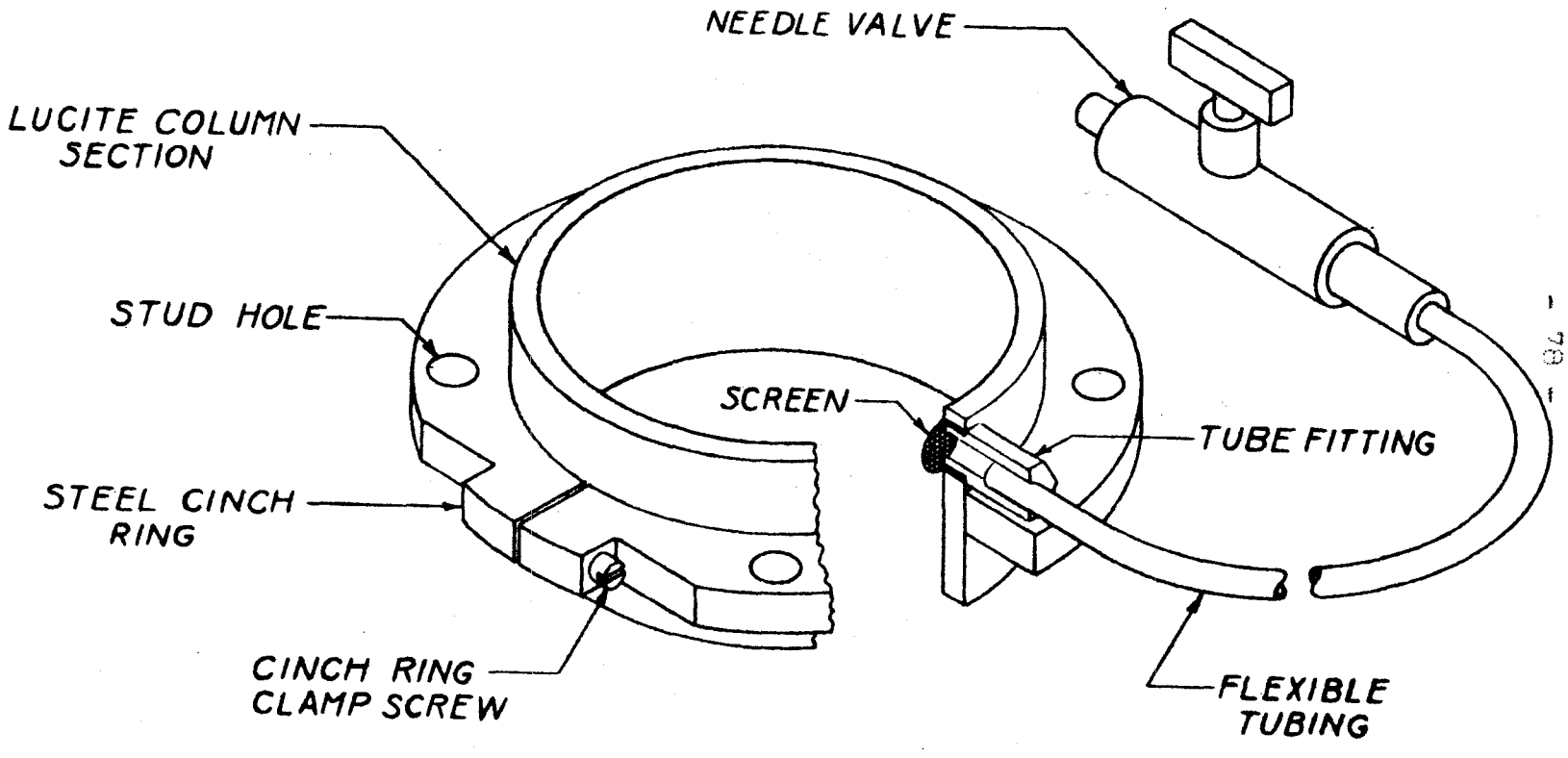

FIG. 2-3
SETTLING COLUMN
CINCH-RING SECTION

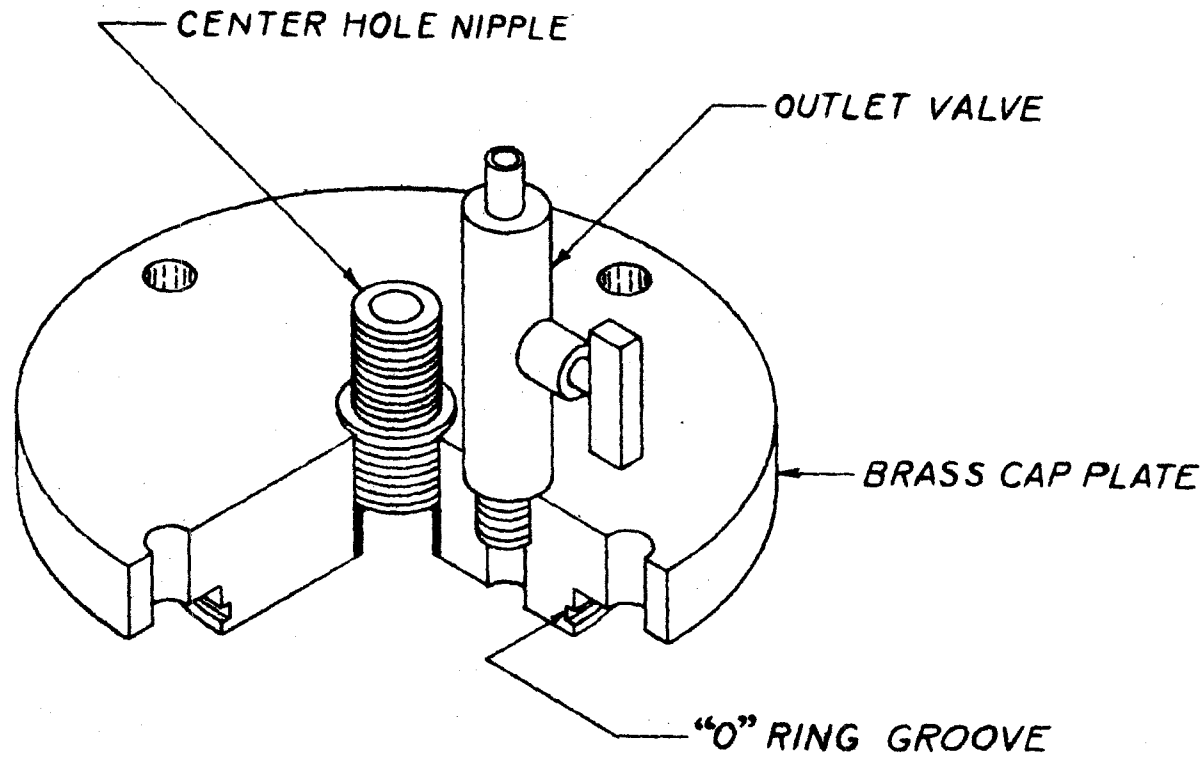

FIG. 2-4
SETTLING COLUMN
CAP PLATE

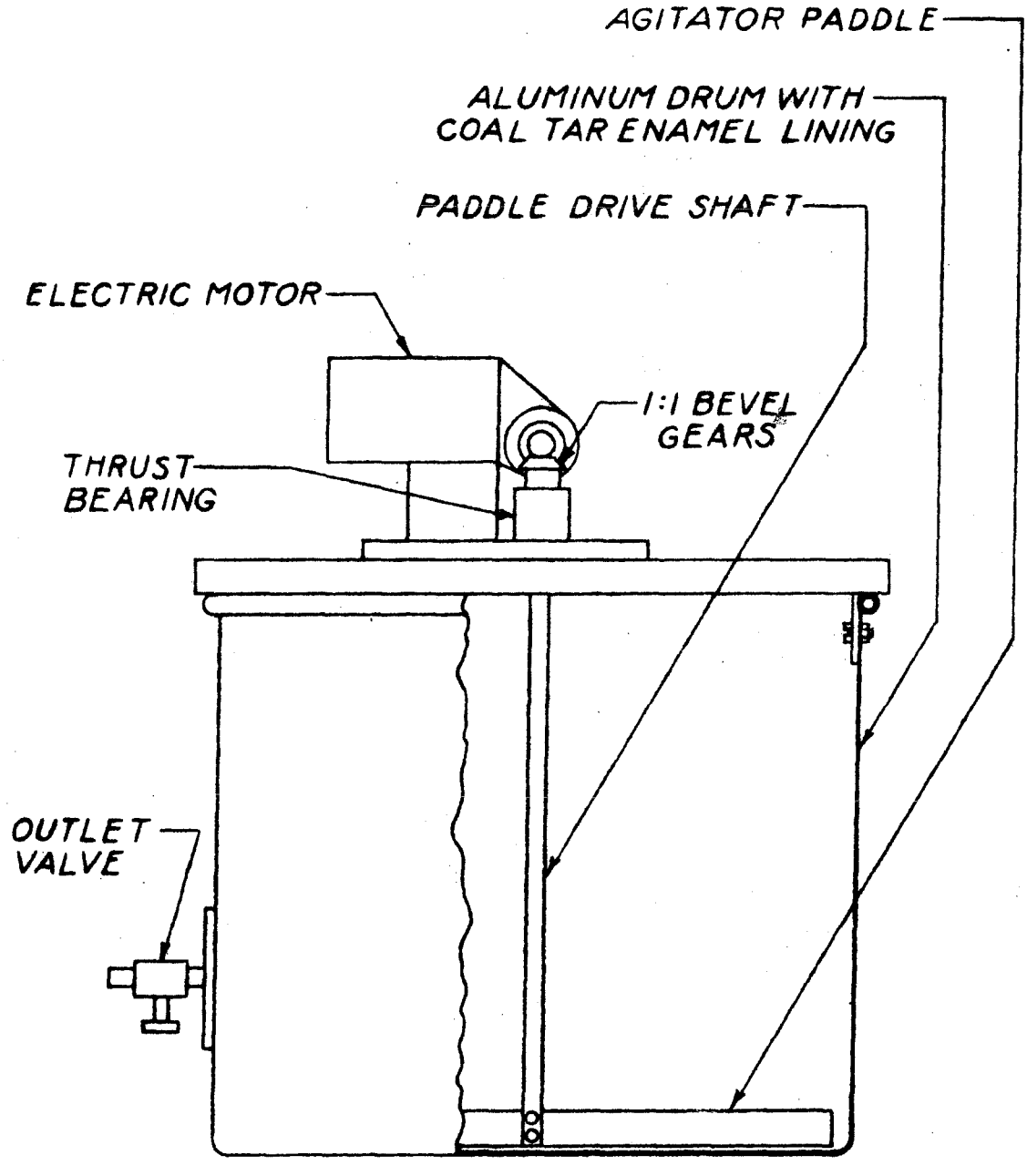

FIG. 2-5
SLURRY AGITATOR TANK

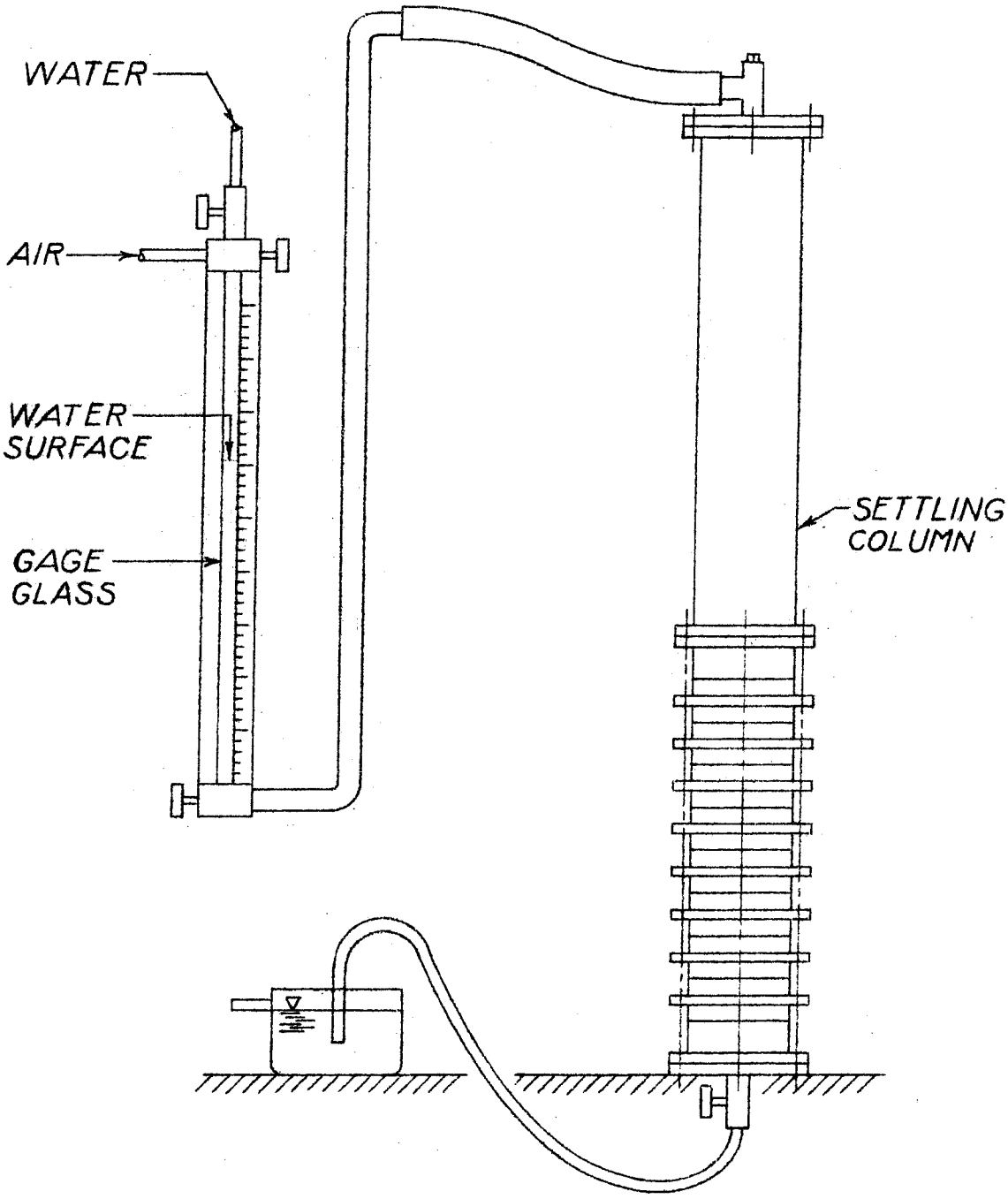

FIG. 2-6
COLUMN PRESSURE GRADIENT APPARATUS

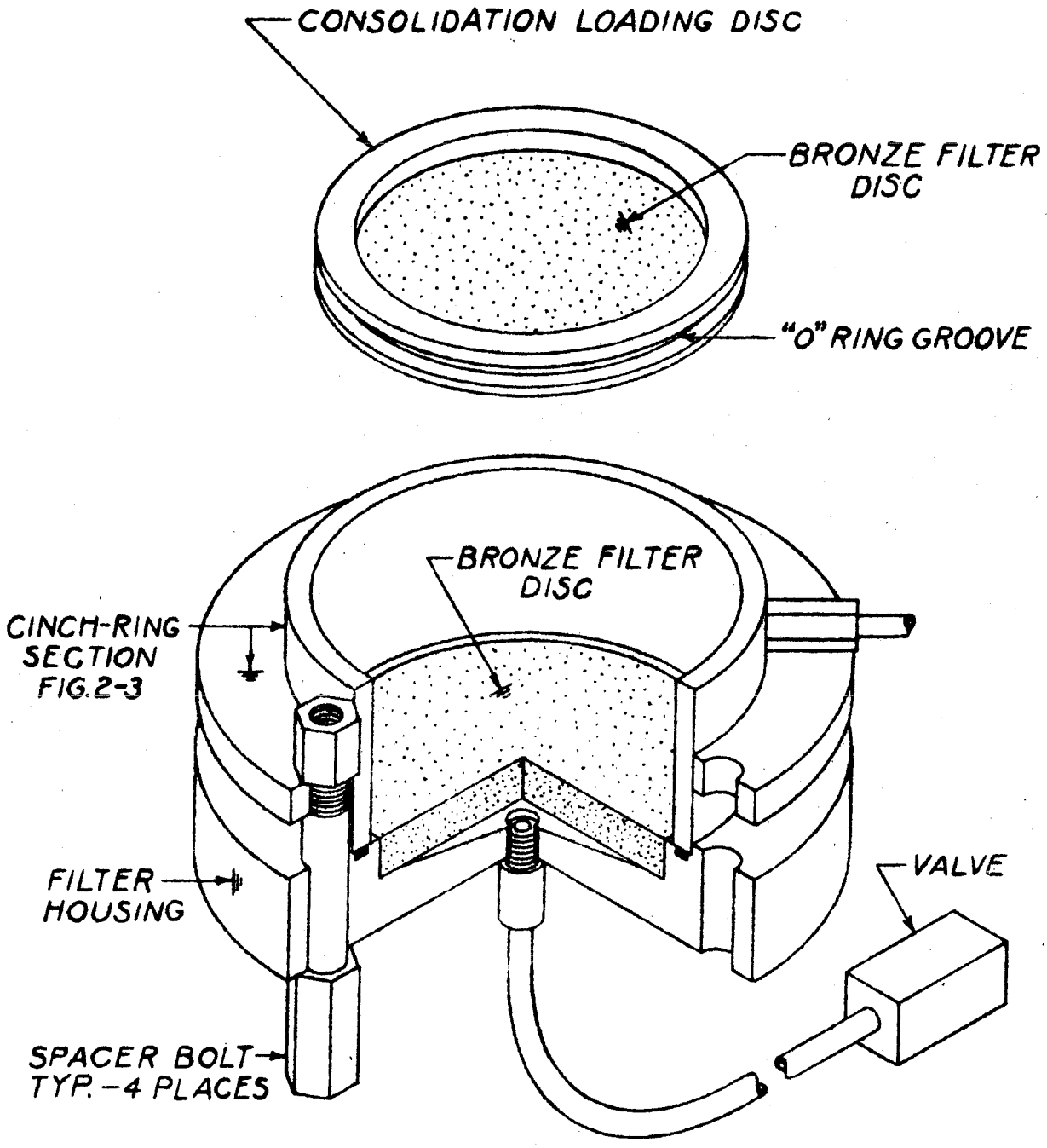

FIG. 2-7
CINCH-RING SECTION-FILTER HOUSING ASSEMBLY AND CONSOLIDATION LOADING DISC

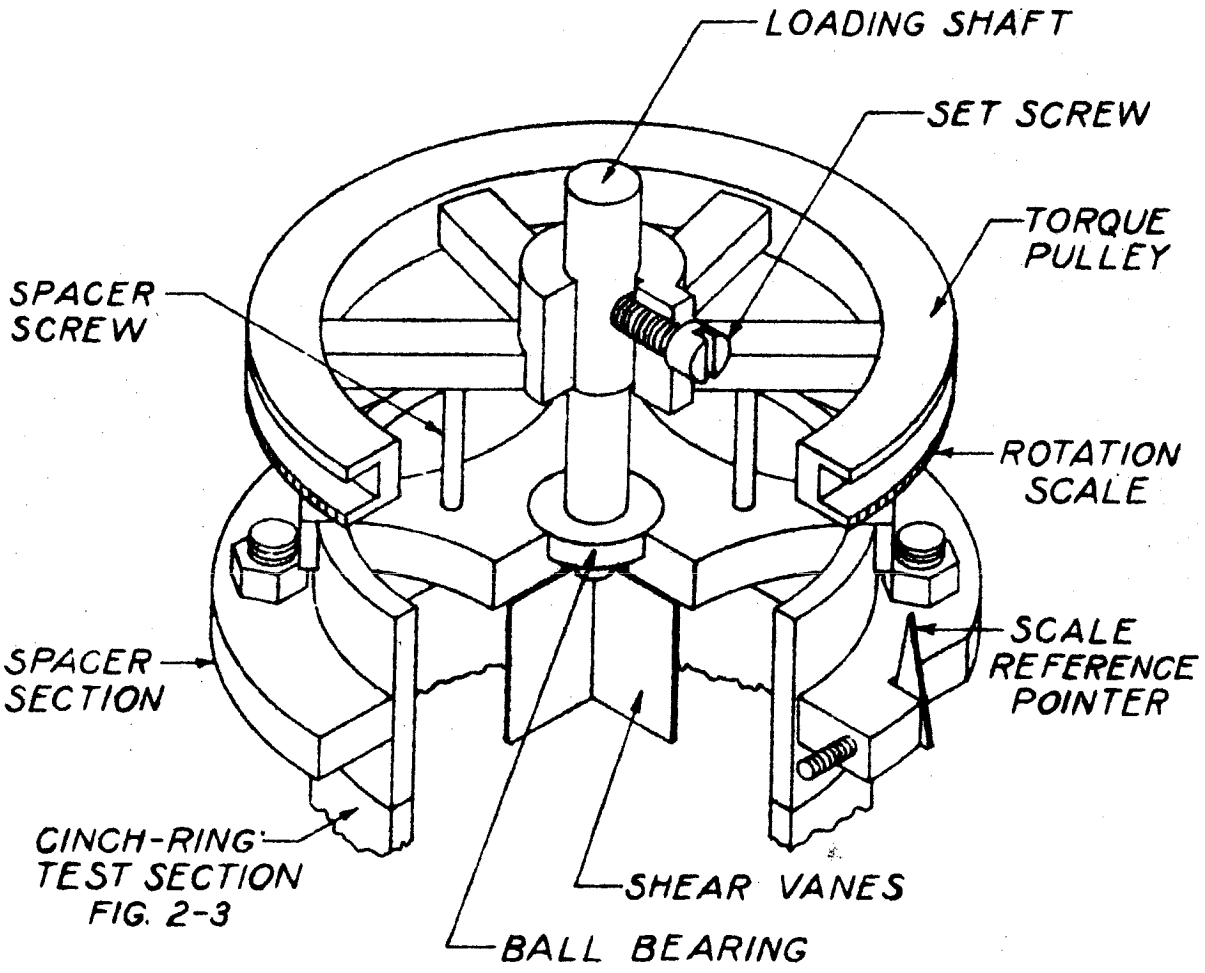

FIG. 2-8
VANE SHEAR TEST APPARATUS

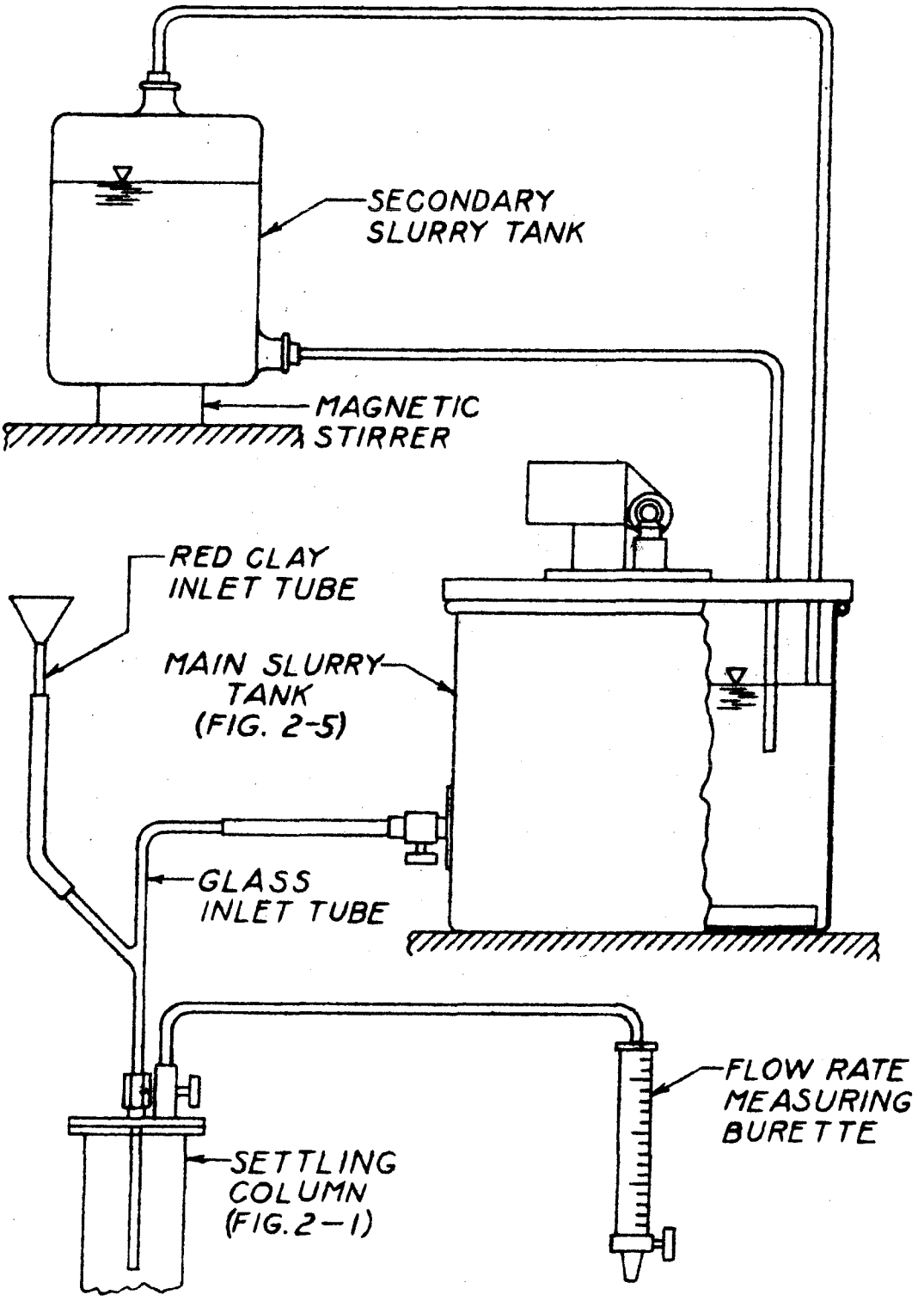

FIG. 2-9
DOUBLE SLURRY TANK SYSTEM

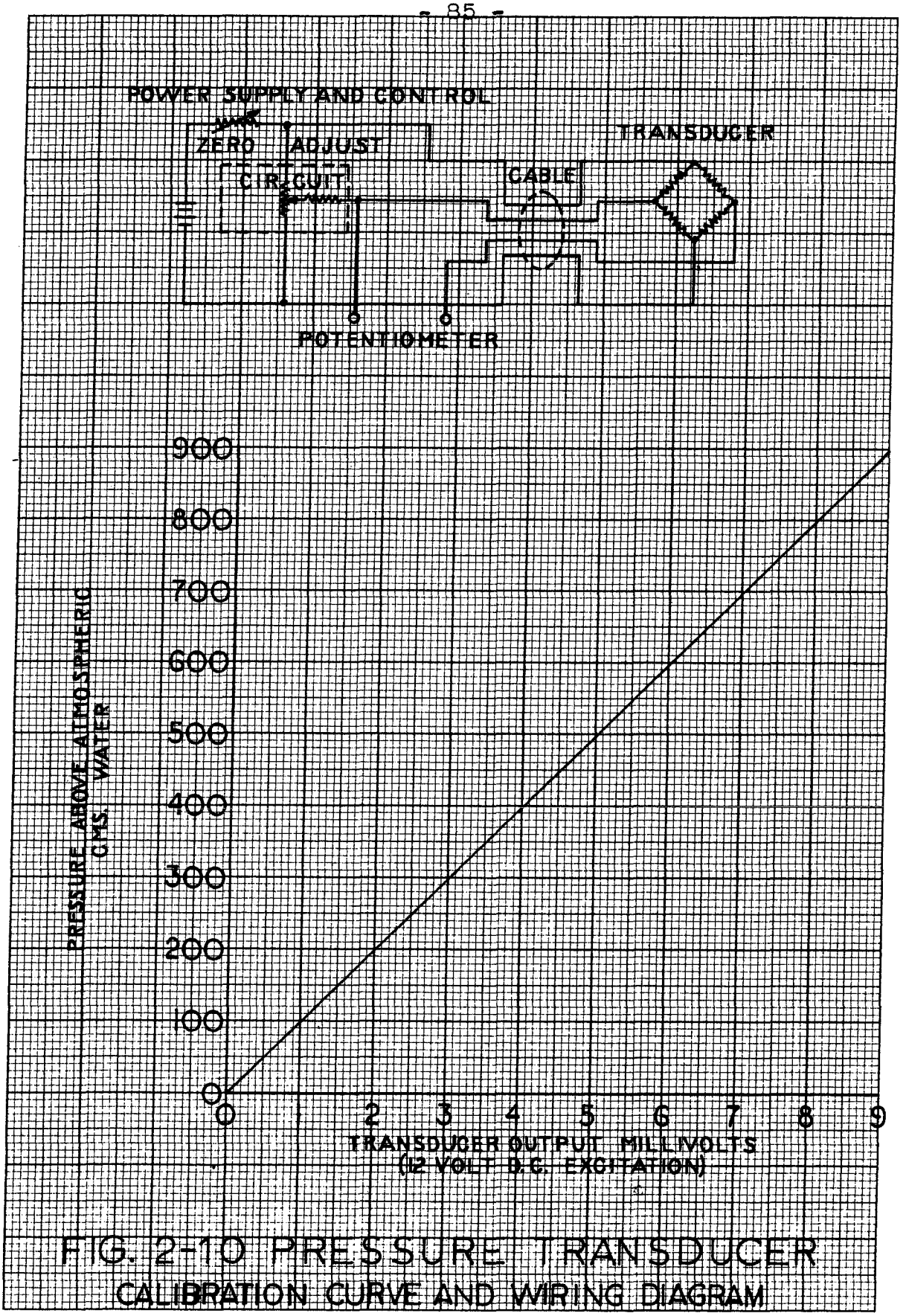

FIG. 2-10 PRESSURE TRANSDUCER
CALIBRATION CURVE AND WIRING DIAGRAM

CHAPTER III

EXPERIMENTS ON PROPERTIES OF SEDIMENTED CLAYS

A. INTRODUCTION

Three experiments with a montmorillonite clay and two with a kaolinite clay are reported in this chapter. Prior to these five, three preliminary experiments were performed with the montmorillonite. These preliminary runs provided general information on what to expect in future runs and brought to light a number of apparatus deficiencies which were corrected to bring the apparatus to the condition described in Chapter II.

For one of the montmorillonite experiments, original data and the various calculations and corrections are recorded in detail to clearly indicate the methods. For the other experiments only data and final results are given.

No record of temperatures was made during the experiments. However, the location of the apparatus was such that the temperature probably did not vary more than $\pm$ 5° F during any one experiment. The effects of this variation are not considered serious.

B. EXPERIMENTS WITH MONTMORILLONITE CLAY

1. Description of Clay.

The montmorillonite used in these experiments was

obtained commercially from the American Colloid Company, Skokie, Illinois. The company quarries the clay from a Wyoming deposit and markets it under the trade name "Volclay No. 200." The following analysis was obtained from the supplier:

Composition

90% Montmorillonite

10% A mixture of a variety of other inorganic minerals, including gypsum, feldspars, micas, etc.

Base exchange capacity (complete sample) 80 - 85 milliequivalents per 100 grams of sample of which

60 milliequivalents is Na ion
20 milliequivalents is Ca ion
15 milliequivalents is Mg ion
1 milliequivalent is K ion

The supplier states further that the deposit from which this clay is obtained is quite uniform and that repeated analyses give results which vary only a few per cent either way from the above figures.

2. Clay bed formation and consolidation in Settling Column.

Some general features of the three experiments are shown in table 1.

Table 1

	Experiment 1	2	3
Slurry agitator system	Single tank	Double tank	Single tank
Initial slurry concentration			
Clay, gms/liter	10.42	10.50	6.83
Salt, gms/liter	1.79	1.80	1.10
Average slurry feed rate, Cm^3/min.	3.90	3.86	3.07
Average clay feed rate, grams clay/min.	.0406	.0405	.0210
Total weight of clay in bed	371.2	412.4	227.2

Experiments 1 and 2 were performed in nearly identical ways, both to check reproducibility and because this particular feed rate produced some interesting results which are analyzed in Chapter IV.

a. Experiment 1

For this experiment all data and computations are recorded in detail.

The total volume of slurry fed into the column is computed in two ways: 1. Summing increments as computed from measured flow rates and, 2. Agitator tank measurements

corrected for evaporation. Table 2 gives the results from the first process.

The second method of computing total slurry input is as follows: At the conclusion of slurry input, the slurry surface in the tank was 4.3 cm. below the starting level, of which, from the evaporation pan record shown in figure 3-1, 1.1 cm. was due to evaporation. Thirty liters of slurry were added during the input period.

Slurry tank cross-sectional area = 1490 cm^2

Total volume of slurry = (4.3 - 1.1) (1.490) + 30

= 34.77 liters

Thus, the total volume of slurry is between 34.77 and 35.35 liters. Weighting the adjusted total somewhat towards the figure obtained from tank measurements, the total slurry volume is taken as 35.0 liters.

Slurry Concentration and Clay Input Calculations

Since the single slurry tank system was used in this experiment, equation 2:5 is the appropriate formula for computing slurry concentration. The measured evaporation rate is 1.1 cm. in 9150 minutes, from which a slurry volume of 34.77 liters was computed. The adjusted volume of 35.0 liters requires an adjustment to the evaporation rate.

$$v = \frac{1.1 - \frac{35.0 - 34.77}{1.48}}{9150} = 1.04 \times 1.0^{-4} \text{ cm/min}$$

q = average outflow rate

$$q = \frac{35000}{9150} = 3.82 \text{ cm}^3/\text{min}$$

Then the exponent in equation 2:5 is

$$\frac{1}{1 + \frac{q}{Av}} = \frac{1}{1 + \frac{3.82}{(1.48)(1.04)(10^{-1})}}$$

$$= .037,$$

and equation 2:5 becomes

$$C = Co \left[\frac{Ho}{Ho - (2.68)(10^{-3})} \right]^{.037}$$

The calculations are shown in table 3, and a plot of slurry concentration vs. time is shown in figure 3-2.

From figure 3-2, concentration is read for each time increment in the flow record of table 1 and the weight of clay in the bed is computed for each time increment as shown in table 4. The individual flow rates are adjusted from the values in table 1 to conform to the total slurry flow figure of 35.0 liters.

Figure 3-3 is a plot of depth of bed and grams of clay in the bed vs. time. The rate of clay input is seen to be essentially constant. At this particular feed rate, the bed surface rose linearly with time after a short initial period during which the rate of surface rise was increasing. Figure 3-4 shows the location of the red marker lines during the period of bed formation. Varying degrees of success were attained in installing the marker lines, some being much smoother than others. However, the marker lines retained their initial configuration as they moved down the column, so that it was possible to accurately trace the history of rough lines by referencing the same spot on the line to the column scale for all readings.

Consolidation of Clay Under Its Own Weight

After slurry input was stopped, the clay was allowed to consolidate under its own weight until it reached equilibrium. Figure 3-5 shows the location of bed surface and marker lines during this period. The curve for the bed surface indicates that some very slow movement was still occurring when this portion of the test was terminated. However, the curve indicates the bed was nearly at equilibrium.

Recalling the consolidation equation development in Chapter I and anticipating the discussion of Chapter IV, the equilibrium location of the red lines will be used to

determine a $\overline{\sigma}$ - C relationship.

Although the average concentration of the clay between pairs of red lines may be calculated from the known weight of clay in each section, the levels at which these average concentrations should be plotted to form a concentration profile is open to question. However, any assumed concentration profile may be checked directly against the location of the surface and marker lines.

In Chapter IV, a $\overline{\sigma}$ - C relation is used which satisfies the equation

$$\frac{dC}{d\bar{\sigma}} = a = \text{a constant.} \qquad (3:1)$$

At equilibrium, $\overline{\sigma}$ must satisfy the following relation:

$$\frac{d\bar{\sigma}}{dz} = -\gamma C$$

Combining the above two equations gives

$$\frac{dC}{dz} = -a\gamma C$$

from which

$$C = A\varepsilon^{-a\gamma z} \qquad (3:2)$$

where A is a constant of integration. The volume of clay particles per unit plan area up to the l'th marker line is

$$\int_0^{z_l} C\,dz = [C]_l \qquad (3:3)$$

where Z_1 is the level of the 1'th line. Combining equations 3:2 and 3:3 gives

$$\int_0^{Z_1} AE^{-a\gamma z} = [C]_1$$

or

$$\frac{A}{a\gamma} \quad 1 - E^{-a\gamma z_1} = [C]_1 \qquad (3:4)$$

The quantities $[C]_1$ are known from the data. Thus, the problem is to see if two constants, a and A, can be found to satisfy equation 3:4 for all 1. If this can be done, equation 3:2 is confirmed as the correct equation for the equilibrium concentration profile. If equation 3:3 is written for any two lines, say the 1'th and the m'th lines, and a ratio formed, then one equation in "a" results:

$$\frac{1 - E^{-a\gamma z_1}}{1 - E^{-a\gamma z_m}} = \frac{[C]_1}{[C]_m} \qquad (3:5)$$

The only unknown in equation 3:5 is "a." If equation 3:5 is formed for all possible pairs of lines, the same value of "a" should be obtained each time, if equation 3:2 is correct. This procedure gives a good fit for the values,

$$a = .0083$$

$$A = .032$$

The dry clay data show γ to have the value 1.64. Insertion of these numerical values in equation 3:2 gives the

concentration profile

$$C = 0.032\,\varepsilon^{-0.0136\,z} \qquad (3:6)$$

Returning now, to equation 3:4 and using the known $[C]_1$ values and the constants found above, the various Z_1 values are computed and shown in figure 3-5 for comparison with the observed values. The agreement is seen to be quite good, confirming equation 3:6 to be a fair representation of the concentration profile.

Using equation 3:6, the C - $\overline{\sigma}$ relation may be derived from equation 3:1 as follows: integrating 3:1 gives

$$C = a\overline{\sigma} + C_o \qquad (3:7)$$

where C_o is a constant of integration equal to C when $\overline{\sigma}$ is zero. The value of C_o may be obtained from equation 3:6, as C evaluated at the surface elevation.

$$C_o = .032\,\varepsilon^{-(.0136)(78.4)} = .011 \qquad (3:8)$$

Using this value of C_o and the value of "a" obtained above, equation 3:7 becomes

$$C = .0083\overline{\sigma} + .011 \qquad (3:9)$$

Consolidation of Clay By Pressure Gradient

An attempt was made to consolidate this bed under an hydraulic gradient. Figure 3-6 shows the location of the bed

surface and marker lines during this period. It will be noted that the lowest layer consolidated quickly to a concentration value of some 30 times the value at the beginning of this period, while the upper layers show only a small change. This was the expected behavior. However, after the lowest portion of the bed consolidated, it formed a barrier of very low permeability which greatly retarded consolidation of the upper portions of the bed. After a period of 22 days, there was still no detectable pressure drop at the lowest pore pressure tap, indicating the entire head drop through the bed occurred in the bottom 2 or 3 centimeters. It was obvious that development of an equilibrium state with this clay under these conditions would require a total elapsed time of many months, and thus the experiment was terminated.

b. Experiment 2

The clay bed was formed under essentially identical conditions as in experiment 1. Original data and adjustments are presented in Table 5. Corresponding curves are shown in figures 3-7 through 3-11.

No attempt was made to consolidate this bed under an hydraulic gradient.

It will be noted that all results agree with those of experiment 1.

c. Experiment 3

In this experiment, a bed of clay was formed under different conditions from those used for experiments 1 and 2. Original data and adjustments are presented in Table 6. Curves as with experiments 1 and 2, above, are plotted in figures 3-12 through 3-16.

During the process of bed formation, the average concentration was at first lower and later higher than this average in experiments 1 and 2. These differences persist in the equilibrium concentration profile after the bed settled under its own weight. No equation of the form of equation 3:6 will agree with the marker line locations.

The variations between experiments 1 and 2 and experiment 3 are discussed in Chapter IV.

Figure 3-14 shows that the rate of clay input was not held constant but was twice decreased. This would appear to be the cause of the bed surface actually falling for a short period during the bed formation period. Apparently, under these conditions, the consolidation effects in the bed tending to lower the surface were greater than the surface raising effects due to accretion of more clay.

3. Tests on column sections

a. Permeability Tests

The data and calculations for permeability tests are shown in table 7. Tests were run on sections from experiments 1 and 3. The results are plotted in figure 3-17. There is no apparent distinction in results between the two clay columns.

The curve $k = KE^2$, where $K = 4.5 \times 10^{-5}$, is sketched in to fit the pattern of points. There is a lot of scatter, much of which is probably due to the method of measurement. This is discussed in section D-1 of chapter II.

b. Consolidation Test

The bottom section of the bed formed in experiment 1 was used for a consolidation test. The results are shown in the form of the E-log $\overline{\sigma}$ curve of figure 3-18. The curve includes equation 3:9 (in terms of E) at the low end of the $\overline{\sigma}$ scale.

Of the several methods availabe for finding the coefficient of consolidation, c_v, from the time-displacement data of a consolidation test, the one recently suggested by Scott (3,1) has the distinct advantage, in this case, of proving that this consolidation test cannot be described by the Terzaghi equation. Ratios of displacements at various times are outside the domains of the appropriate curves in figure of reference 3,1. Since these curves apply to any one

dimensional consolidation test which behaves in accordance with the Terzaghi theory, then any test to which these curves do not apply must not conform to this theory.

c. Vane Shear Tests

Vane shear tests were conducted on column sections from experiments 1 and 3. The failure shear stress as computed from equation 2:23 is plotted against E in figure 3-19. From the surface appearance of the samples during the tests, the failures all took place along smooth cylindrical surfaces at the outer edges of the vanes.

C. EXPERIMENTS WITH KAOLINITE CLAY

1. Description of clay

The kaolin was obtained from the Braun Chemical Company, Los Angeles, California. It is labeled as "Kaolin-China Clay." No detailed information was available from the supplier. An x-ray diffraction pattern of a sample was obtained from facilities at Caltech. No lines other than those for kaolin could be detected on this pattern, indicating the clay to be at least 95% kaolin mineral.

2. Clay bed formation

Two experiments were performed under essentially identical conditions. The slurry concentrations were 20 grams of dry clay and 3 grams of salt per liter. The average slurry feed rate was about 9.0 cm^3/min.

As noted in section D of chapter II, the pore-pressure taps through the walls of the cinch ring sections were installed for these experiments, and, during the experiments they were found to respond quickly to changes in water manometer levels and thus apparently were not plugged by clay. During the bed formation process, the manometer levels, with slight variations, all rose linearly with time, after being covered by the clay bed, as shown in figure 3-20. However, the behavior of the red marker lines makes it difficult to give these pressures any significance.

The marker lines formed nicely at the bed surface, but, as the clay moved down in the column, the lines were immediately erased at the column wall.

The red line behavior indicated that the clay was adhering to the column wall. This was confirmed when the columns were disassembled. The clay was removed from several column sections and sliced in half. The red lines were found to be distinct and clear in the interior, but near the edge, the lines curved sharply upward and disappeared.

One of the columns was allowed to stand for a period of 30 days under its own weight The list of dry weights of clay in each section, tabulated below, shows quite clearly that tests of this type in a lucite column are of doubtful significance with a kaolin clay.

Bottom elevation of column section, cm	Dry weight of clay in section, gms
0	278
5.1	248
10.1	252
15.1	260
20.2	267
25.3	261
30.4	248
35.5	252
40.5*	38

*Partial section; 1.0 cm of clay

3. Consolidation under hydraulic gradient

One column of kaolin was subjected to a total head difference of 775 cms of water. Figure 3-21 shows bed height vs. time during this period. The pore pressure taps continued to function well.

The equilibrium pore pressure profile is shown in figure 3-22.

The importance of the wall drag effect, under these conditions, is not known. The results are presented in figure 3-23 as plots of k and $\overline{\sigma}$, computed from the gradients and dry weights of column sections, as functions of E.

4. Vane shear tests

It will be noted from the above that the kaolin beds formed at much greater densities than the montmorillonite beds. This is the expected result. However, the density and strength of the kaolin beds were such that the shear strength could not be measured in the apparatus described in chapter II. Instead of failing along a cylindrical surface, cracks radiated out from the vane tips towards the lucite wall, while, at the same time, clay heaped up on the pressure sides of the vanes. These conditions are illustrated in figure 3-24. No attempt has been made to analyze the stress distribution leading to this sort of failure.

Table 2

MONTMORILLONITE RUN NO. 1 - SLURRY FLOW DATA

(1) Time (min.)	(2) Interval min.	(3) Slurry flow rate $Cm^3/min.$	(4) Average flow rate for interval $Cm^3/min.$	(5) Slurry volume for interval Cm^3	Notes
0		6.12			Start slurry input
	40		6.12	245	
40		6.12			Change flow rate
		3.74			
	130		3.74	486	
170		3.74			
	196		3.765	738	
366		3.79			
	134		3.78	506	
500		3.77			
	500		3.775	1890	
1000		3.78			
	320		3.785	1210	
1320		3.79			
	80		3.785	303	
1400		3.78			
	340		3.76	1280	
1740		3.74			

Table 2

(1) Time (min.)	(2) Interval min.	(3) Slurry flow rate $Cm^3/min.$	(4) Average flow rate for interval $Cm^3/min.$	(5) Slurry volume for interval Cm^3	Notes
	210		3.74	785	
		3.74			
1950		3.90			Change flow rate
	890		3.86	3435	
2840		3.82			
	70		3.83	268	
2910		3.84			
	350		3.815	1340	
3260		3.79			
	140		3.785	529	
3400		3.78			
	430		3.77	1620	
		3.76			
3830		3.97			Change flow rate
	430		3.97	1710	
4260		3.97			
	560		3.93	2200	
4820		3.89			
	530		3.86	2045	
5350		3.83			

Table 2

(1) Time (min.)	(2) Interval min.	(3) Slurry flow rate $Cm^3/min.$	(4) Average flow rate for interval $Cm^3/min.$	(5) Slurry volume for interval Cm^3	Notes
	400		3.81	1525	
5750		3.79			
	20		3.79	76	
		3.79			
5770		4.03			Change flow rate
	430		4.02	1730	
6200		4.01			
	100		4.02	402	
6300		4.03			
	570		3.99	2275	
6870		3.95			
	370		3.935	1460	
7240		3.92			
	460		3.39	1790	
7700		3.86			
	600		3.83	2300	
8300		3.80			
	375		3.785	1420	

Table 2

(1)	(2)	(3)	(4)	(5)	
Time (min.)	Interval min.	Slurry flow rate $Cm^3/min.$	Average flow rate for interval $Cm^3/min.$	Slurry volume for interval Cm^3	Notes
8675		3.77			
	475		3.745	1780	
9150		3.72		____	Stop slurry input

Total slurry input = 35.35 liters

Table 3

MONTMORILLONITE RUN NO. 1 - SLURRY CONCENTRATIONS

At $t = o$, $c_o = 10.42$, $H_o = 23.2$ cm

$$c = 10.42 \left[\frac{23.2}{23.2 - (2.68)(10^{-3})\, t} \right]^{.037}$$

t, min	c, gms/liter	volume in tank, liters
0	10.42	33.55
500	10.44	
1000	10.47	
1500	10.49	
1950	10.52	25.8

At $t =$ 1950 minutes, add 10 liters of slurry at $c = 10.42$ gms/liters, bringing c to:

$$c = \frac{(10.52)(26.1) + (10.42)(10)}{36.1} = 10.49$$

$$H = 24.8 \text{ cm}$$

$$c = 10.49 \left[\frac{24.8}{24.8 - (2.68)(10^{-3})\, t} \right]^{.037}$$

Table 3

t, min	c, gms/liter	volume in tank, liters
1950	10.49	36.1
2450	10.51	
2950	10.54	
3450	10.56	
3830	10.58	28.3

At t = 3830 add 10 liters of slurry at
c = 10.42 gms/liter, bringing
c to:

$$c = \frac{(28.3)(10.53) + (10)(10.42)}{38.3} = 10.54 \text{ gms/liter}$$

$$H = 26.5 \text{ cm}$$

$$c = 10.54 \left[\frac{26.5}{26.5 - (2.68)(10^{-3})\, t}\right]^{.037}$$

t, min	c, gms/liter	volume in tank, liters
3830	10.54	38.3
4330	10.56	
4830	10.58	
5330	10.60	
5770	10.63	30.6

Table 3

At t = 5770 add .10 liters of slurry at c = 10.42 gms/liter, bringing c to:

$$c = \frac{(30.6)(10.63) + (10)(10.42)}{40.6} = 10.58 \text{ gms/liter}$$

$$H = 28.1 \text{ cm}$$

$$c = 10.58 \left[\frac{28.1}{28.1 - (2.68)(10^{-3})\, t}\right]^{.037}$$

t, min	c, gms/liter	
5770	10.58	
6270	10.60	
6770	10.62	
7270	10.64	
7770	10.66	
8270	10.69	
8770	10.71	
9150	10.73	Stop slurry input

Table 4

MONTMORILLONITE RUN NO. 1 - CLAY INPUT CALCULATIONS

(1) Time (min.)	(2) Interval (min.)	(3) Average adj. slurry flow rate $cm^3/min.$	(4) Slurry input cm^3	(5) Conc. gms/liter (from figure 3-2)	(6) Grams of clay fed into column during interval	(7) Total weight of clay in column, grams
0						
	40	6.08	243	10.42	2.53	2.53
40						
	130	3.72	483	10.42	5.04	7.57
170						
	196	3.75	734	10.43	7.66	15.23
366						
	34	3.77	128	10.44	1.34	16.57
400						
	100	3.75	375	10.44	3.92	20.49
500						
	500	3.75	1876	10.46	19.62	40.11
1000						
	320	3.75	1200	10.48	12.58	52.69
1320						
	80	3.75	300	10.48	3.14	55.83
1400						
	340	3.74	1270	10.50	13.34	69.17
1740						
	210	3.72	782	10.51	8.22	77.39
1950						

Table 4

(1) Time (min.)	(2) Interval (min.)	(3) Average adj. slurry flow rate $cm^3/min.$	(4) Slurry input cm^3	(5) Conc. gms./liter (from figure 8-2)	(6) Grams of clay fed into column during interval	(7) Total weight of clay in column, grams
	20	3.88	78	10.49	0.81	78.20
1970						
	870	3.83	3335	10.51	35.05	113.25
2840						
	20	3.79	76	10.53	0.80	114.05
2860						
	50	3.79	190	10.54	2.01	116.06
2910						
	350	3.79	1320	10.54	14.00	130.06
3260						
	140	3.76	527	10.56	5.56	135.62
3400						
	430	3.74	1610	10.57	17.01	152.63
3830						
	430	3.94	1694	10.55	17.87	170.50
4260						
	30	3.94	118	10.56	1.25	171.75
4290						
	530	3.90	2069	10.57	21.86	193.61
4820						
	530	3.84	2035	10.59	21.55	215.16

Table 4

(1)	(2)	(3)	(4)	(5)	(6)	(7)
Time (min.)	Interval (min.)	Average adj.slurry flow rate $cm^3/min.$	Slurry input cm^3	Conc. gms/liter (from figure 3-2)	Grams of clay fed into column during interval	Total weight of clay in column, grams
5350						
	20	3.81	76	10.60	0.81	215.97
5370						
	380	3.79	1440	10.62	15.29	231.26
5750						
	20	3.77	75	10.63	0.80	232.06
5770						
	430	4.00	1720	10.59	18.21	250.27
6200						
	100	4.00	400	10.60	4.24	254.51
6300						
	570	3.96	2258	10.61	23.95	278.46
6870						
	370	3.91	1446	10.63	15.37	293.83
7240						
	330	3.88	1280	10.64	13.62	307.45
7570						
	130	3.85	500	10.65	5.33	312.78
7700						
	600	3.81	2285	10.68	24.41	337.79

Table 4

(1)	(2)	(3)	(4)	(5)	(6)	(7)
Time (min.)	Interval (min.)	Average adj. slurry flow rate $cm^3/min.$	Slurry input cm^3	Conc. gms/liter (from figure 3-2)	Grams of clay fed into column during interval	Total weight of clay in column, grams
8300						
	375	3.76	1410	10.70	15.09	352.28
8675						
	475	3.72	1767	10.72	18.94	371.22
9150						

Table 5

MONTMORILLONITE RUN NO. 2 - CLAY INPUT DATA

(1)	(2)	(3)	(4)	(5)	(6)	(7)	(8)
Time (min.)	Interval (min.)	Slurry Flow Rate $cm^3/min.$	Average Flow Rate $cm^3/min.$	Slurry quantity cm^3	Concentration gms/liter	Grams of Clay in Interval	Total weight of clay
0		6.12					
	50		6.12	310	10.0	3.10	
50		6.12 4.00					3.10
	190		3.98	760	10.01	7.61	
240		3.96					10.71
	270		3.95	1070	10.025	10.73	
510		3.94					21.44
	220		3.94	870	10.040	8.73	
730		3.94					30.17
	270		3.94	1060	10.055	10.66	
		3.94					
1000							40.83
		4.10					
	210		4.11	860	10.07	8.66	
1210		4.12					49.49
	420		4.14	1740	10.085	17.55	
1630		4.16 4.04					67.04
	180		4.06	730	10.10	7.37	
1810		4.08					74.41

Table 5

(1) Time (min.)	(2) Interval (min.)	(3) Slurry Flow Rate $cm^3/min.$	(4) Average Flow Rate $cm^3/min.$	(5) Slurry quantity cm^3	(6) Concentration gms/liter	(7) Grams of Clay in Interval	(8) Total weight of clay
	190		4.08	760	10.11	7.68	
		4.08					
2000							82.09
		4.00					
	280		3.99	1120	10.125	11.34	
2280		3.98					93.43
	220		3.99	880	10.135	8.92	
2500		4.00					102.35
	270		3.99	1080	10.145	10.96	
2770		3.98					113.31
	230		3.97	910	10.155	9.24	
3000		3.96					122.55
	240		3.96	950	10.165	9.66	
3240		3.96					132.21
	590		3.97	2340	10.18	23.82	
3830		3.98					156.03
	170		3.99	680	10.195	6.93	
4000		4.00					162.96
	620		3.99	2470	10.21	25.22	
4620		3.98					188.18
	220		3.97	870	10.225	8.90	

Table 5

(1)	(2)	(3)	(4)	(5)	(6)	(7)	(8)
Time (min.)	Interval (min.)	Slurry Flow Rate $cm^3/min.$	Average Flow Rate $cm^3/min.$	Slurry quantity cm^3	Concentration gms/liter	Grams of Clay in Interval	Total weight of clay
4840		3.96					197.08
	160		3.92	630	10.235	6.45	
5000		3.88 4.02					203.53
	300		4.02	1210	10.24	12.39	
5300		4.02					215.92
	320		3.99	1280	10.255	13.13	
5620		3.96					228.05
	170		3.95	670	10.26	6.27	
5790		3.94					235.92
	210		3.94	830	10.265	8.52	
6000		3.94					244.44
	420		3.92	1650	10.275	16.95	
6420		3.90					261.39
	220		3.885	860	10.285	8.85	
6640		3.87					270.24
	230		3.865	890	10.295	9.16	
6870		3.86					279.40
	130		3.83	500	10.30	5.15	
7000		3.80 3.94					284.55
	250		3.94	990	10.305	10.20	

Table 5

(1)	(2)	(3)	(4)	(5)	(6)	(7)	(8)
Time (min.)	Interval (min.)	Slurry Flow Rate $cm^3/min.$	Average Flow Rate cm^3/min	Slurry quantity cm^3	Concentration gms/liter	Grams of Clay in Interval	Total weight of clay
7250		3.94					294.75
	280		3.92	1100	10.31	11.34	
7530		3.90					306.09
	230		3.86	890	10.315	9.18	
7760		3.82					315.27
	340		3.77	910	10.320	9.39	
8000		3.72 3.90					324.66
	410		3.895	1600	10.33	16.53	
8410		3.89					341.19
	370		3.88	1440	10.39	14.89	
8780		3.87					356.08
	220		3.855	850	10.345	8.79	
9000		3.84					364.87
	150		3.84	580	10.345	6.00	
9150		3.84					370.87
	360		3.835	1380	10.35	14.28	
9510		3.83					385.15
	270		3.875	1030	10.355	10.67	
9780		3.82					395.82

Table 5

(1)	(2)	(3)	(4)	(5)	(6)	(7)	(8)
Time (min.)	Interval (min.)	Slurry Flow Rate $cm^3/min.$	Average Flow Rate cm^3/min	Slurry quantity cm^3	Concentration gms/liter	Grams of Clay in Interval	Total weight of clay
	220		3.82	840	10.355	8.70	
10000		3.82					404.52
	110		3.82	420	10.355	4.35	
10110		3.82					408.87
	90		3.82	340	10.36	3.52	
10200		3.82					412.39

Table 6

MONTMORILLONITE RUN NO. 3 - CLAY INPUT DATA

(1) Time (min)	(2) Interval (min)	(3) Average adj. slurry flow rate cm^3/min	(4) Slurry input cm^3/min	(5) Conc. gms/liter (from figure 3-14)	(6) Grams of clay fed into column during interval	(7) Total weight of clay in column, grams
0						
	23	12.20	280.6	6.83	1.916	1.92
23						
	215	4.63	995.4	6.835	6.804	8.72
238						
	512	3.99	2042.9	6.85	13.994	22.71
750						
	53	3.79	200.9	6.86	1.378	24.09
803						
	220	3.76	827.2	6.865	5.679	29.77
1023						
	455	3.75	1706.2	6.831	11.740	41.51
1478						
	50	3.75	187.5	6.892	1.292	42.80
1528						
	60	3.75	225.0	6.894	1.551	44.35
1588						
	50	3.74	187.0	6.897	1.290	45.64
1638						
	475	3.70	1757.5	6.912	12.148	57.79

Table 6

(1) Time (min.)	(2) Interval (min.)	(3) Average adj. slurry flow rate cm^3/min	(4) Slurry input $cm^3/min.$	(5) Conc. gms/liter (from figure 3-14)	(6) Grams of clay fed into column during interval	(7) Total weight of clay in column, grams
2113						
	195	3.68	717.6	6.932	4.974	62.77
2308						
	170	3.71	630.7	6.937	4.375	67.14
2478						
	170	3.71	630.7	6.951	4.384	71.52
2648						
	215	3.67	789.0	6.959	5.491	77.02
2863						
	45	3.79	170.6	6.964	1.188	78.20
2908						
	770	3.65	2810.5	6.989	19.643	97.85
3678						
	50	3.41	170.5	7.006	1.195	99.04
3728						
	220	3.40	748.0	7.008	5.242	104.28
3948						
	20	3.54	70.8	7.010	.496	104.78
3968						
	300	3.70	1110.0	6.967	7.733	112.51

Table 6

(1) Time (min)	(2) Interval (min)	(3) Average adj. slurry flow rate cm^3/min	(4) Slurry input cm^3/min	(5) Conc. gms/liter (from figure 3-14)	(6) Grams of clay fed into column during interval	(7) Total weight of clay in column, grams
4268						
	790	3.71	2930.9	6.982	20.464	132.98
5058						
	35	3.71	129.8	6.992	.908	133.88
5093						
	360	3.65	1317.0	7.000	9.219	143.10
5453						
	110	2.64	290.4	7.008	2.035	145.14
5563						
	235	2.61	613.4	7.015	4.303	149.44
5798						
	710	2.58	1831.8	7.033	12.883	162.32
6508						
	210	2.49	522.9	7.044	3.683	166.01
6718						
	80	2.49	199.2	7.050	1.404	167.41
6798						
	360	2.47	889.0	7.058	6.275	173.69
7158						

Table 6

(1) Time (min)	(2) Interval (min)	(3) Average adj. slurry flow rate cm^3/min	(4) Slurry input cm^3/min	(5) Conc. gms/liter (from figure 3-14)	(6) Grams of clay fed into column during interval	(7) Total weight of clay in column, grams
	120	2.46	295.2	7.069	2.087	175.77
7278						
	600	2.40	1438.0	7.085	10.188	185.96
7878						
	670	1.78	1192.6	7.114	8.484	194.45
8548						
	720	1.40	1008.0	7.148	7.205	201.65
9268						
	60	2.29	137.4	7.167	.985	202.64
9328						
	330	2.28	752.4	7.177	5.400	208.04
9658						
	360	2.26	811	7.194	5.834	213.87
10018						
	170	2.25	382.5	7.209	2.757	216.63
10188						
	660	2.20	1455.0	7.234	10.525	227.151
10848						

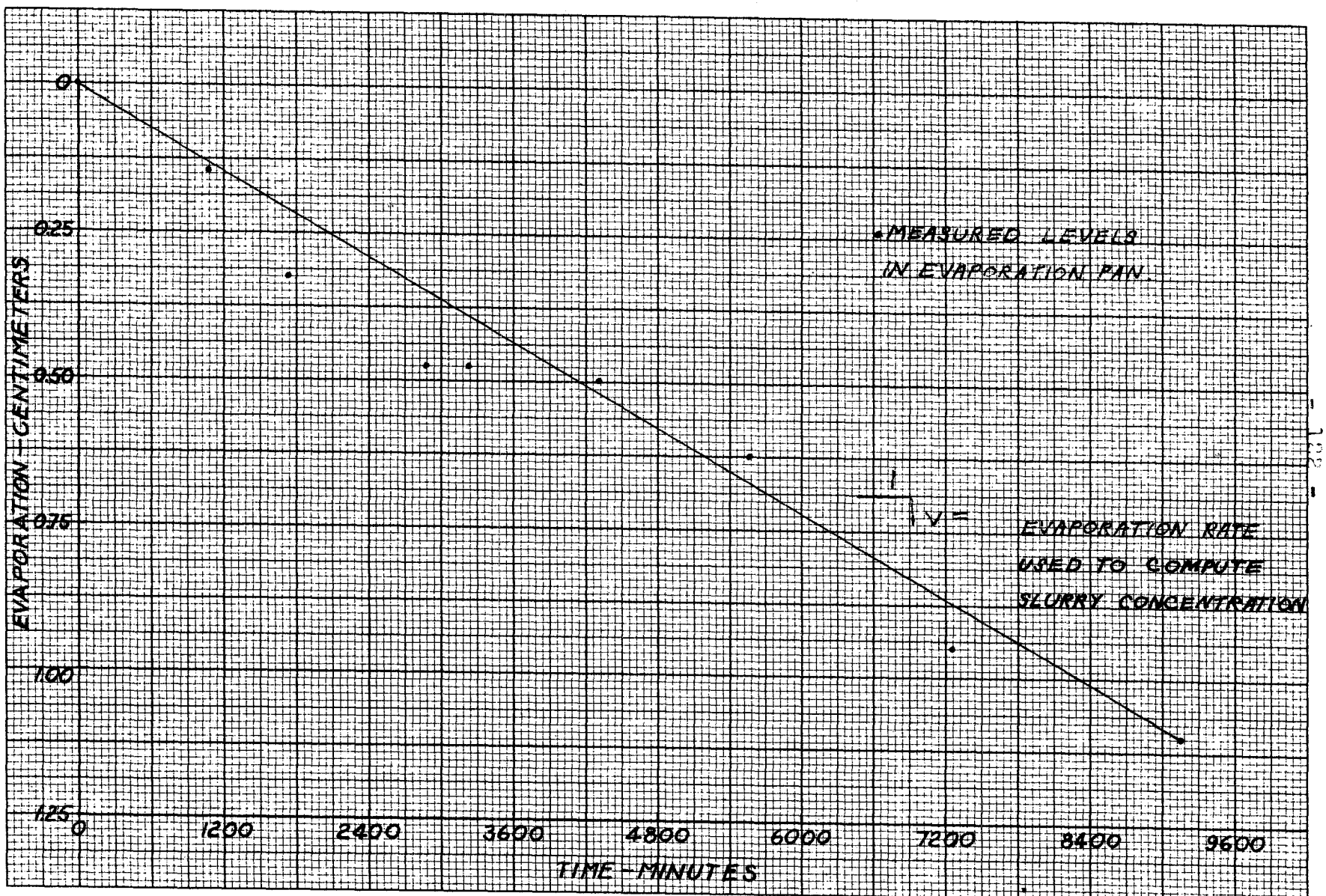

FIG. 3-1

EVAPORATION PAN RECORD - MONTMORILLONITE RUN NO. 1

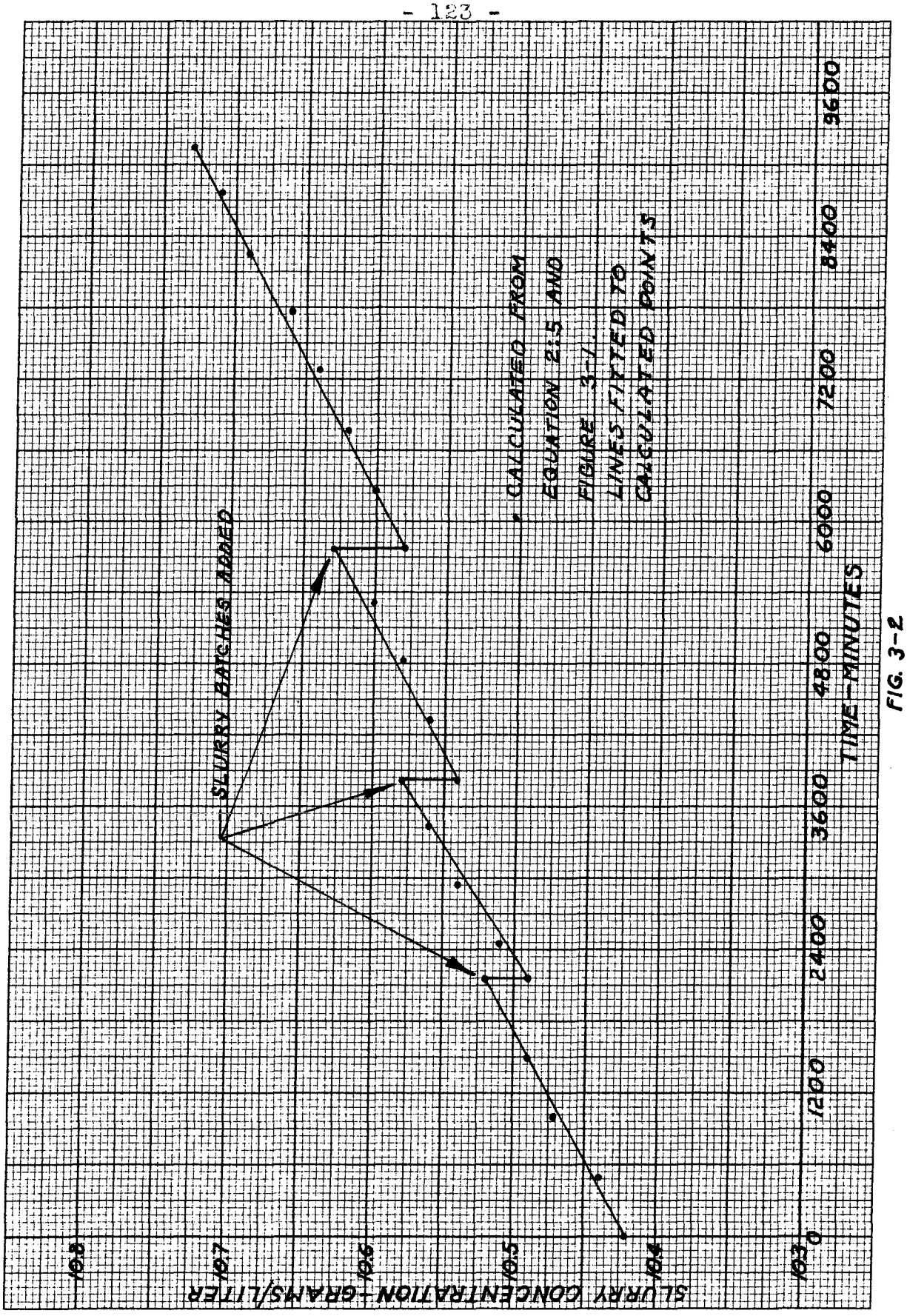

FIG. 3-2
AGITATOR TANK SLURRY CONCENTRATION - MONTMORILLONITE RUN NO. 1

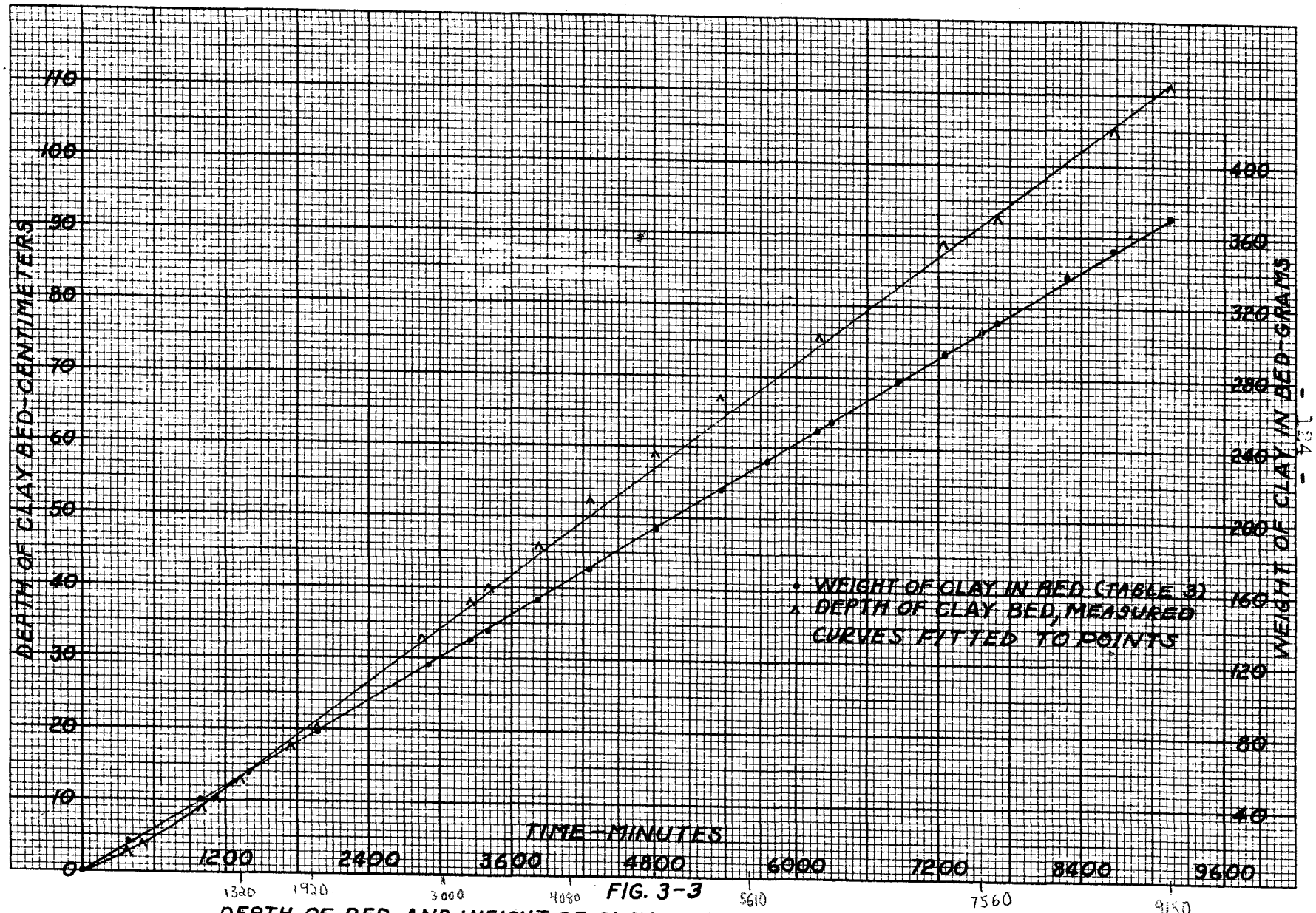

FIG. 3-3

DEPTH OF BED AND WEIGHT OF CLAY IN BED-MONTMORILLONITE RUN NO. 1

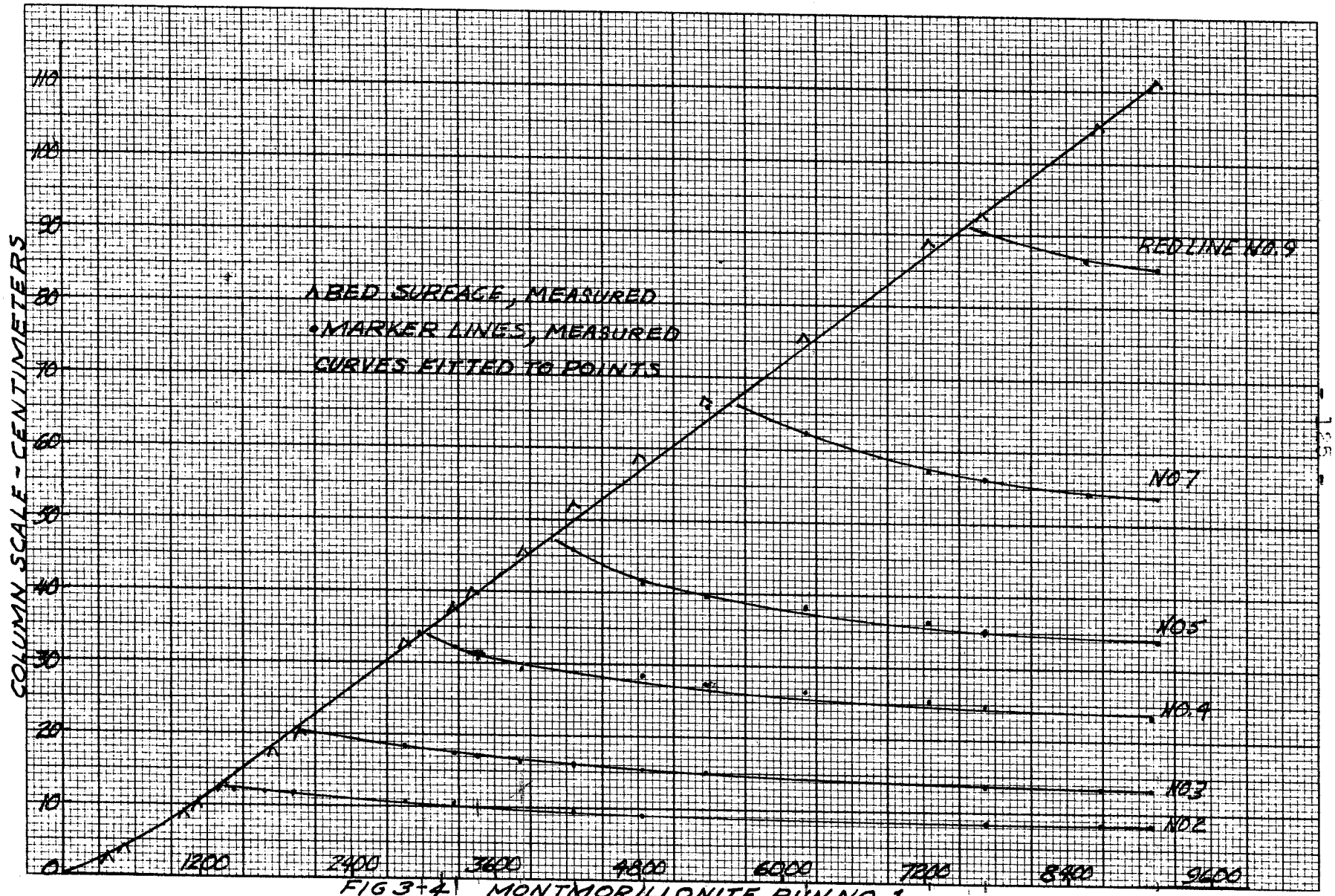

FIG 3+4 MONTMORILLONITE RUN NO. 1

ELEVATION OF BED SURFACE AND MARKER LINES vs. TIME

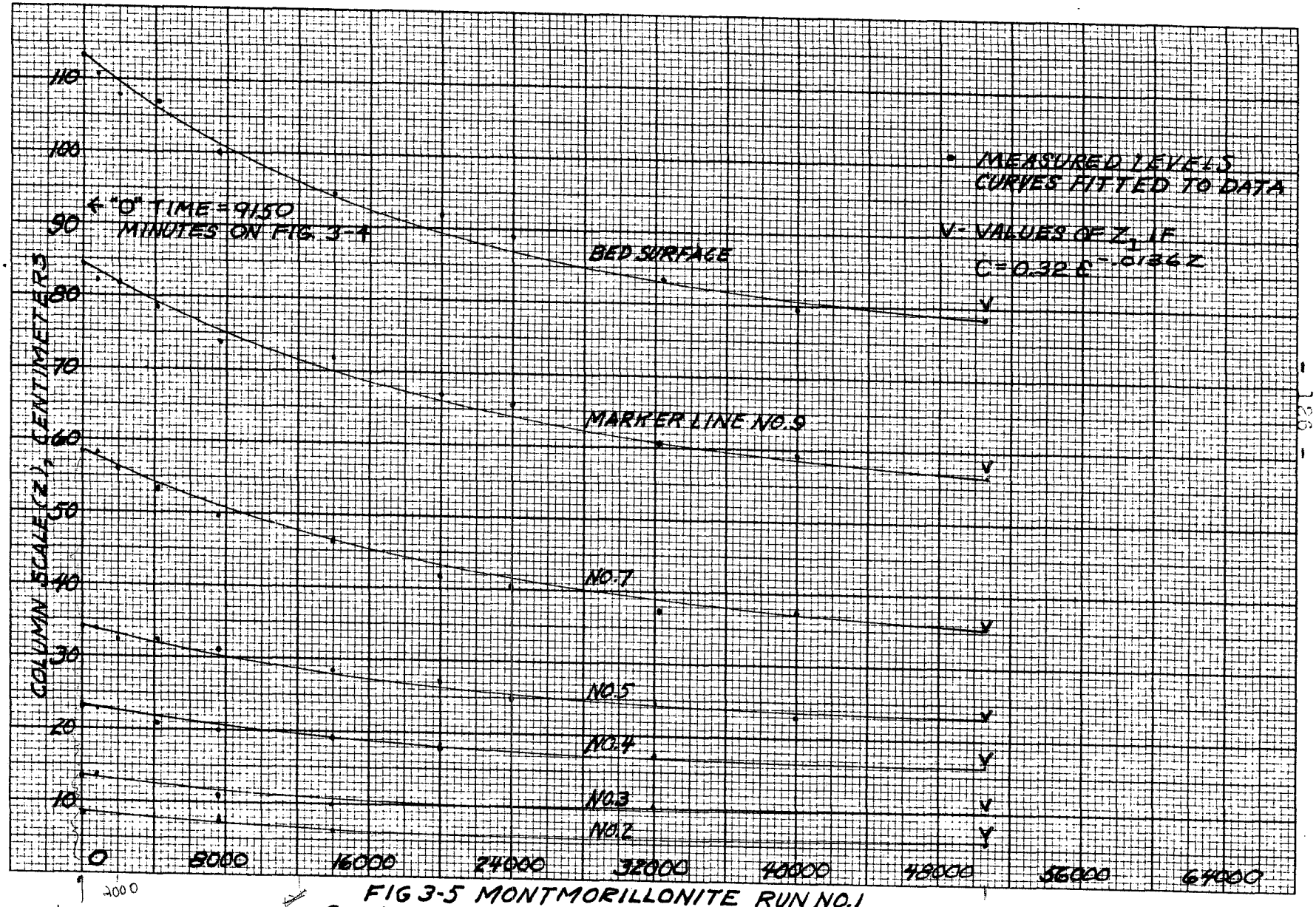

FIG 3-5 MONTMORILLONITE RUN NO. 1
CONSOLIDATION OF CLAY BED UNDER GRAVITY

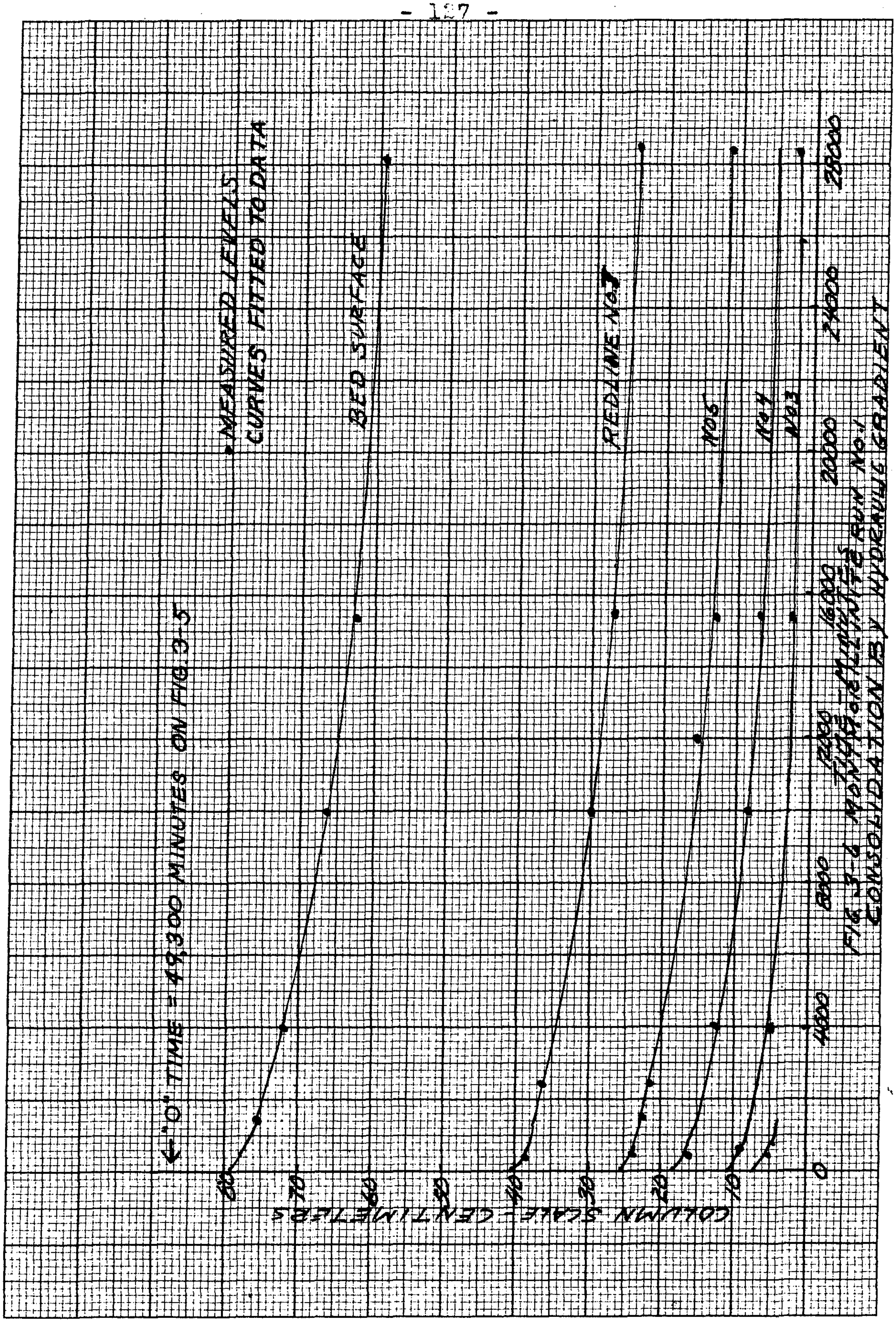

FIG. 3-6 MONTMORILLONITE RUN No.1
CONSOLIDATION BY HYDRAULIC GRADIENT

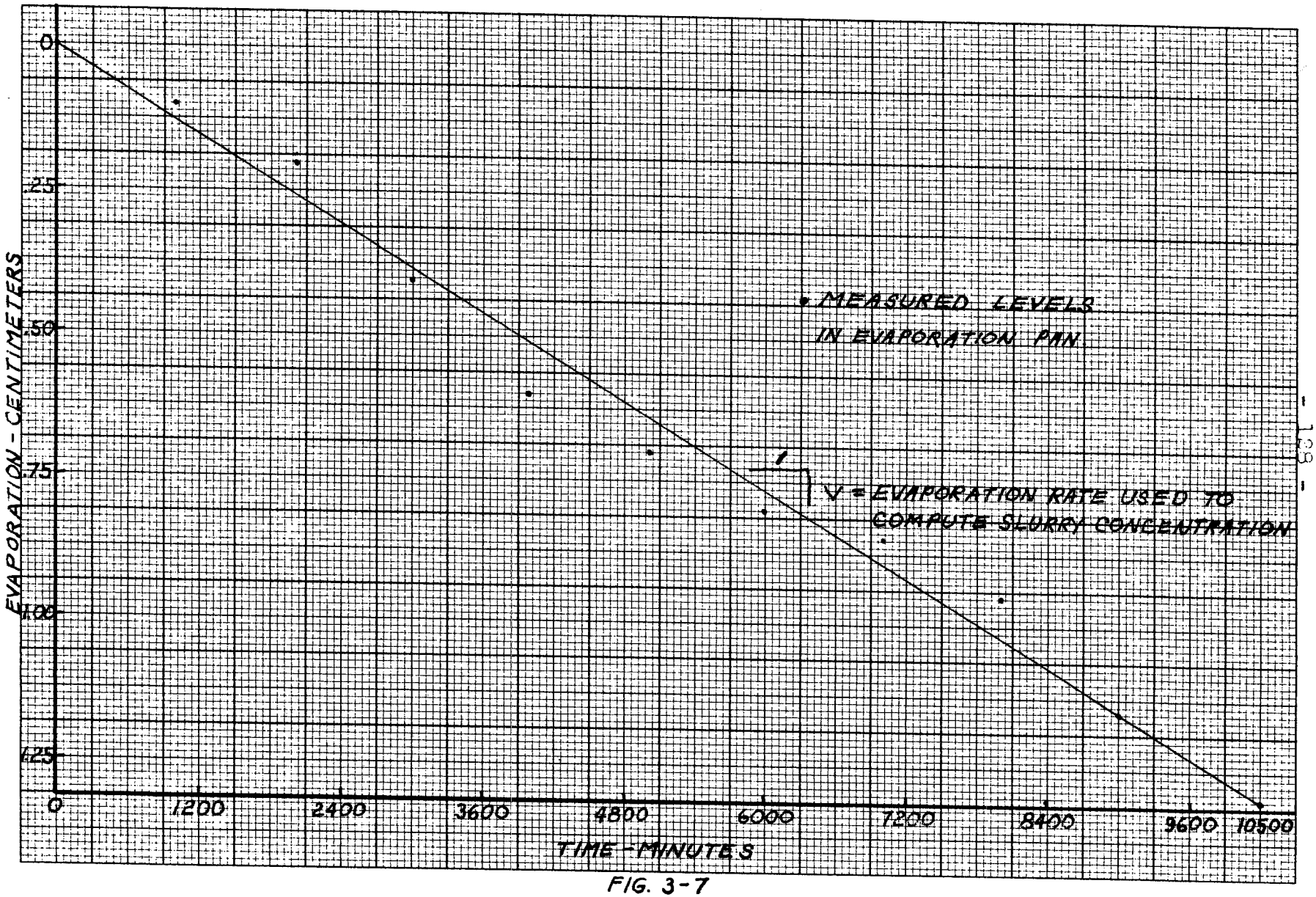

FIG. 3-7

EVAPORATION PAN RECORD - MONTMORILLONITE RUN NO. 2

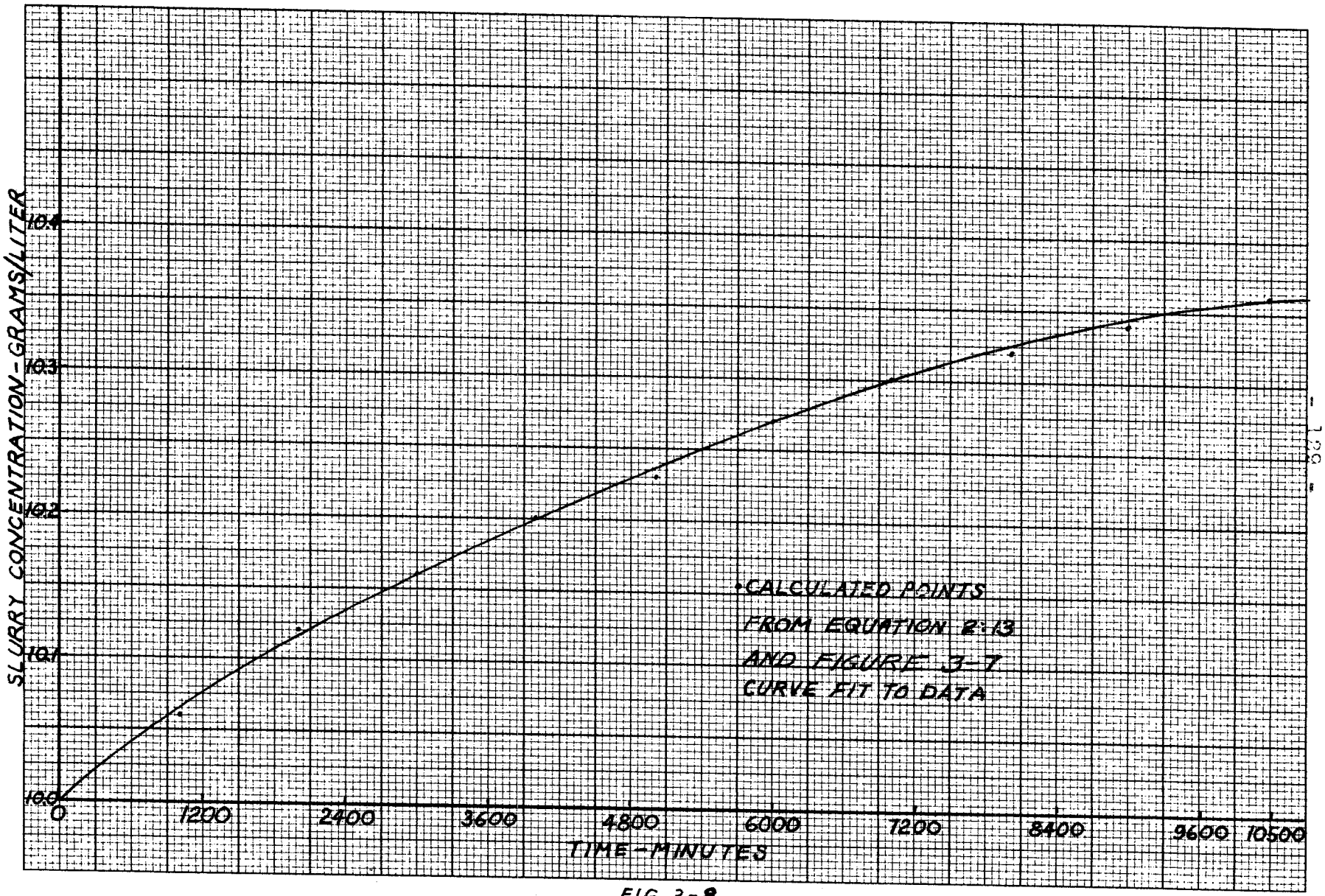

FIG. 3-8

AGITATOR TANK SLURRY CONCENTRATION - MONTMORILLONITE RUN NO. 2

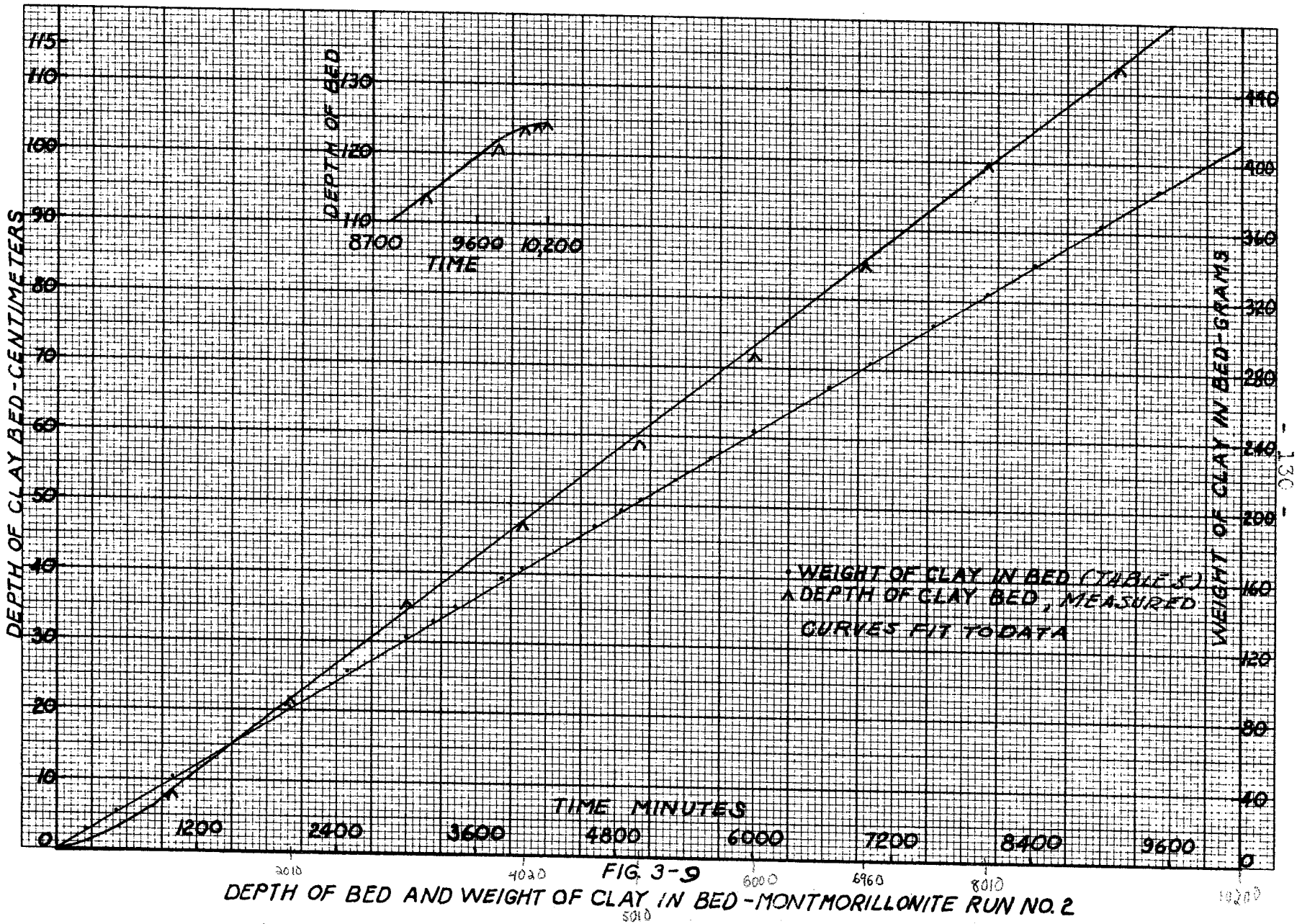

FIG. 3-9

DEPTH OF BED AND WEIGHT OF CLAY IN BED - MONTMORILLONITE RUN NO. 2

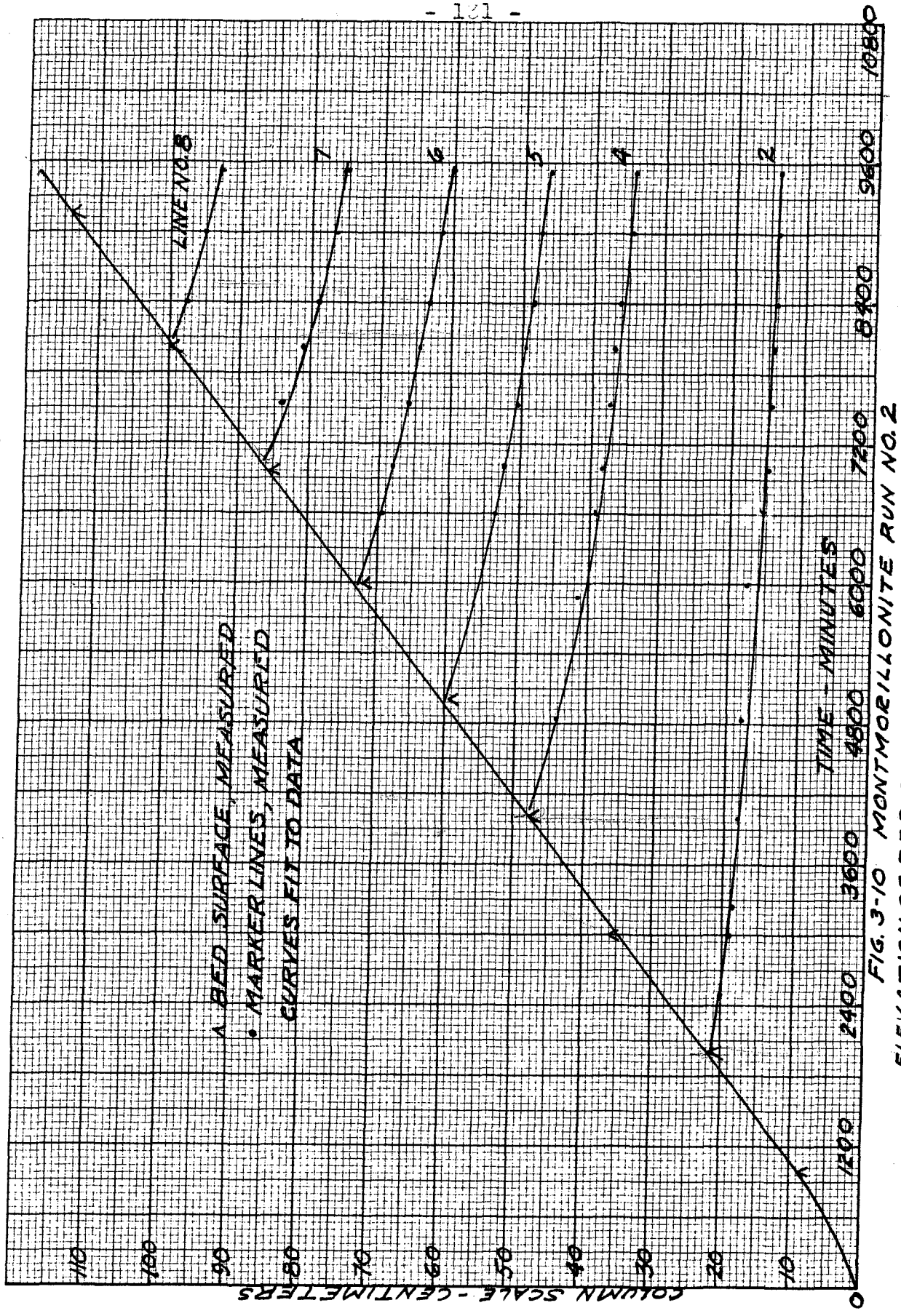

FIG. 3-10 MONTMORILLONITE RUN NO. 2
ELEVATION OF BED SURFACE AND MARKER LINES vs. TIME

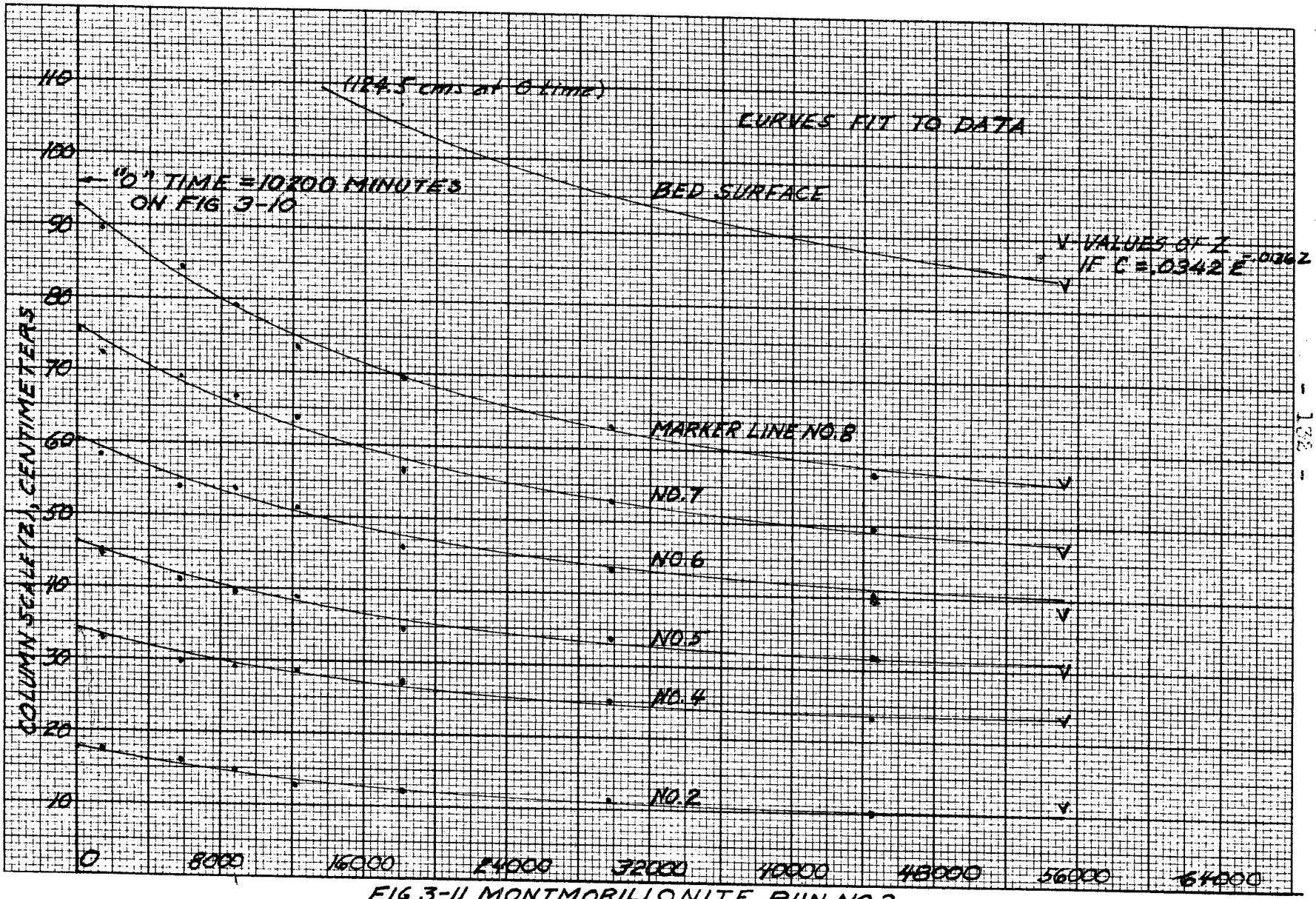

FIG 3-11 MONTMORILLONITE RUN NO.2
CONSOLIDATION OF CLAY BED UNDER GRAVITY

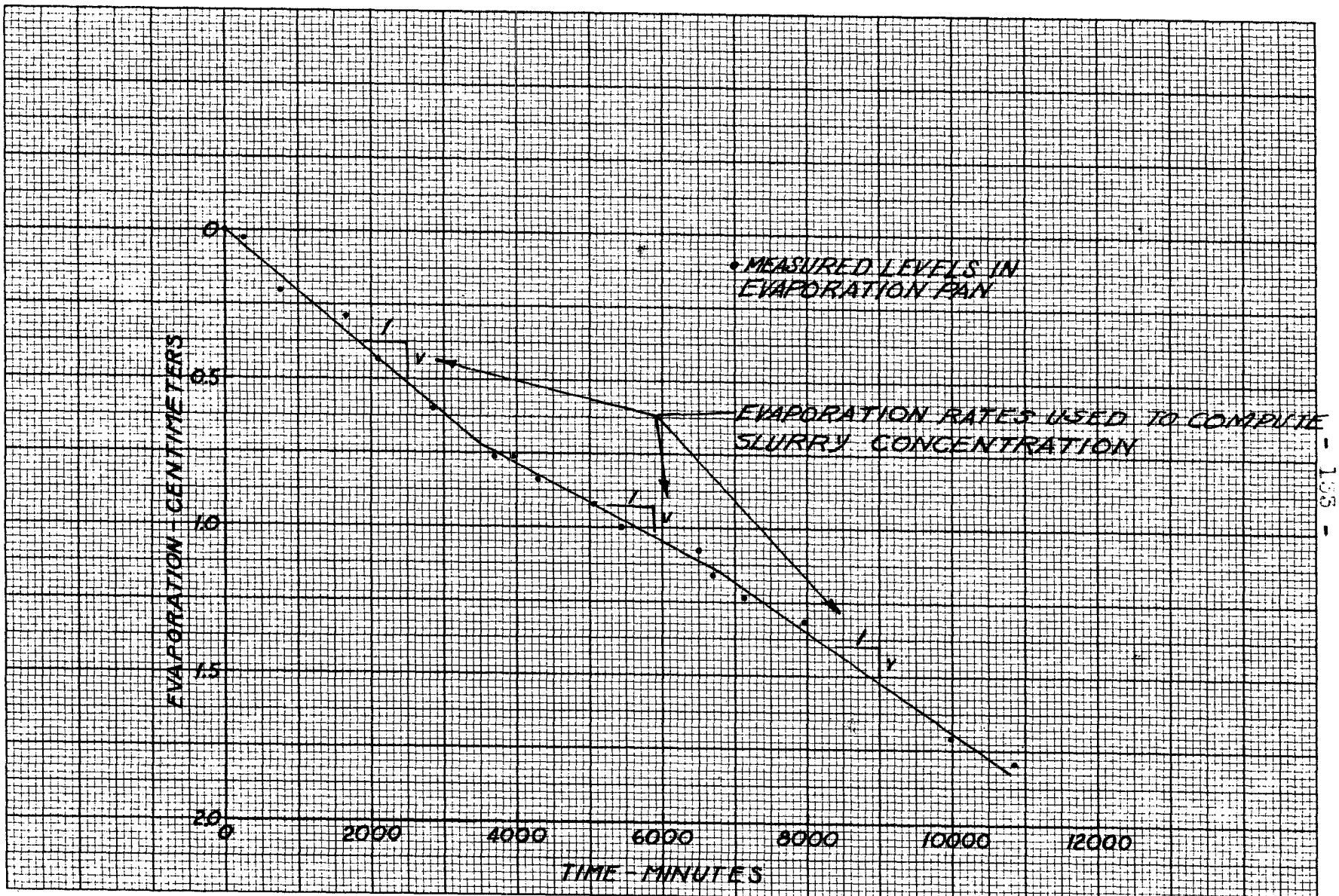

FIG. 3-12.

EVAPORATION PAN RECORD - MONTMORILLONITE RUN NO. 3

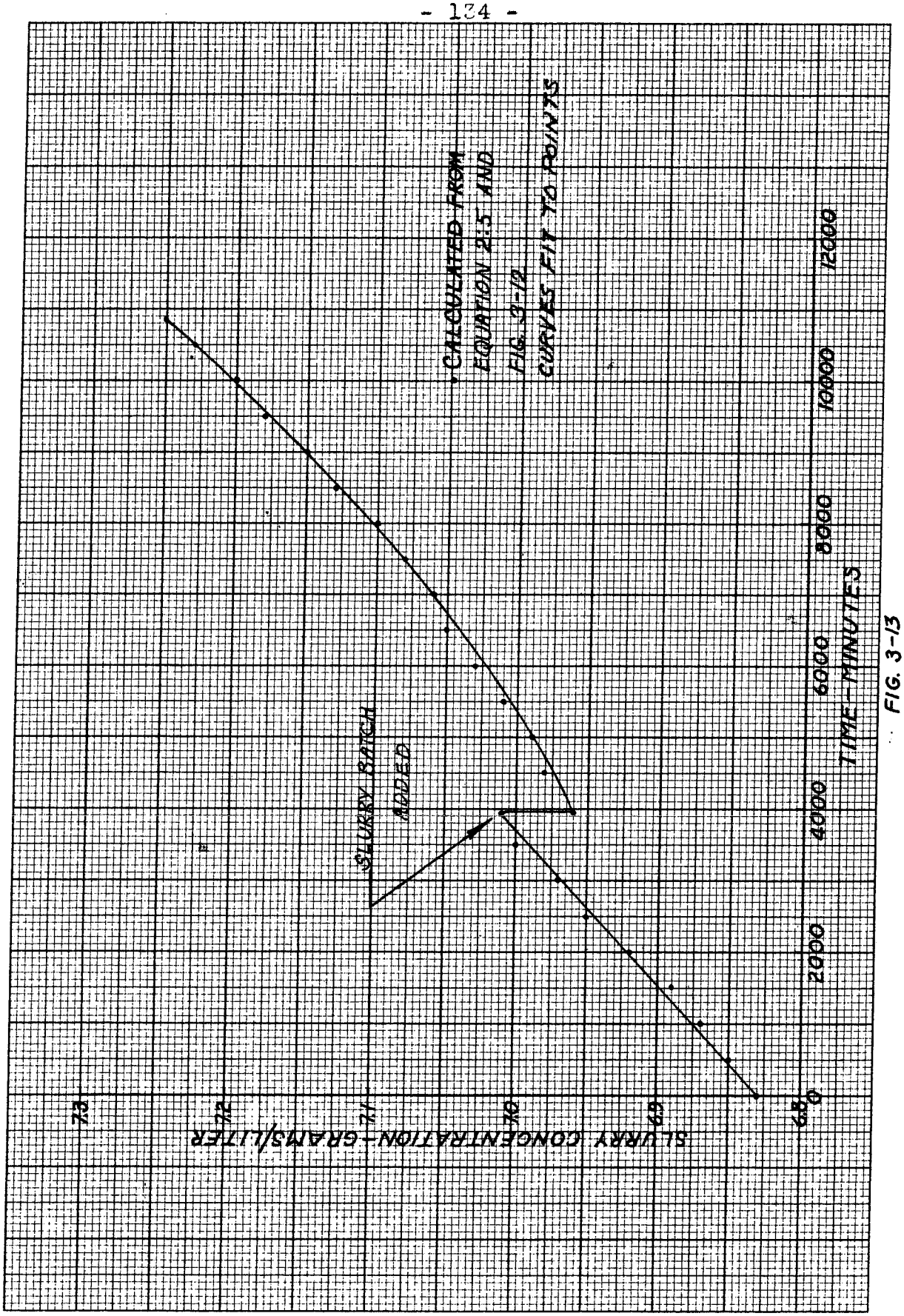

FIG. 3-13
AGITATOR TANK SLURRY CONCENTRATION - MONTMORILLONITE RUN NO. 3

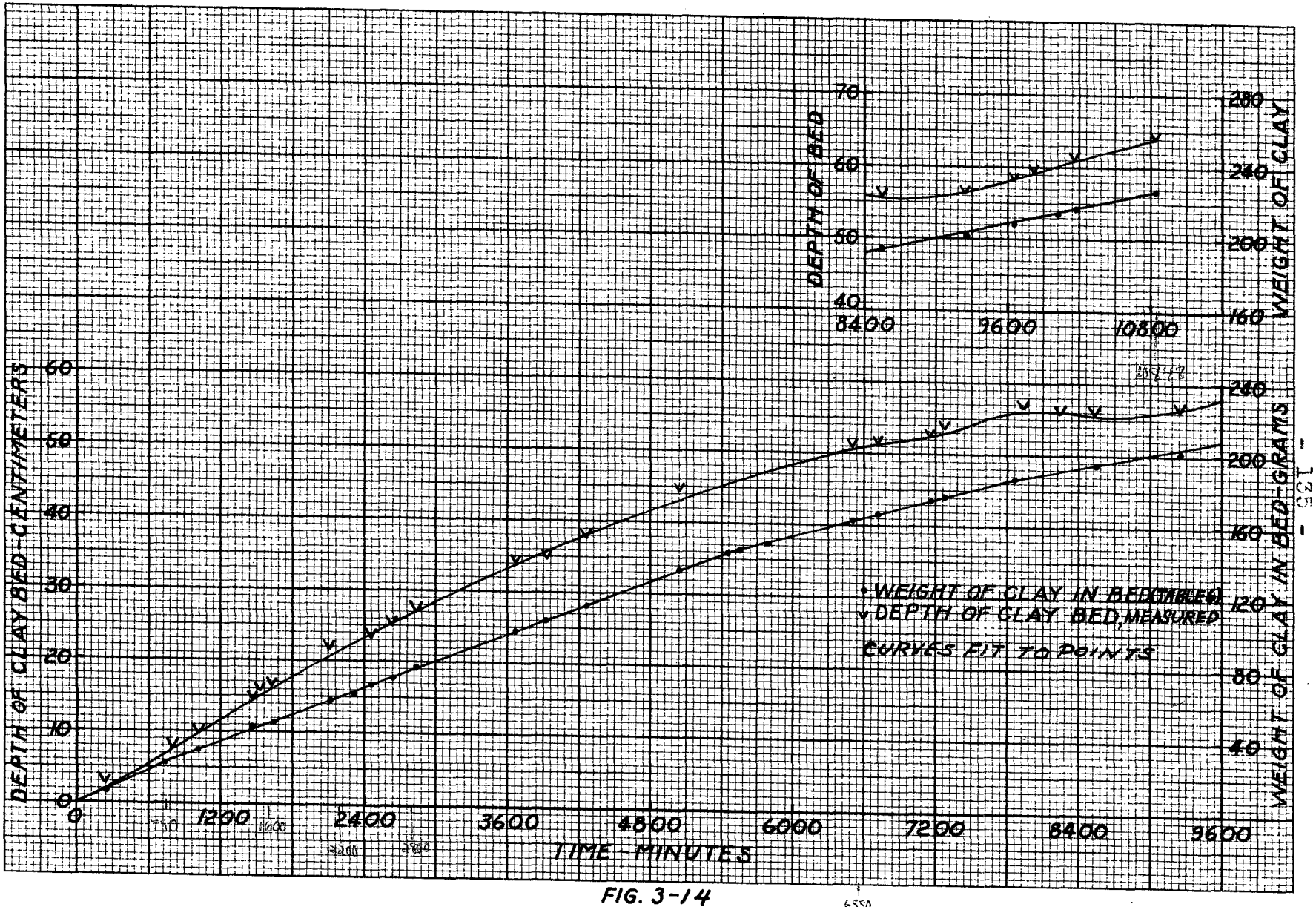

FIG. 3-14

DEPTH OF BED AND WEIGHT OF CLAY IN BED - MONTMORILLONITE RUN NO. 3

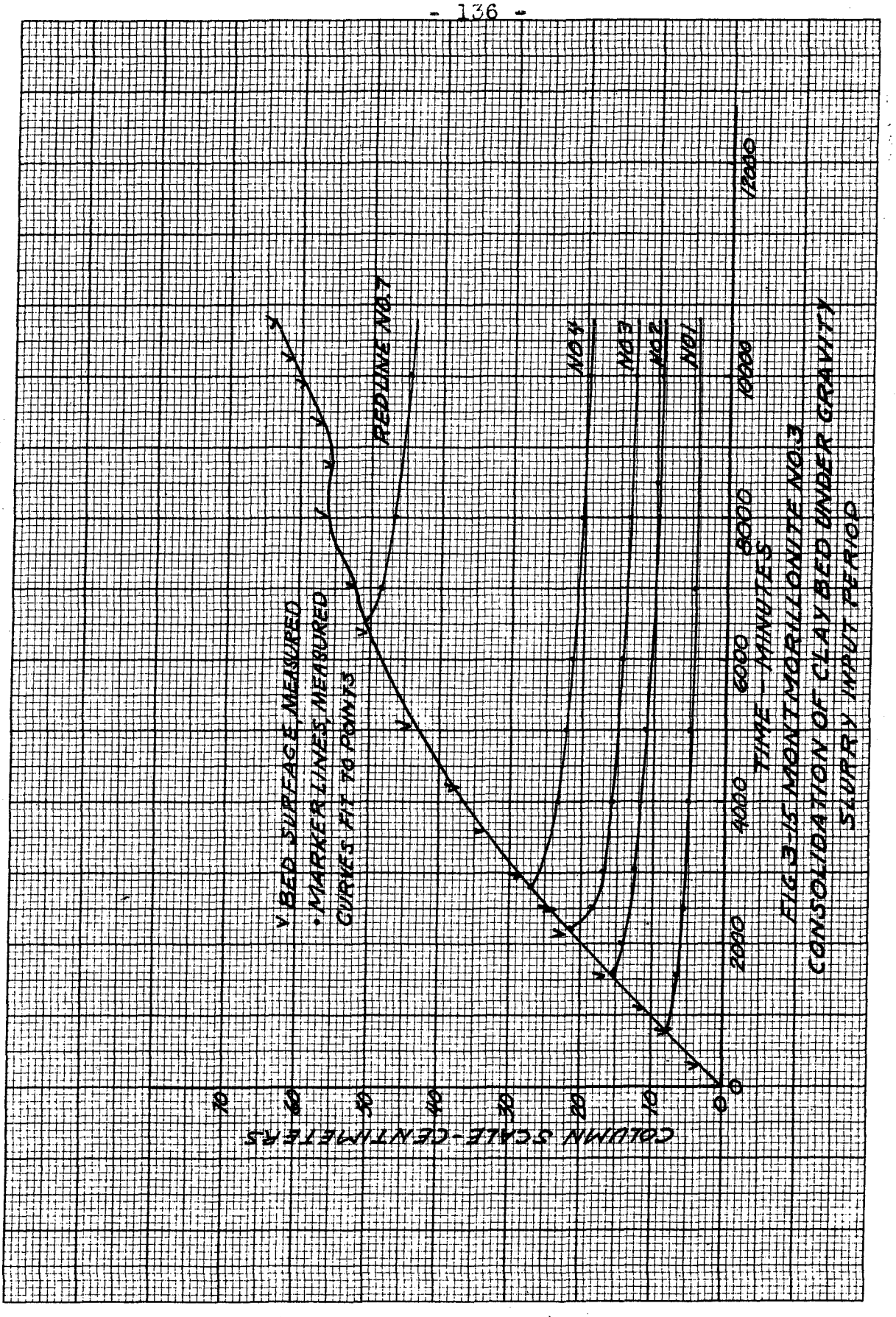
FIG 3-15 MONTMORILLONITE NO 3
CONSOLIDATION OF CLAY BED UNDER GRAVITY
SLURRY INPUT PERIOD
TIME — MINUTES
0
2000
4000
6000
8000
10000
12000
H01
H02
H03
H04
REDLINE NO 7
V BED SURFACE, MEASURED
• MARKER LINES, MEASURED
CURVES FIT TO POINTS
COLUMN SCALE - CENTIMETERS
0
10
20
30
40
50
60
70

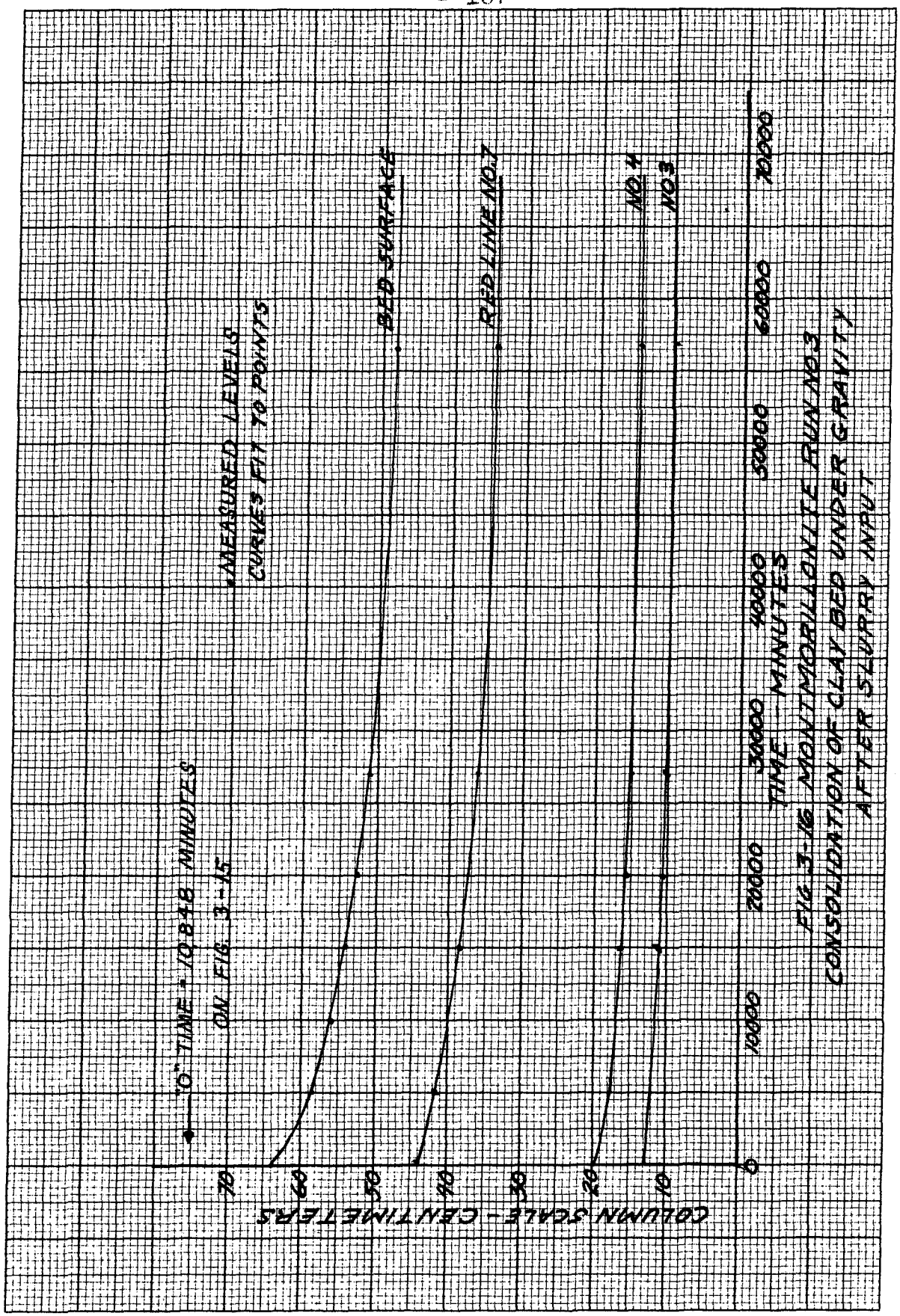

FIG. 3-16 MONTMORILLONITE RUN NO. 3
CONSOLIDATION OF CLAY BED UNDER GRAVITY
AFTER SLURRY INPUT

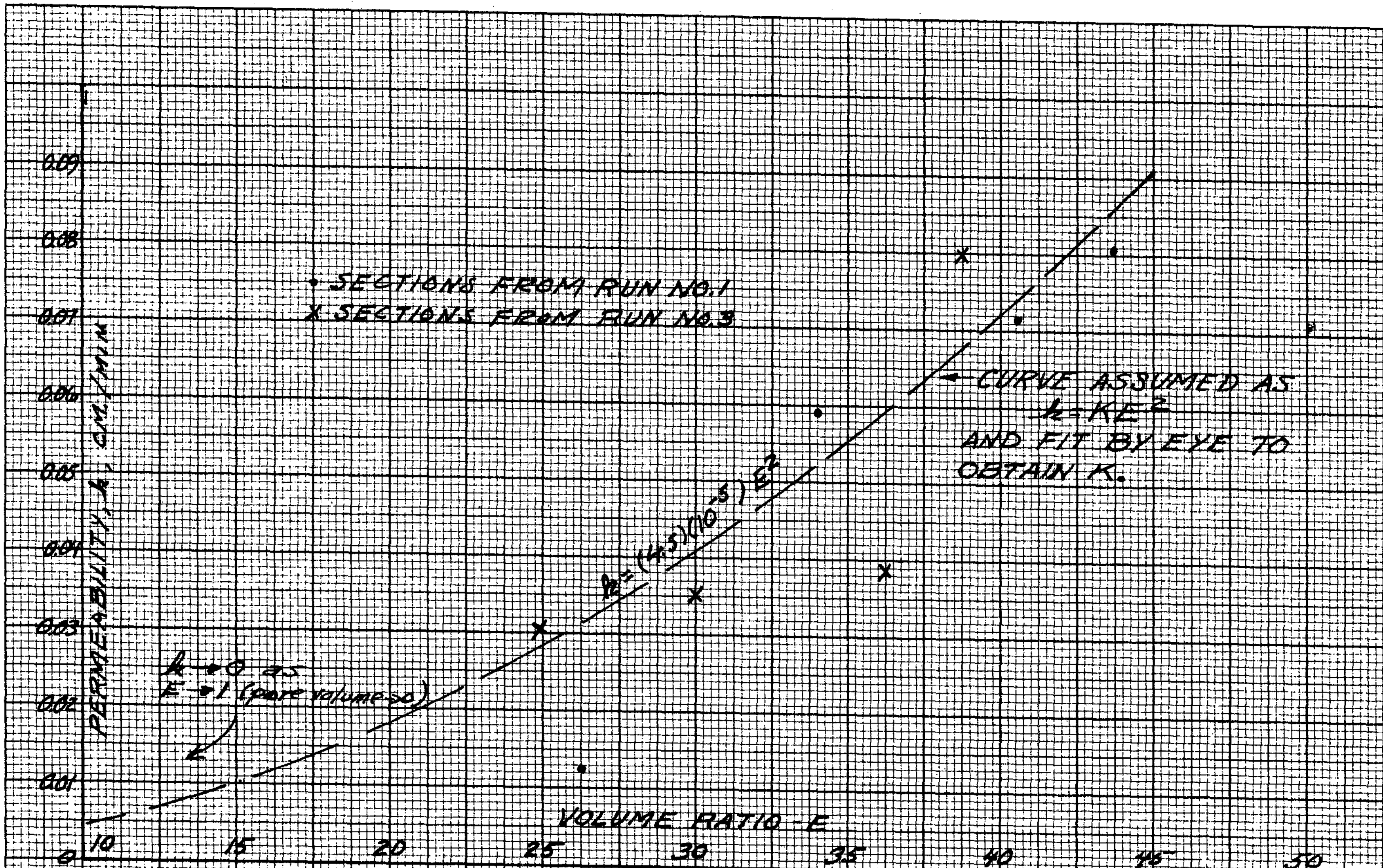

FIG 3-17 MONTMORILLONITE BE SECTIONS
PERMEABILITY vs. E

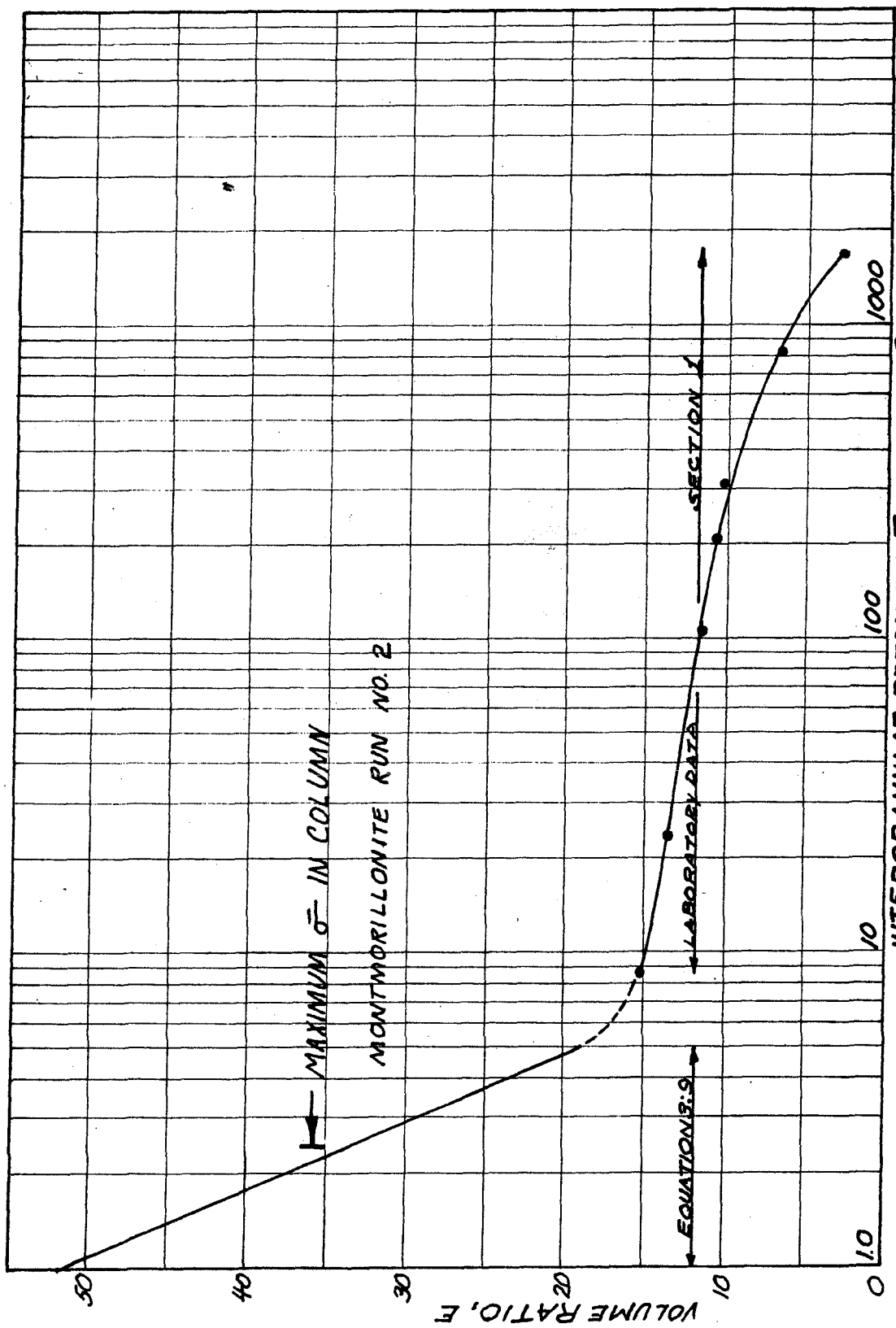

FIG 3-18 MONTMORILLONITE RUN NO. 1
CONSOLIDATION TEST SECTION 1

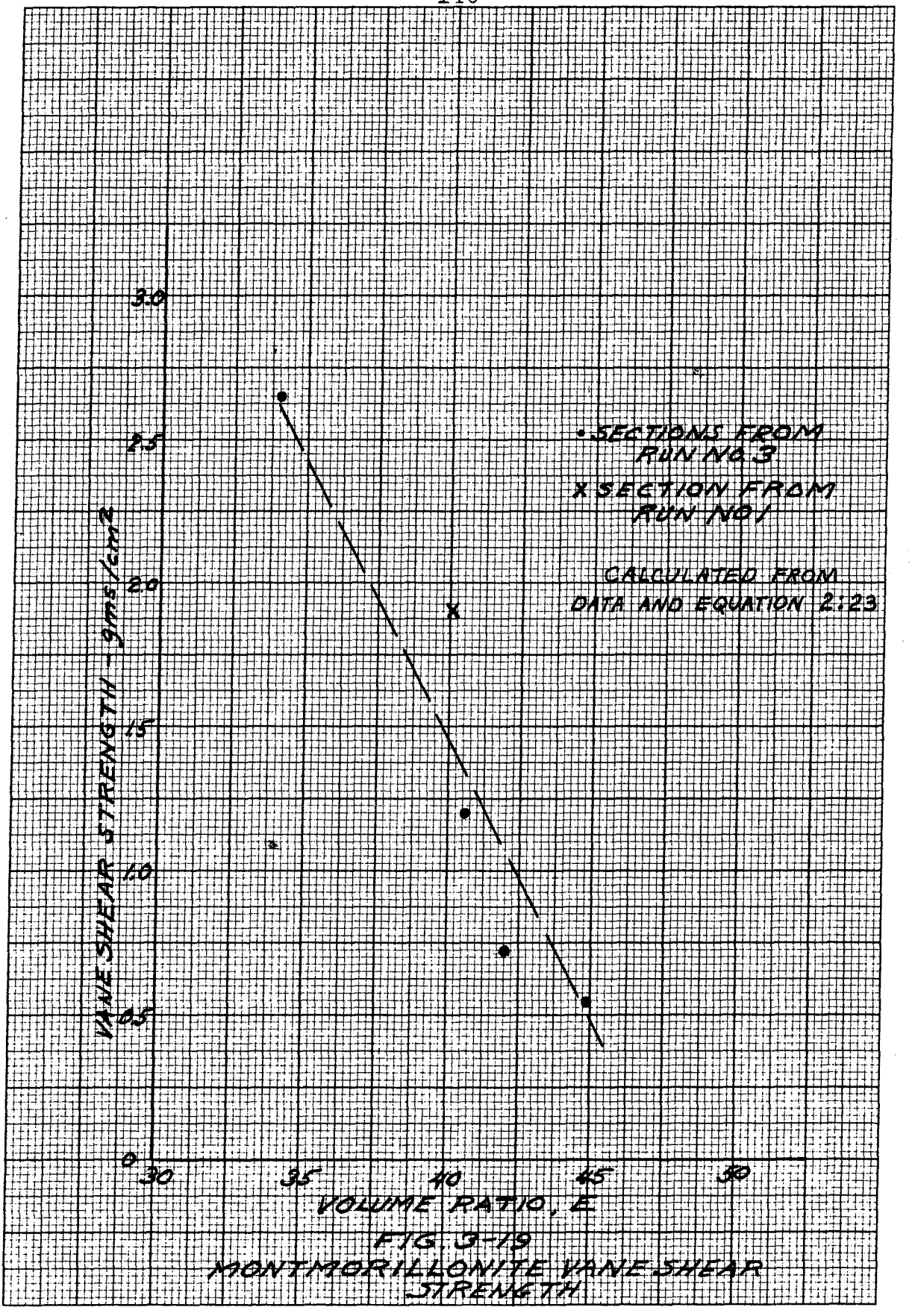

FIG. 3-19
MONTMORILLONITE VANE SHEAR STRENGTH

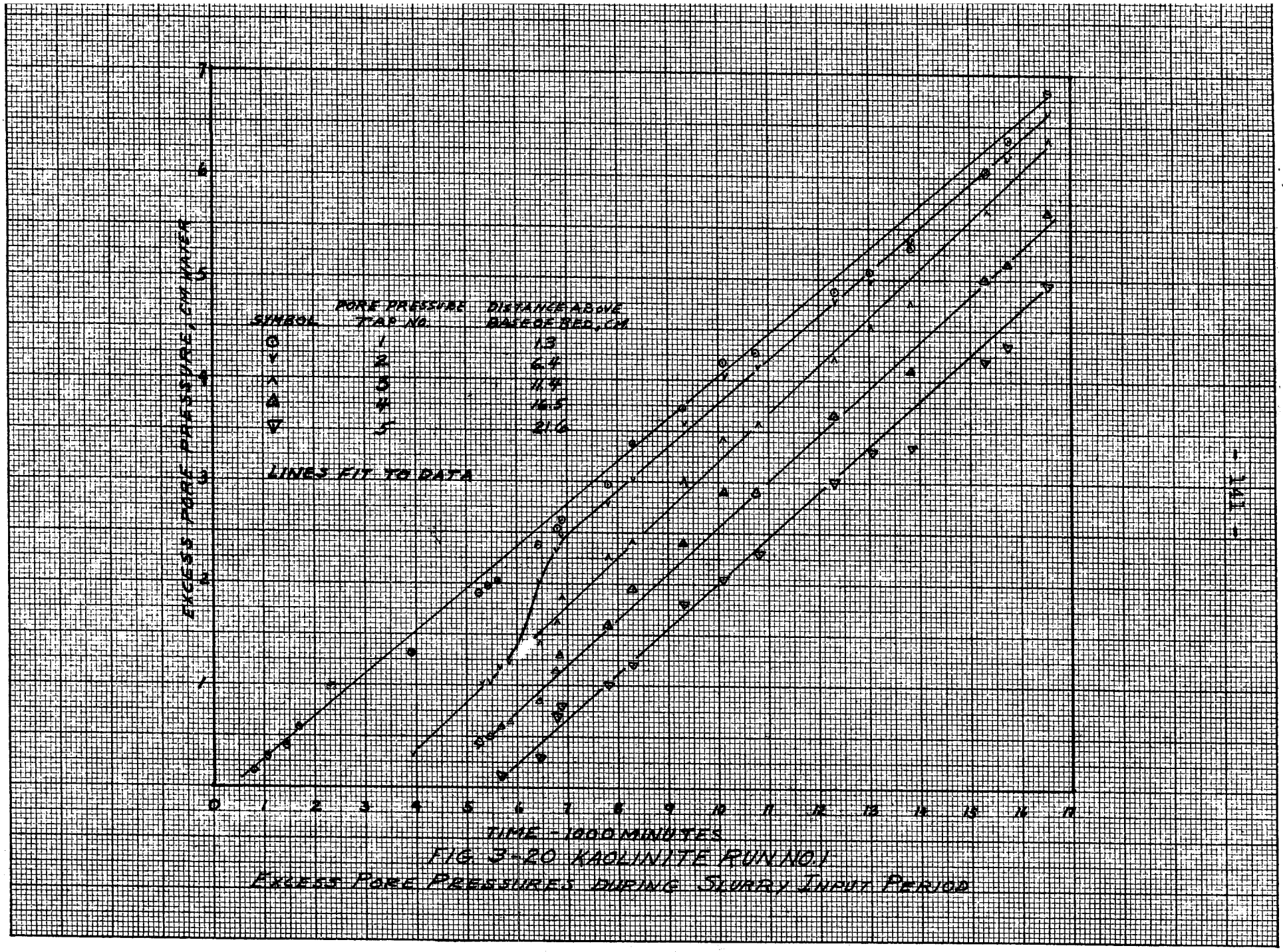

FIG. 3-20 KAOLINITE RUN NO.1
EXCESS PORE PRESSURES DURING SLURRY INPUT PERIOD

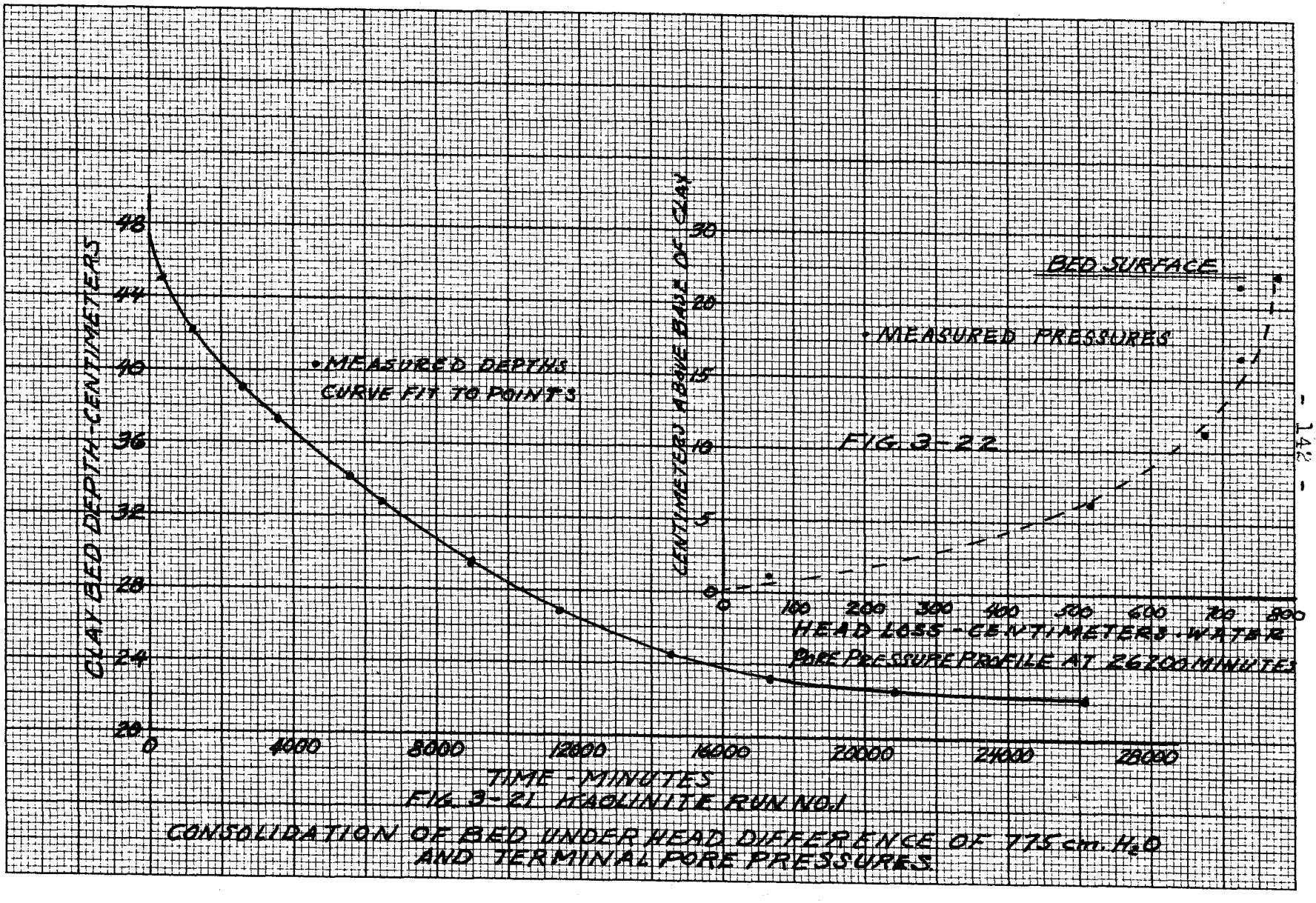

FIG. 3-21 KAOLINITE RUN NO. 1

CONSOLIDATION OF BED UNDER HEAD DIFFERENCE OF 775 cm. H_2O AND TERMINAL PORE PRESSURES

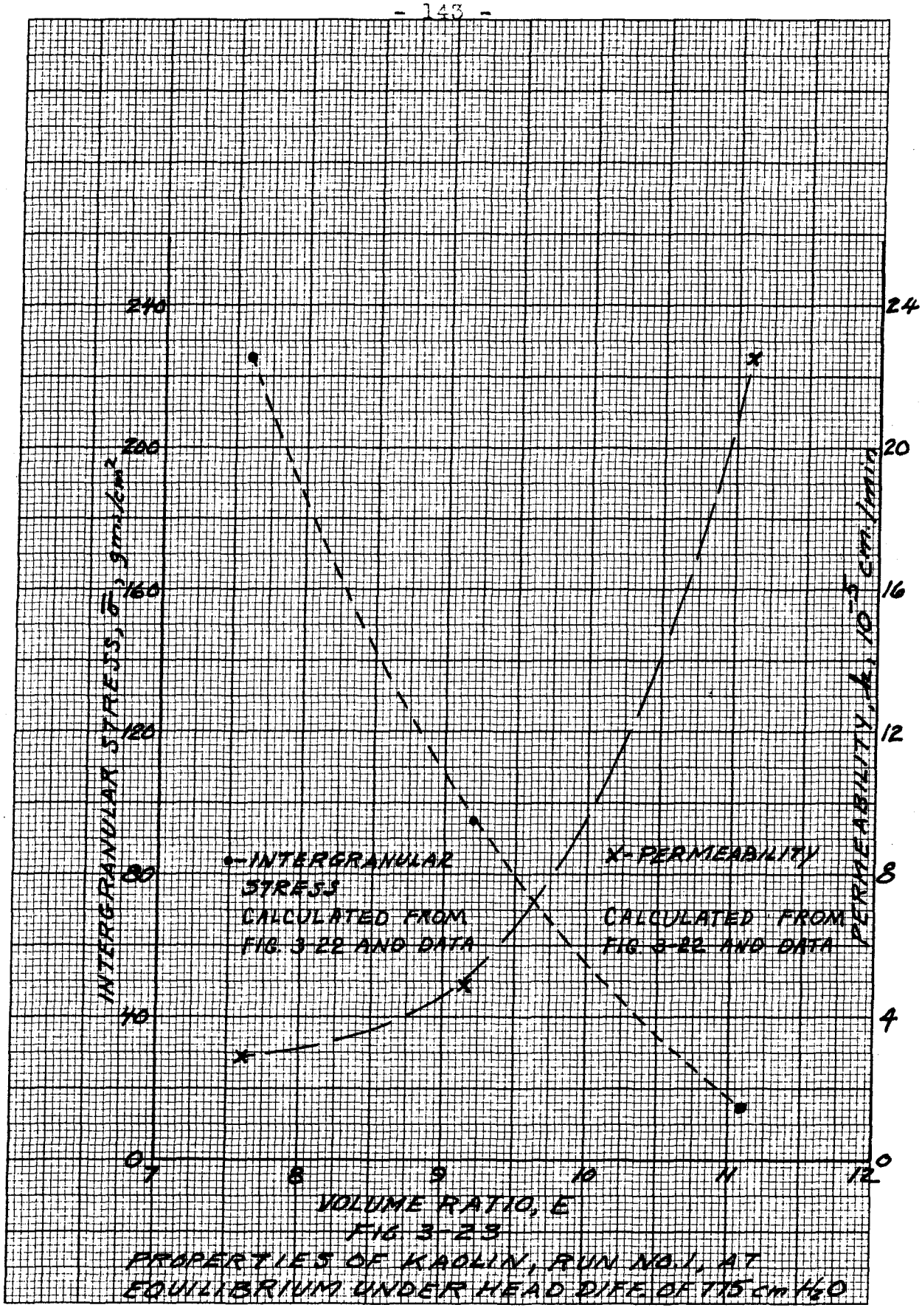

FIG. 3-23

PROPERTIES OF KAOLIN, RUN NO. 1, AT EQUILIBRIUM UNDER HEAD DIFF. OF 715 cm H_2O

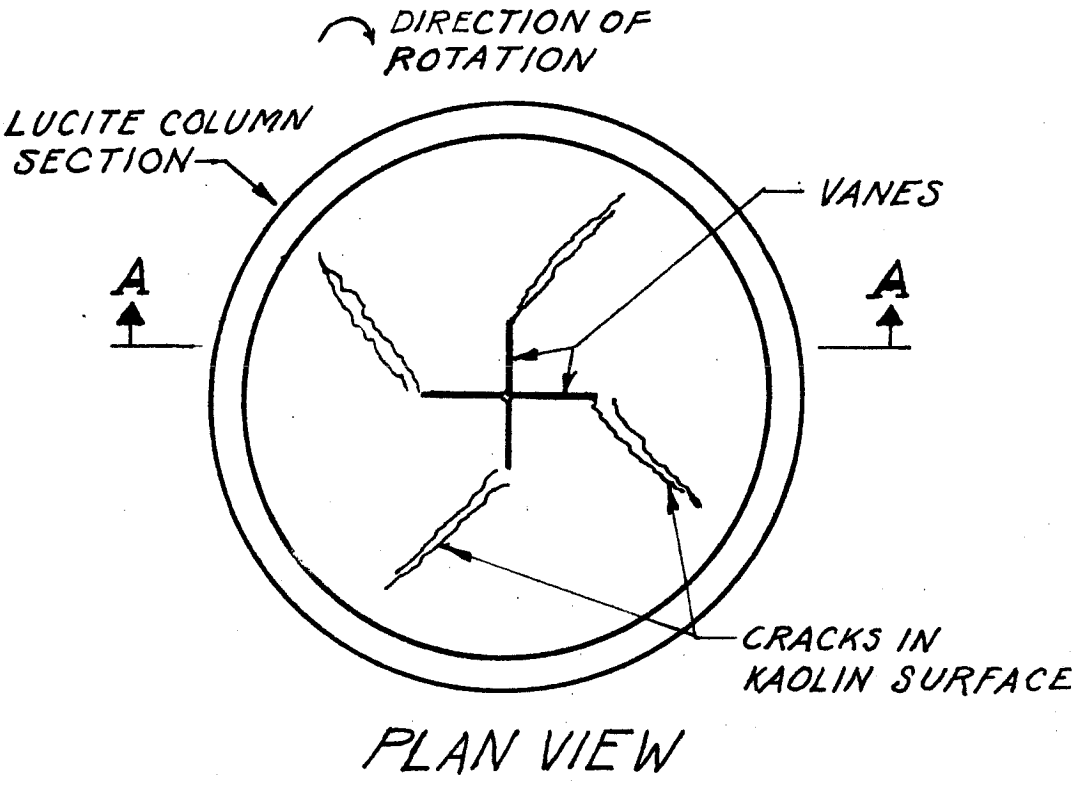

FIG. 3-24

BEHAVIOR OF KAOLIN COLUMN SECTION IN VANE SHEAR TEST

CHAPTER IV

DATA ANALYSIS AND CONCLUSIONS

A. INTRODUCTION

In Chapter I, consolidation theories are discussed with regard to the physical assumptions concerning the mechanics of the consolidation process and to the assumptions commonly used to obtain a linear mathematical model to describe the process. The linear equation was seen to be unsuitable for consolidation problems in which large strains occur. With the purpose of finding a suitable mathematical model for cases of large strain, equation 1:12 (and its alternate forms, equations 1:22 and 1:32) was developed by avoiding the linearizing assumptions. A finite difference method of solution was outlined to indicate how this equation might be applied in practice.

The experiments on sedimented clays, reported in Chapter III, represent perhaps the most extreme possible example of a consolidation process with large strains. Accordingly, the first point of discussion in this chapter is to analyze these experiments in relation to the theory developed in Chapter I.

Finally, there are presented some general conclusions resulting from this study.

B. SOLUTIONS TO THE CONSOLIDATION EQUATION AND CORRELATION WITH EXPERIMENTS.

1. Particular Solutions of the Consolidation Equation.

Since the experimental data are more simply expressed in terms of concentration than volume ratio, the consolidation equation of Chapter I will be considered here in the form of equation 1:32, which is reproduced below for ready reference:

$$\frac{\partial C}{\partial \tau} = \frac{\partial}{\partial x}\left[\frac{G}{CF}\frac{\partial C}{\partial x} + GC^2\right] \qquad (1:32)$$

where, it will be recalled, G and F are functions of E and, by equation 1:31, $E = \frac{1}{C}$.

From inspection of equation 1:32, it is apparent that if solutions of the product form are sought, i.e., if C may be expressed as

$$C = \Theta(\tau)\phi(x) \qquad (4:1)$$

where Θ is a function of τ only and ϕ is a function of x only, then only certain special forms of F and G are possible. For equation 1:32 to be separable, F and G must be power functions of C, i.e.,

$$F = C^p \qquad (4:2)$$

$$G = C^q \qquad (4:3)$$

In terms of equations 4:1, 4:2 and 4:3, equation 1:32 becomes

$$\Phi \frac{d\Theta}{d\tau} = \frac{d}{d\eta}\left[\Phi^{q-p-1}\frac{d\Phi}{d\tau}\Theta^{q-p} + \Phi^{q+2}\Theta^{q+2}\right] \tag{4:4}$$

Equation 4:4 is separable for values of p and q as follows:

q = -2 all p

p = -2 all q

For p = -2 equation 4:4 becomes:

$$\frac{1}{\Theta^{q+2}}\frac{d\Theta}{d\tau} = \frac{1}{\Phi}\frac{d}{d\eta}\left[\Phi^{q+1}\frac{d}{d\eta} + \Phi^{q+2}\right] \tag{4:5}$$

By the usual reasoning, the two sides of this equation must equal a constant, say L. Then,

$$\frac{1}{\Theta^{q+2}}\frac{d\Theta}{d\tau} = L \tag{4:6}$$

which may be integrated directly to give

$$\Theta^{-(q+1)} = -(q+1)(L\tau + M),\ q \neq -1 \tag{4:7}$$

where M is a constant of integration. Obviously, the solution for q = -1 is also easily found.

The equation in Φ is

$$\frac{1}{\Phi}\frac{d}{d\eta}\left(\Phi^{q+1}\frac{d\Phi}{d\eta}\right) + \frac{1}{\Phi}\frac{d}{d\eta}\left(\Phi^{q+2}\right) = L$$

or

$$\frac{1}{\Phi}\frac{d}{d\eta}\left(\Phi^{q+1}\frac{d\Phi}{d\eta}\right) + (q+2)\frac{1}{\Phi}\left(\Phi^{q+1}\frac{d}{d\eta} = L\right. \tag{4:8}$$

This is a non-linear ordinary differential equation of the second order. Solutions must be considered separately for

each value of q. Analytic solutions are presumably possible only for some special values of q. However, it is always possible to reduce equation 4:8 to a first order equation by the substitution,

$$\rho = \phi^{q+1} \frac{d\phi}{dx} \tag{4:9}$$

Then

$$\frac{d\rho}{d\phi} = \left[\frac{d}{dx}\left(\phi^{q+1}\frac{d\phi}{dx}\right)\right]\frac{dx}{d\phi}$$

or

$$\frac{d}{dx}\left(\phi^{q+1}\frac{d\phi}{dx}\right) = \frac{\rho}{\phi^{q+1}}\frac{d\rho}{d\phi} \tag{4:10}$$

Substituting equations 4:9 and 4:10 in equation 4:8, the following first order equation is obtained:

$$\frac{\rho}{\phi^{q+2}}\frac{d\rho}{d\phi} + (q+2)\frac{\rho}{\phi} = L \tag{4:11}$$

Here again, equation 4:11 must be examined separately for each value of q.

For the case q = -2, equation 4:4 becomes

$$\Theta^{p+2}\frac{d\Theta}{d\tau} = \frac{d}{dx}\left[\phi^{-(p+3)}\frac{d\phi}{dx}\right] = L \tag{4:12}$$

The equation in Θ is again directly integrated,

$$\Theta^{p+2}\frac{d\Theta}{d\tau} = L$$

$$\Theta^{p+3} = (p+3)(L\tau + M), \quad p \neq -3 \tag{4:13}$$

where M is a constant of integration. The solution for p = -3 also may be obtained by direct integration. The

equation in ϕ is solved by integrating twice,

$$\frac{d}{dx}\left[\phi^{-(P+3)}\frac{d\phi}{dx}\right]=L$$

Integrating once gives

$$\phi^{-(P+3)}\frac{d\phi}{dx}=Lx+N$$

Integrating a second time yields the solution:

$$\phi^{-(P+2)}=-(P+2)\left[\frac{L}{2}x^2+Nx+P\right]\quad P\neq -2 \tag{4:14}$$

where N and P are constants of integration. Again, the special case, p = -2, presents no problem.

The above discussion indicates quite a large group of solutions are obtainable by the "separation of variables" technique in the two cases, p = -2 and q = -2. Of course, these solutions are valid only if the boundary and initial conditions are satisfied by them in a given problem. Although these solutions are applicable only in certain special cases, they are presented to indicate some analytic solutions are possible for equation 1:32, and because one of these solutions is shown below to be applicable, with some reservations, to some of the experiments described in Chapter III.

Boundary conditions, in general form, are not obvious for equation 1:32. Again, the non-linearity of the equation requires separate consideration of boundary conditions for each case.

2. Solution of Consolidation Equation for Montmorillonite Experiments 1 and 2.

a. The functions F and G.

Figures 3-5, 3-11, and the accompanying discussion show that, at equilibrium under its own weight, the montmorillonite clay formed under the conditions of these two experiments has a $\overline{\sigma}$ - C diagram which is linear, i.e.,

$$\frac{dC}{d\overline{\sigma}} = a = a\ constant \qquad (4:14)$$

The definition of a_v is from Chapter I,

$$a_v = -\frac{dE}{d\overline{\sigma}}$$

In terms of C this becomes

$$\frac{dC}{d\overline{\sigma}} = a_v C^2 \qquad (4:15)$$

But a_v may be expressed as

$$a_v = a\,F\left(\frac{1}{C}\right)$$

(See equations 1:13 and 1:32.)

Thus, from equations 4:14 and 4:15

$$F\left(\frac{1}{C}\right) = \frac{1}{C^2} \qquad (4:16)$$

In figure 3-17 there is considerable scatter but the permeability may be roughly expressed functionally as

$$k = K\frac{1}{C^2} \qquad (4:17)$$

(See equation 1:18.)

Thus, for these experiments the values of p and q in equation 4:4 are

$$q = p = -2 \ .$$

A discussion of the legitimacy of using the value of p obtained from the equilibrium state of the clay is reserved for the next section below. Assuming for the moment that the above values of p and q may be used, equation 1:32 becomes

$$\frac{\partial c}{\partial \tau} = \frac{\partial}{\partial x}\left(\frac{1}{c}\frac{\partial c}{\partial x}\right) \qquad (4:18)$$

b. <u>The solution of equation 4:18</u>.

The solution by separation of variables will now be examined with regard to the progress of consolidation in a clay-bed during its formation.

Again, assuming C may be represented as

$C = \Theta(\tau)\,\Phi(x)$, equation 4:18 becomes

$$\frac{d\Theta}{d\tau} = \frac{1}{\Phi}\frac{d}{dx}\left(\frac{1}{\Phi}\frac{d\Phi}{dx}\right) = L \qquad (4:19)$$

The Θ function is obtained directly,

$$\Theta = L\tau + M \qquad (4:20)$$

where M is a constant of integration. For the Φ equation, the substitution of equation 4:9 is made.

$$\rho = \frac{1}{\phi} \frac{d\phi}{dx} \tag{4:21}$$

Differentiating with respect to ϕ gives

$$\frac{d\rho}{d\phi} = \frac{d}{dx}\left(\frac{1}{\phi}\frac{d\phi}{dx}\right)\frac{dx}{d\phi}$$

or

$$\frac{d}{\phi x}\left(\frac{1}{\phi}\frac{d\phi}{dx}\right) = \phi\rho\frac{d\rho}{d\phi} \tag{4:22}$$

With this substitution the equation in ρ and ϕ is

$$\rho\frac{d\rho}{d\phi} = L$$

Which may be integrated to give

$$\rho^2 = 2L\phi - N$$

or $$\rho = \sqrt{2L\phi - N} \tag{4:23}$$

where N is a constant of integration.

Substitution of equation 4:23 into equation 4:21 gives

$$\frac{1}{\phi}\frac{d\phi}{dx} = \sqrt{2L\phi - N} \tag{4:24}$$

which may be integrated to give.

$$\int \frac{d\phi}{\phi\sqrt{2L\phi - N}} = x + P, \tag{4:25}$$

where P is a constant of integration.

The integral on the left side of equation 4:25 takes various forms, depending on the relationship between $2L\phi - N$ and N and whether N is positive or negative.*

Assuming for the moment, $N > 0$, and, $2L\phi - N > 0$, then equation 4:25 becomes

$$\frac{2}{\sqrt{N}} \tan^{-1} \sqrt{\frac{2L\phi - N}{N}} = \varkappa + P$$

or

$$\sqrt{\frac{2L\phi - N}{N}} = \tan \sqrt{\frac{N}{2}} (\varkappa + P)$$

or

$$\phi = \frac{N}{2L} \left[1 + \tan^2 \sqrt{\frac{N}{2}} (\varkappa + P) \right] \qquad (4:26)$$

---

* See, for example, reference 4,1 (page 42).

Thus, C from equations 4:1, 4:20, and 4:26 is

$$C = N\left(\tfrac{1}{2} + M_1\right)\left[1 + \tan^2 \sqrt{\tfrac{N}{2}}\,(x + P)\right] \qquad (4:27)$$

where $M_1 = \frac{M}{2L}$

Equation 4:27 is a solution of equation 4:18 using the technique of separation of variables. As expected, there are three constants, N, M_1, and P to be determined from conditions of the problem.

c. Boundary Conditions.

Only one of the three necessary conditions is immediately obvious. The other two are obtained from the experimental data and some reasoning concerning the particle structure in the clay-bed. The accompanying sketch of the domain of the problem in the $\chi - \tau$ plane is helpful in visualizing the conditions. It will be recalled that

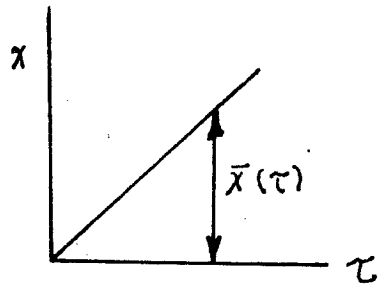

in the two experiments under consideration, the clay-bed surface rose linearly with time during the clay input period (see figures 3-3, and 3-9). Then, in the $\chi - \tau$ plane, the elevation of the surface, $\bar{x}(\tau)$, is also linear as indicated in the sketch. Figure 3-9 shows,

further, that a time was reached after which the bed surface no longer rose linearly with time.

The above observations yield the three conditions required to fix the constants of equation 4:27.

i. The base of the settling column was sealed so there is no movement of water or clay particles at $z = x = o$.

ii. The bed surface rose linearly with time for most of the clay input period. (It will be recalled from Chapter III that the rate of clay input was constant for these two experiments.)

iii. In experiment No. 2 (figure 3-9), a time was reached at which the bed surface no longer rose linearly with time.

These three conditions are developed below.

Condition i.

The impermeable base yields an equation in C at $x = o$. (See equation 1:36.)

$$\frac{1}{C}\frac{\partial C}{\partial x} = -1 \quad at \; x = o \tag{4:28}$$

Condition ii.

The second condition resulting from specifying $\overline{x}\,(\tau)$, is, in a sense, related to a boundary condition at $x = \overline{x}$. The equilibrium relationship of Chapter I (equation

1:9) is, in terms of C

$$\bar{\sigma} + u = \sigma_o - \int_o^z \gamma C \, dz \qquad (4:29)$$

At the surface $z = \bar{z}, (x = \bar{x}), \bar{\sigma} + u = 0$

The term, σ_o , was defined as

$$\sigma_o = \bar{\sigma} + u \text{ at } z = 0, (x = 0)$$

In this case

$$\sigma_o = \frac{W}{\gamma_s} \gamma t$$

so equation 4:29 becomes

$$\int_o^{\bar{z}} \gamma C \, dz = \frac{W}{\gamma_s} \gamma t$$

where W is the rate of clay input in grams per square centimeter per minute. In terms of x and τ this is (see equations 1:17 and 1:21)

$$\int_o^{\bar{x}} C \, dx = \frac{W \gamma_w}{\gamma_s \gamma K} \tilde{\tau} \qquad (4:30)$$

Since the bed surface rose linearly with time, $\tilde{\tau}$ may be expressed in terms of $\bar{x}$ the constant rate of surface rise. In terms of z and t , α is defined by

$$\bar{z} = \alpha t \qquad (4:31)$$

Replacing $\bar{z}$ and t by $\bar{x}$ and τ in equation 4:31 gives

$$\frac{\bar{x}}{a\gamma} = \alpha \frac{\gamma_a}{a\gamma^2 K} \tilde{\tau}$$

or

$$\tilde{\tau} = \frac{K\gamma}{\alpha \gamma_w} \bar{x} = \beta \bar{x} \qquad (4:32)$$

where $\beta = \frac{K\gamma}{\alpha \gamma_w}$

Inserting this expression for τ in equation 4:30 gives

$$\int_o^{\bar{x}} C \, dx = \frac{W}{\gamma_s \alpha} \qquad (4:33)$$

Since the bed surface rises at a uniform rate and clay is fed in at a uniform rate, the average value of C, is a constant C_a for all τ .

$$C_a = \frac{Wt}{\gamma_s \alpha t} = \frac{W}{\gamma_s \alpha}$$

The final form of the second condition is given by

$$\int_0^{\bar{x}} C \, d\, x = C_a \, \bar{x} \qquad (4:34)$$

Discussion of Condition ii.

A brief discussion of this equation is appropriate before proceeding to the third condition. Equation 4:34 is identical with the definition of C_a, i.e.,

$$C_a = \frac{1}{\bar{x}} \int_0^{\bar{x}} C \, dx$$

A comparison between the conditions of this problem and the hypothetical problem discussed in section D, Chapter I helps to show the relation between this condition and a boundary condition at $x = \bar{x}$.

In the Chapter I problem, a bed of clay is initially at equilibrium under its own weight, and, from the characteristics of the clay the initial concentration profile is known, i.e.,

$$C = C\,(x) \text{ at } \tau = o \, .$$

At x = o, the boundary condition is the same as here.

$$\frac{1}{C} \frac{\partial C}{\partial x} = -1 \text{ AT } x = 0 \; \tau \gg 0$$

At $x = \bar{x}$, the value of C is given from the known loading conditions at the surface, i.e.,

$$C = C(\tau) \text{ at } x = \bar{x},$$

prescribed, since consolidation takes place immediately at the surface. Finally, the movement of the clay surface is determined from the fact that the total amount of clay in the bed is a known constant, i.e.,

$$\int_0^{\bar{x}} C\,dx = \text{a constant.}$$

In principle at least, these last two conditions may be interchanged. If the clay-bed could be compressed in some way so that $\bar{x}(\tau)$ is prescribed, then C at $x = \bar{x}$ would not be a known boundary condition (since the required load would not be known) but would be obtained from the conservation relationship, $\int_0^{\bar{x}} C\,dx = \text{a constant}$. In this case, the conservation relation may be thought of as a boundary condition for the upper clay surface, since it fixes C at this boundary.

The above reasoning applies to the problem here. Examination of figure 3-4 shows quite clearly that the lower levels of the clay-bed undergo considerable consolidation during the period of bed formation. Since (1) C is increasing with time within the bed, (2) the average C over the bed remains constant, and (3) the slurry feed rate and other conditions remain constant, then the concentration at the surface must decrease as the surface rises. The only other possibility is that C is not a monotonic function of depth.

Assuming no changes in floc characteristics as they reach the bed, a reversal in the concentration profile does not seem physically reasonable, nor is any such condition indicated by the data.

The surface value of C, C_s, is not known as a boundary condition, but, in analogy with the above discussion, equation 4:34 may be thought of as the boundary condition on the upper surface which will fix C_s if the form of $\bar{x}$ (?) is taken as known.

Condition iii.

Equations 4:28 and 4:34 provide two conditions on equation 4:27. The third condition, which results from a change in the rate of bed surface rise, is obtained from some reasoning concerning C_s .

It is noted, above, that the experimental evidence indicates C_s must decrease with time. Since the intergranular stress must always be zero at the surface, one might expect C_s to be a constant, but this is contrary to the evidence.

In Chapter II, section C-3-a, there is a brief discussion of the environmental factors which permit the particles in an aqueous clay suspension to aggregate into flocs. The necessary condition for floc formation is that the net effect of attractive and repulsive forces between clay particles is attractive. One might expect,

further, that a net attractive force may exist between flocs. Such a force is thought to explain a structural characteristic commonly present in clay soils formed by deposition under water and referred to as "honeycomb structure."

The process of formation is explained* by consideration of the static equilibrium of individual flocs as they make contact with the clay surface. When a floc strikes the surface at a protrusion or high point of a previous floc it is thought that in a suitable environment, the forces of attraction at the contact between the two floc are large enough to overcome the gravity force tending to roll the floc off its high resting place into a more stable position. As the process is repeated the flocs may bridge over and enclose small volumes in which there are no soil particles; hence, the name "honeycomb structure." In this way a soil may be constructed with a very high average porosity. That this surface structure becomes progressively more porous during the period of bed formation must be due to some effect of the consolidation process occurring within the bed. Some possible mechanisms are considered in the next section below.

---

*Reference 1, 5, pp. (59 - 61).

Whatever the process may be, one might reasonably expect some limit to this steadily decreasing C_s . In the given environment the attractive forces at the contacts between flocs should eventually be overcome as the structure becomes more and more open. The bed surface rising linearly with time is explained by C_s decreasing with time. If C_s reaches some minimum value then, conversely, the bed surface can no longer continue to rise at the same rate. In the second of the two montmorillonite experiments, the bed formation process was continued until there was a slight but clear tendency for the rate of bed surface rise to start decreasing as shown in figure 3-9. The third condition for equation 4:27, then, is that C_s decreases until it reaches some minimum value. This condition is expressed as

$$\frac{dC_s}{d\tau} = 0 \quad \text{AT} \quad \tau = \tau_m \tag{4:35}$$

This is a total derivative, since C_s is a function of τ (or $\bar{x}$) only.

d. Summary of equation solution, and conditions.

To summarize, the applicable form of the consolidation for the montmorillonite experiments is taken as

$$\frac{\partial c}{\partial \tau} = \frac{\partial}{\partial x}\left(\frac{1}{c}\frac{\partial c}{\partial x}\right) \tag{4:18}$$

a solution for which is

$$C = N\left(\tfrac{1}{2}\tau^2 + M_1\right)\left[1 + \tan^2 \sqrt{\tfrac{N}{2}}\,(x + P)\right] \tag{4:27}$$

where N, M, and P are constants determined by the three

conditions:

$$\frac{1}{C}\frac{\partial c}{\partial x} = -1 \quad \text{at } x = 0, \tag{4:28}$$

$$\int_0^{\tau} C\,d\tau = C_a x \qquad 0 < \tau < \tau_m \tag{4:34}$$

and

$$\frac{dC}{d\tau} = 0 \quad \text{at } \tau = \tau_m \tag{4:35}$$

e. Application of conditions.

Using the expression for C from equation 4:27 in equation 4:28 provides a relation between N and P.

$$\frac{1}{C}\frac{\partial c}{\partial x} = \frac{2\tan\frac{\sqrt{N}}{2}(x+p)\left\{\cos^{\sqrt{N}/2}\frac{\sqrt{N}}{2}(x+p)\right\}}{1+\tan^2\frac{\sqrt{N}}{2}(x+p)}$$

Putting x = 0 :

$$\frac{1}{C}\frac{\partial c}{\partial x} = \frac{\sqrt{N}\tan\frac{\sqrt{N}}{2}p}{\cos^2\frac{\sqrt{N}}{2}p + \sin^2\frac{\sqrt{N}}{2}p} = -1 \quad \text{, by equation 4:28}$$

or

$$\tan\frac{\sqrt{N}}{2}p = -\frac{1}{\sqrt{N}} \tag{4:36}$$

The term $\left[1+\tan^2\frac{\sqrt{N}}{2}(x+p)\right]$ in equation 4:27 may be expanded.

$$1+\tan^2\frac{\sqrt{N}}{2}(x+p) = 1+\left[\frac{\tan\frac{\sqrt{N}}{2}x+\tan\frac{\sqrt{N}}{2}p}{1-\tan\frac{\sqrt{N}}{2}x\tan\frac{\sqrt{N}}{2}p}\right]^2$$

Using equation 4:36 and simplifying, this becomes

$$1+\tan^2\frac{\sqrt{N}}{2}(x+p) = \frac{(N+1)}{\sqrt{N}\cos\frac{\sqrt{N}}{2}x+\sin\frac{\sqrt{N}}{2}x)^2}$$

which, when substituted in equation 4:27, gives

$$C = N\left(\frac{1}{2}\tau + M\right)\frac{N+1}{\left(\sqrt{N}\cos\frac{\sqrt{N}}{2}x+\sin\frac{\sqrt{N}}{2}x\right)^2} \tag{4:37}$$

In applying condition 4:34, c is integrated over $\bar{x}$. This integration is facilitated by making the substitution.

$$\sqrt{N}\cos\frac{\sqrt{N}}{2}x + \sin\frac{\sqrt{N}}{2}x = \sqrt{N+1}\sin\left(\frac{\sqrt{N}}{2}x + \delta\right)$$

where $$\sin\delta = \frac{\sqrt{N}}{\sqrt{N+1}}$$

and $$\cos\delta = \frac{1}{\sqrt{N+1}}$$

In this notation equation 4:37 is

$$c = N\left(\tfrac{1}{2}\tau + M_1\right)\frac{1}{\sin^2\left(\frac{\sqrt{N}}{2}x + \delta\right)}$$

Condition 4:34 may now be applied.

$$\int_0^{\bar{x}} c\,dx = N\left(\tfrac{1}{2}\tau + M_1\right)\int_0^{\bar{x}}\frac{dx}{\sin^2\left(\frac{\sqrt{N}}{2}x+\delta\right)}$$

$$= N\left(\tfrac{1}{2}\tau + M_1\right)\frac{2}{\sqrt{N}}\left[-\cot\left(\frac{\sqrt{N}}{2}x+\delta\right)\right]_0^{\bar{x}}$$

$$= 2\sqrt{N}\left(\tfrac{1}{2}\tau+M_1\right)\left[\cot\delta - \cot\left(\frac{\sqrt{N}}{2}\bar{x}+\delta\right)\right]$$

$$\int_0^{\bar{x}} c\,dx = 2\left(\tfrac{1}{2}\tau+M_1\right)\frac{(N+1)\tan\frac{\sqrt{N}}{2}\bar{x}}{\sqrt{N}+\tan\frac{\sqrt{N}}{2}\bar{x}}$$

Setting this expression equal to Ca $\bar{x}$ gives the relation

$$\left(\tfrac{1}{2}\tau + M_1\right) = \frac{Ca}{2}\bar{x}\,\frac{\sqrt{N}\cos\frac{\sqrt{N}}{2}\bar{x} + \sin\frac{\sqrt{N}}{2}\bar{x}}{(N+1)\sin\frac{\sqrt{N}}{2}\bar{x}} \qquad (4:38)$$

Substitution of equation 4:38 in equation 4:37 gives

$$C = \frac{N}{2} C_a \frac{\bar{x}\left(\sqrt{N}\cos\frac{\sqrt{N}}{2}\bar{x} + \sin\frac{\sqrt{N}}{2}\bar{x}\right)}{\sin\frac{\sqrt{N}}{2}\bar{x}\left(\sqrt{N}\cos\frac{\sqrt{N}}{2}x + \sin\frac{\sqrt{N}}{2}x\right)^2} \qquad (4:39)$$

Since the linearity of $\bar{x}$ (τ) has been used to obtain equation 4:39, the solution must be considered valid only up to that point where $\bar{x}$ (τ) is no longer linear. Replacing x by $\bar{x}$ in equation 4:39 gives an expression for the surface concentration, C_s:

$$C_s = \frac{N}{2} C_a \frac{\bar{x}}{\sin\frac{\sqrt{N}}{2}\bar{x}\left(\sqrt{N}\cos\frac{\sqrt{N}}{2}\bar{x} + \sin\frac{\sqrt{N}}{2}\bar{x}\right)}$$

or

$$C_s = \frac{N C_a \bar{x}}{1 - \cos\sqrt{N}\bar{x} + \sqrt{N}\sin\sqrt{N}\bar{x}} \qquad (4:40)$$

Since, from equation 4:32, $\tau = \beta\bar{x}$, the condition of equation 4:35 may be modified to

$$\frac{dC_s}{d\bar{x}} = 0 \qquad at \quad \bar{x} = \bar{x}_m$$

Application of this to C_s as expressed in equation 4:40 yields the value of N.

$$\frac{dC_s}{d\bar{x}} = NC_a\left\{\frac{1}{1-\cos\sqrt{N}\bar{x}+\sqrt{N}\sin\sqrt{N}\bar{x}} - \bar{x}\frac{\sqrt{N}\sin\sqrt{N}\bar{x} + N\cos\sqrt{N}\bar{x}}{(1-\cos\sqrt{N}\bar{x}+\sqrt{N}\sin\sqrt{N}\bar{x})^2}\right\}$$

By equation 4:35, this expression is o at $\bar{x} = \bar{x}_m$ so that

$$\sqrt{N}(\bar{x}_m - 1)\sin\sqrt{N}\bar{x}_m + (1+\sqrt{N}\bar{x}_m)\cos\sqrt{N}\bar{x}_m = 1 \qquad (4:41)$$

f. Numerical values of constants of integration.

To complete the solution, some numerical values from Chapter III must be introduced. The unit weight of the montmorillonite clay is, from Chapter III,

$$\gamma_s = 2.64 \text{ gms/cm}^3 ,$$

so that

$$\gamma_s' = \gamma_s - \gamma_w = 1.64 \text{ gms/cm}^3 .$$

From figure 3-5

$$a = 0.0083$$

From figure 3-9 the value of $\bar{z}$ at which $\bar{z}(t)$ is no longer linear is in the neighborhood of 123 cm. Then

$$\bar{x}_m = 1.68$$

Checking with equation 4:41, it is found that if $\bar{x}_m = 1.675$ then $\sqrt{N} = 0.8$. This is taken as the value of $\sqrt{N}$.

Introducing the above value of N into equation 4:39, the final expression for C is

$$C = 0.32 C_d \frac{\bar{x}\,(0.8 \cot 0.4\bar{x} + 1)}{(0.8 \cos 0.4x + \sin 0.4x)^2} \qquad (4:42)$$

g. Assumptions used in finding the solution.

Before testing this result against the data, two assumptions used in the solution must be confirmed. The form of the integral used in proceeding from equation 4:25 to equation 4:26 assumed $N > 0$ and $2L\phi - N > 0$. The value of N found above satisfies the first condition. From equation 4:26,

$$2L\phi - N = N\left[1 + \tan^2 \frac{\sqrt{N}}{2}(x+p)\right] - N$$
$$= N \tan^2 \frac{\sqrt{N}}{2}(x+p)$$

This expression is positive for all x. Thus, the first assumption is confirmed.

The second assumption is the use of equation 4:38. The question is: Can a constant, M_1, be found to satisfy the relation?

$$\int_0^{\bar{x}} c\,dx = 2\left(\tfrac{1}{2}\tau + M_1\right)\frac{(N+1)\tan\frac{\sqrt{N}}{2}\bar{x}}{\sqrt{N} + \tan\frac{\sqrt{N}}{2}\bar{x}} \stackrel{?}{=} C_a\bar{x}$$

From equation 4:32

$$\tau = \beta\bar{x} = \frac{K\tau}{\alpha\gamma_w}\bar{x}$$

The rate of a bed surface rise, α, is essentially the same for both experiments under consideration. From the data for montmorillonite experiment number 1,

$$\alpha = \frac{113.5\ cms}{9150\ mins} = 0.0124\ cm/min$$

From figure 3-17 , the value of K is, roughly, 4.5×10^{-5} cm./min. Thus,

$$\beta = \frac{K\tau}{\alpha\gamma_w} = \frac{(4.5)(10^{-5})(1.64)}{(0.0124)(1)}$$

$$\beta = 0.00595$$

Inserting numerical values for β, N and C_a, the required

relation is

$$\frac{0.00975\ (\bar{x} + M_2)}{0.8\cot\ 0.4\bar{x} + 1} = 0.01355\ \bar{x}, \qquad (4:43)$$

where $M_2 = \frac{2}{\beta} M_1$

or $\bar{x} + M_2 = 1.39\ \bar{x}\ (0.8\cot\ 0.4\bar{x} + 1)$

The term cot $0.4\bar{x}$ may be replaced by the first two terms of its series form with less than 1% error even at the maximum $\bar{x}$ value of 1.675. Making this substitution and simplifying the relation becomes

$$\bar{x} + M_2 = 2.78 + 1.39\bar{x} - .135\bar{x}^2 \qquad (4:44)$$

Obviously, this equation cannot be satisfied for all values of $\bar{x}$. In that it is not satisfied, $\int_0^{\bar{x}} C dx$ does not equal the known volume of clay in the bed. The range of $\bar{x}$ is $0 \le \bar{x} \le 1.675$. Solving equation 4:44 for M_2,

$$M_2 = 2.78 + 0.39\bar{x} - 0.135\bar{x}^2,$$

it is seen that M_2 varies from 2.78 at $\bar{x} = 0$ to 3.05 at $\bar{x} = 1.675$. Choosing $M_2 = 3$, the two sides of equation 4:43 are plotted against $\bar{x}$ in figure 4:1, and the differences are seen to be small.

Assuming M_2 to be constant, yielded the final expression for C, equation 4:42. When this equation is integrated over

$\bar{x}$, the resulting expression is very nearly linear in $\bar{x}$ for the range of $\bar{x}$ encountered in the experiments. For much higher values of $\bar{x}$, the assumption would no longer be valid. It was noted above that this solution for C is valid only while $\bar{x}$ is linear in τ . Since the solution is quite good over the maximum range of $\bar{x}$, for which $\bar{x}$ is linear in τ , then the problem of higher $\bar{x}$ is of no concern in applying the solution to these particular experiments. This may not be the case for experiments conducted in different environments and/or with different clays.

3. Comparison of Equation 4:42 and Experimental Data.

To check equation 4:42 for C against experimental data, there is available only the locations of the red marker lines during the period of bed formation. The amount of clay, and thus the average C, is known for the sections of bed between pairs of marker lines, but there is a question as to just where this average C value should be plotted to form a concentration profile at a given time for comparison with equation 4:42. However, equation 4:42 may be used to compute the theoretical location of the marker lines at any time. In this way a check can be made between the theory and original data. Define

$x_l = x_l(\tau)$ as the distance from the base to the l'th marker line and $\bar{x}_l$ as that distance when the line is first laid down. Then

$$\int_o^{x_1} C dx = C_a \bar{x}_1 = \text{a constant} \qquad (4:45)$$

The method of performing the integration has been discussed following equation 4:37 and is not repeated here. The equation for x_1 is

$$x_1 = 2.5 \tan^{-1} \left[\frac{0.8\bar{x}_1}{\bar{x}\,(0.8 \cot 0.4\bar{x} + 1) - \bar{x}_1} \right] \qquad (4:46)$$

In figures 3-3 and 3-9 , it is seen that there is an initial period during which the rate of bed surface rise is increasing after which the rate is uniform. If the straight line portions of the curves of bed surface vs. time are extended back to zero depth, they intersect the time axes at approximately 300 minutes in both figures. The time at which the red lines were first installed is taken, then, as the recorded time less 300 minutes. The various values of $\bar{x}_1$ are computed from these times. The corresponding x_1 curves are then plotted from equation 4:46 in figures 4-2 and 4-3, together with the corresponding data observations. The initial data points are slightly above or below the $x = \bar{x}$ line, since the bed surface curve varied slightly about the straight line as shown in figures 3-3 and 3-9 . The agreement between the theoretical curves and the data is seen to be quite close, both in the form of the curves and in the values of x_1.

4. Discussion of Solution.

Although a solution to the consolidation equation has been obtained which agrees well with certain experimental data, there remain several points for discussion before any conclusions may be drawn.

In formulating the three requisite conditions necessary to obtain a mathematical solution, two were easily obtained from conditions of the problem. The third condition involved the observed phenomenon of decreasing surface concentration during the clay input period. That the surface concentration did, in fact, decrease during the period of bed formation is clear from the evidence. If other conditions are not changing, this changing bed surface concentration must result from some effect of the consolidation process occurring in the bed.

a. Surface Concentration.

Replacing x by $\overline{x}$ in equation 4:42 yields an expression for C_s as a function of $\overline{x}$ (or time), which is plotted in figure 4-4. The indicated values of surface concentration vary between extremes of 0.01354 and 0.00934. There are no measurements to check these computed values of surface concentration, and the fact that the theory shows close agreement with data in the total quantity of clay up to various levels in the bed does not imply that the theoretical values of C at particular points are in such close agreement with actual values. The

range of values of C_s in the experiments could be considerably smaller or larger than that indicated in figure 4-4 without seriously affecting the agreement between theory and experiment shown in figures 2-2 and 2-3.

Besides providing values of C_s, the theory also may be used to analyze two effects of the consolidation process which explain, in part, the changing surface concentration.

Seepage Velocity.

The pore water escaping from the bed surface reduces the impact velocity of floc reaching the surface and provides support for the loose assemblages of floc at the bed surface.

From equation 1:6a, the seepage velocity is

$$j = -\frac{i}{E} = -iC ,$$

where i is the velocity of soil particles. If Z_1 (t) is the trace of a layer of particles with time, then

$$i = \frac{dz_1}{dt}$$

If this derivative is evaluated at the bed surface an expression is obtained for (t), the soil particle velocity at the surface.

$$\frac{dz_1}{dt} = \frac{d\left(\frac{x_1}{a\tau}\right)}{d\left(\frac{\bar{x}}{a\tau_\alpha}\right)} = \alpha \frac{dx_1}{d\bar{x}} \qquad (4:47)$$

The derivative is found from equation 4:46. The seepage velocity is obtained as

$$j = -\alpha \left(c \frac{dx_1}{d\bar{x}} \right)_{\bar{x}} , \qquad (4:48)$$

where the quantity in the brackets is evaluated at $\bar{x}$ from equation (4:46). The mathematics is straightforward and the final form of j is

$$j = -\alpha Ca \left[0.4 \sin 0.8\bar{x} + 0.5 (1-\cos 0.8\bar{x}) - 0.32\bar{x} \right] \qquad (4:49)$$

In the range $0 \leq x \leq 1.675$, j increases from 0 to 0.4×10^{-4} cm/min. Since the observed settling velocity of the floc is on the order of 1 - 2 cm/min, this influence can hardly be appreciable.

Bed Surface Movement.

There is another effect, which, though small, is of considerably greater magnitude than the seepage velocity. Although the clay surface is rising, each clay floc strikes a receding surface and its impact velocity is reduced by the velocity of the receding surface. This velocity is $\frac{dz_1}{dt}$, evaluated at the surface. Some approximations will be used to put this in simple terms. From equation 4:46

$$\tan 0.4x_1 = \frac{0.8\bar{x}_1}{\bar{x} (0.8 \cot 0.4\bar{x} + 1) - \bar{x}_1}$$

The tangent and cotangent terms may be roughly approximated by the first terms of their series for the range of

values of $\bar{x}$ and x_1 in figures 4:2 and 4:3.

$$x_1 = \frac{2\bar{x}_1}{2 + \bar{x} - \bar{x}_1}$$

Then the receding surface velocity is

$$\left(\frac{dz_1}{dt}\right)_{\bar{z}} = \propto \left(\frac{dx_1}{d\bar{x}}\right)_{\bar{x}}$$

$$= \propto 2\bar{x}_1 \left(- \frac{1}{(2 + \bar{x} - \bar{x}_1)^2} \right)$$

or

$$\left(\frac{dz_1}{dt}\right)_{\bar{z}} = - \frac{\propto}{2} \bar{x}$$

$$= 0 \text{ at } \bar{x} = o$$

$$= 0.0104 \text{ cm/min at } \bar{x} = 1.675$$

This is still very small compared to the floc settling velocity.

Decreasing surface concentration and the apparent existence of a minimum concentration in a given environment have been used to prescribe the mathematical solution. To be sure, these conditions are applied after the fact. Certainly, none of the above discussion is meant to imply that these phenomena were anticipated prior to the laboratory experiments. In an area in which published theoretical and/or experimental studies are almost non-existent, the initial approach has been to attempt to explain admittedly arbitrary

experiments conducted under controlled conditions in the light of some basic concepts of the consolidation process.

Summary.

Experimental observation and physical reasoning indicate a decreasing surface concentration and two possible explanations for this phenomenon. The theoretical solution has been used to find some numerical values for these items. The indicated change in surface concentration is not large and one might expect that clay at such low concentrations to be sensitive to small influences.

If the consolidation equation were solved, assuming a constant surface concentration (say the average of the valves shown in figure 4-4), the solution probably would not be at large variance with the solution obtained here.

b. The $\overline{\sigma}$ - E Relationship.

One result of this process has been to show one of the basic assumptions of the Terzaghi consolidation theory and that developed here to be in error - at least, at very low concentrations. It is perhaps best to use the volume ratio, E, instead of concentration in the following discussion since it is more easily related to the commonly used void ratio ($E = e + 1$).

The volume ratio was assumed to be a continuous single-valued function of intergranular pressure, $\overline{\sigma}$, when $\overline{\sigma}$ is increased from lower to higher values once only. When the clay is considered as a continuum, $\overline{\sigma}$ at the bed surface is always zero. If $\overline{\sigma}$ at the surface is envisioned as the intergranular pressure below the top layer of clay floc, then it is the submerged weight of these floc less the pressure gradient due to upward flow of pore water. In this sense, the changing surface volume ratio may be partially accounted for by the changing upward velocity of pore fluid as discussed previously. Still the evidence indicates E is not single-valued at $\overline{\sigma} = o$.

Of more interest, perhaps, is a comparison of figures 3-5, 3-10, and 3-15, in which it is clearly seen that the equilibrium C (or E) vs. $\overline{\sigma}$ curves of the montmorillonite beds in experiments 1 and 2 are essentially identical and different from that in experiment 3. The only difference in the formation of these beds was that the clay input rate in experiment 3 was considerably lower than the rate

for the other two. For this clay, then, E is a function not only of $\overline{\sigma}$ but also of the manner in which the bed was formed, other things being equal.

In developing the consolidation equation in Chapter I, the uniqueness of E with $\overline{\sigma}$ assumption was used in making the substitution.

$$\frac{\partial \overline{\sigma}}{\partial z} = \frac{d\overline{\sigma}}{dE} \frac{\partial E}{\partial z} = -\frac{1}{a_v} \frac{\partial E}{\partial z} \qquad (4:50)$$

In solving the consolidation equation for montmorillonite experiments 1 and 2, above, the equilibrium C - $\overline{\sigma}$ relation of equation 3:8 was used. Equation 3:8 is

$$C = .0083\ \overline{\sigma} + .011,$$

which in terms of E, is

$$E = \frac{90.9}{.775\ \overline{\sigma} + 1} \qquad (4:51)$$

The equilibrium profile of E over the depth of the bed is (see equation 3:6)

$$E = 31.25\ \mathfrak{E}^{x} \qquad (4:52)$$

During the process of bed formation the total volume of clay (per unit plan area) in the bed at a given time is, from equation 4:34, $C_a \langle \bar{x} \rangle$. The brackets signify a specific $\bar{x}$. The layer of particles on the surface at $\langle \bar{x} \rangle$

may be located in the bed at equilibrium from equation 4:52 since the volume of clay below it does not change.

$$\int_0^{\langle x \rangle} C\, dx = \int_0^{\langle x \rangle} \frac{dx}{31.25C^x} = C_a \langle \bar{x} \rangle \qquad (4:53)$$

The values of $\langle x \rangle$ for various values of $\langle \bar{x} \rangle$ obtained from equation 4:53 may then be used to compute the corresponding E value at equilibrium in equation 4:52. In figure 4-5, the solid curve is the equilibrium E - $\overline{\sigma}$ diagram (equation 4:51). The labeled points on the $\overline{\sigma}$ = o axis and on this curve represent the initial and final E - $\overline{\sigma}$ conditions for various layers of the bed. Each pair of points is connected by a curve which is the E - $\overline{\sigma}$ curve for that part of the bed from $\overline{\sigma}$ = o to the maximum value of $\overline{\sigma}$ occurring at equilibrium. Thus, the equilibrium E - $\overline{\sigma}$ curve is the locus of the terminal points of a continuous sequence of $\overline{\sigma}$ - E curves, one for each layer of particles.

The curves connecting the known end points of these individual $\overline{\sigma}$ - E curves are sketched in by assuming they are continuous and of the same general shape of the equilibrium curve. If these assumed curves are approximately correct, their slopes do not differ greatly from the equilibrium curve for a given E. However, the $\frac{d\overline{\sigma}}{dE}$ term in equation 4:50 is not the slope of a particular $\overline{\sigma}$ - E

curve. In proceeding from z to $z + \Delta z$, the intergranular pressure goes from $\overline{\sigma}$ to $\overline{\sigma} - \Delta \overline{\sigma}$, but, in addition, moving up Δz is accompanied by a jump to a new $\overline{\sigma}$ - E curve. Assuming that the slopes of all $\overline{\sigma}$ - E curves continually increase, those curves above the equilibrium curve in figure 4-4 have slopes less than the equilibrium curve for the same E value. Conversely, those curves below the equilibrium curve have larger slopes. The appropriate $\frac{d\overline{\sigma}}{dE}$ slopes for equation 4:50 are the slopes of the lines A - B in the figure. It is seen that these slopes are probably quite close to the slope of the equilibrium curve for $\overline{\sigma}$ - E conditions below that curve at a given E, while for conditions above the curve the slopes must always be less. The use of equation 4:50 requires that $\frac{d\overline{\sigma}}{dE}$ be the same as the slope of the equilibrium curve at a given E. This is seen to be nearly true for the lower levels of the clay bed, but there is appreciable error in the upper levels.

c. Summary.

A short summary may be useful to properly relate the various facets of this part of the investigation.

i. Based on commonly accepted principles of the soil consolidation process, but without the commonly used linearizing assumptions, a consolidation equation is developed in Chapter I.

ii. The equation is non-linear, however the results

of experiments on montmorillonite clay, presented in Chapter III, show the variation of a_v and k with C to be such that the consolidation equation is separable.

iii. Of the three conditions necessary to prescribe the solution, two involve observed phenomena for which no clear physical explanation is apparent at this time.

iv. One of the basic assumptions used in formulating the consolidation equation is refuted by the results of the experiments. However, in application to the mathematics of the problem, the assumption still appears to be reasonable.

v. The solution to the equation correlates well with experimental data.

Despite the many reservations, the agreement between theory and experiment is felt to be good enough to support the proposition that the consolidation equation developed in Chapter I is a good mathematical model for the physics of soil consolidation involving large strains.

Much more is required before the equation may be applied in general with confidence. The results presented here would seem to justify further investigation.

This completes the discussion of the consolidation equation and its application to the montmorillonite experiments. The results suggest some other matters of interest which are considered below.

5. Hydrostatic Excess Pressures.

In figure 4-4, the $\overline{\sigma}$ - E curves for various layers of the bed were sketched in by assuming their general form, but only the ends of the curves were actually known. If reliable pore-pressure data were available, intermediate points on these curves could be calculated. Since the quantity of clay above any layer of particles is known, the effective stress at that layer is readily found.

$$\overline{\sigma} = \int_{z}^{\overline{z}} \gamma C dz$$

Then, if the hydrostatic excess pressure were available from pore pressure measurements, $\overline{\sigma}$ is found directly from $\overline{\sigma} = \sigma - u$. Despite the lack of data to fix intermediate points on these curves, their relation to the known equilibrium curve and the fact that their end points are known gives some confidence that they are approximately correct. The distribution of hydrostatic excess pressure is of interest in soil mechanics for problems of soil strength besides consolidation. These $\overline{\sigma}$ - E curves may be used to compute hydrostatic excess pressures as follows:

As an example, the profile of hydrostatic excess pressure will be computed at the time corresponding to $\overline{x} = 1.0$. The locations at $\overline{x} = 1.0$ of the layers of particles which were on the surface at $\overline{x} = 0.2$, 0.4, 0.6, and 0.8 are computed from equation 4:46 and tabulated below.

Initial level of clay layers, $\bar{x}$,	Level of same layers at $\bar{x} = 1.0$, x,
0	0
0.2	0.148
0.4	0.319
0.6	0.519
0.8	0.745
1.0	1.0

The indicated C values are computed from equation 4:42. The column of E's is calculated from the C values as $E = \frac{1}{C}$.

Values of C at $\bar{x} = 1.0$ and x,	Corresponding values of E
.0199	50.2
.0173	57.8
.0150	66.7
.0130	76.9
.0110	90.9
.0100	100.0

For these values of E, $\bar{\sigma}$ values are taken from the appropriate curves in figure 4-4, and the hydrostatic excess pressure is computed as indicated. This profile of u is plotted in figure 4-6.

Figure 4-4 Curve	E	$\overline{\sigma}$	$= \frac{Ca(1.0 - \bar{x}_1)}{a\tau}$	$u = \sigma - \overline{\sigma}$
⓪ - ⓪	50.2	0.925	1.631	0.706
⑵ - ⑵	57.8	0.675	1.304	0.629
⑷ - ⑷	66.7	0.460	9.978	0.518
⑹ - ⑹	76.9	0.290	0.652	0.362
⑻ - ⑻	90.9	0.080	0.326	0.246
1.0 - 1.0	101.2	-0-	-0-	-0-

6. The $\overline{\sigma}$ - E Relationship With Reference to General Soil Behavior.

The assumption of uniqueness in the $\overline{\sigma}$ - E relationship is so commonly applied in soil mechanics practice and is substantiated by such a large body of laboratory data that the question of why the non-uniqueness found in this investigation has not been found by others must be considered. First, the range of E values encountered in this study is far beyond those normally encountered in soils engineering problems. A volume ratio of 5 or 6 would be a high value for a soil on dry land. Likewise, the maximum $\overline{\sigma}$ value found here is of the order of one gram per square centimeter, whereas values up to several kilograms per square centimeter are encountered in soil mechanics practice. Secondly, the various $\overline{\sigma}$ - E curves in figure 4-4 tend to come closer together as $\overline{\sigma}$ increases. It is clear from examination of these curves that, as $\overline{\sigma}$ is increased, the differences between the curves will become indistinguishable, and the various curves will fuse

into one. It is not surprising, therefore, that the $\overline{\sigma}$ - E relation is usually found to be unique at values of $\overline{\sigma}$ and E normally encountered in soil mechanics practice.

7. Plasticity Effects.

In all the above discussion of the $\overline{\sigma}$ - E relation, time effects have been ignored. The fact that different $\overline{\sigma}$ - E curves are implied by the data does not, of itself, prove that this is a property of the clay. It may be more a property of the experiments, since it is quite possible that the various portions of the bed, which assumed different E values at the same $\overline{\sigma}$, might all come to the same E value at a given $\overline{\sigma}$ if this $\overline{\sigma}$ remained unchanged for a long time. Clays at the lower volume ratios encountered in engineering problems commonly exhibit such plastic characteristics. In soil mechanics literature this is usually referred to as "secondary consolidation." Under a given load clay samples may continue to compress almost indefinitely at a very slow rate.

In this regard, the difference between the "equilibrium" profiles of experiments numbers 1 and 2 and that for number 3 cannot be considered as permanent and constant. If these beds were allowed to stand for very long times, it may be these differences would disappear.

The consolidation theory developed in Chapter I does not include any plasticity effects. The assumption of a unique $\overline{\sigma}$ - E relation denies any such effects. The fact

that theory agreed well with certain experiments, which showed this assumption to be not quite correct, may be the result of compensating errors. In other words, the theory may be incorrect in two ways: 1. The $\overline{\sigma}$ - E relation is not unique and, 2. Plastic effects do occur. However, the error in the $\overline{\sigma}$ - E assumption is not great, as discussed above, and during the relatively short period when the theory is applied, plasticity effects are probably small.

C. CONCLUSIONS

1. The Consolidation Equation.

a. In Chapter I a consolidation equation is formulated which is not limited to cases of small strain and which is felt to be a more reasonable and accurate mathematical model of the consolidation process than the classical linear equation.

b. In Chapter IV a particular solution to this consolidation equation is found to be in close agreement with some experiments on sedimented clays.

c. These clays represent perhaps the most extreme case possible of large volume changes in a soil. Thus, this consolidation equation may be a useful model for more common cases of large strain consolidation.

2. Experimental Results and Techniques.

a. The apparatus, designed and built for this study, is a useful tool for the study of sedimented clays. As noted in Chapter II, difficulties were encountered in the measurement of

pore pressures, but later developments indicated that these difficulties may be overcome.

b. Some parts of the apparatus should be of more general usefulness in a soils laboratory. The design concepts of the apparatus suggest that equipment of different structure, using the same principles, may find broad application in soil testing. This is discussed in Chapter II.

c. The results of experiments with kaolin are of questionable value because of the affinity exhibited between the kaolin and the lucite column. Since minerals of the kaolin group are perhaps the most common of all clay minerals, the results of investigations on consolidation of natural fine sediments in lucite columns are questionable. Columns of some material other than lucite must be used, or some other type of experiment must be devised to study natural sediments.

D. RECOMMENDATIONS FOR FUTURE WORK

The consolidation equation developed in Chapter I should be applied to some field examples of large strain consolidation to test its utility as a means of computing settlements. Applications of this type almost certainly will require the use of numerical techniques to find solutions. A more thorough analysis of the numerical calculation technique than that presented in Chapter I probably is required before a successful method can be formulated.

For future studies of consolidation in fine sediments, solutions must be found to the two main apparatus problems discussed in Chapters II and III: The pore-pressure measurement problem and the problem of finding some means of testing kaolin under one-dimensional conditions.

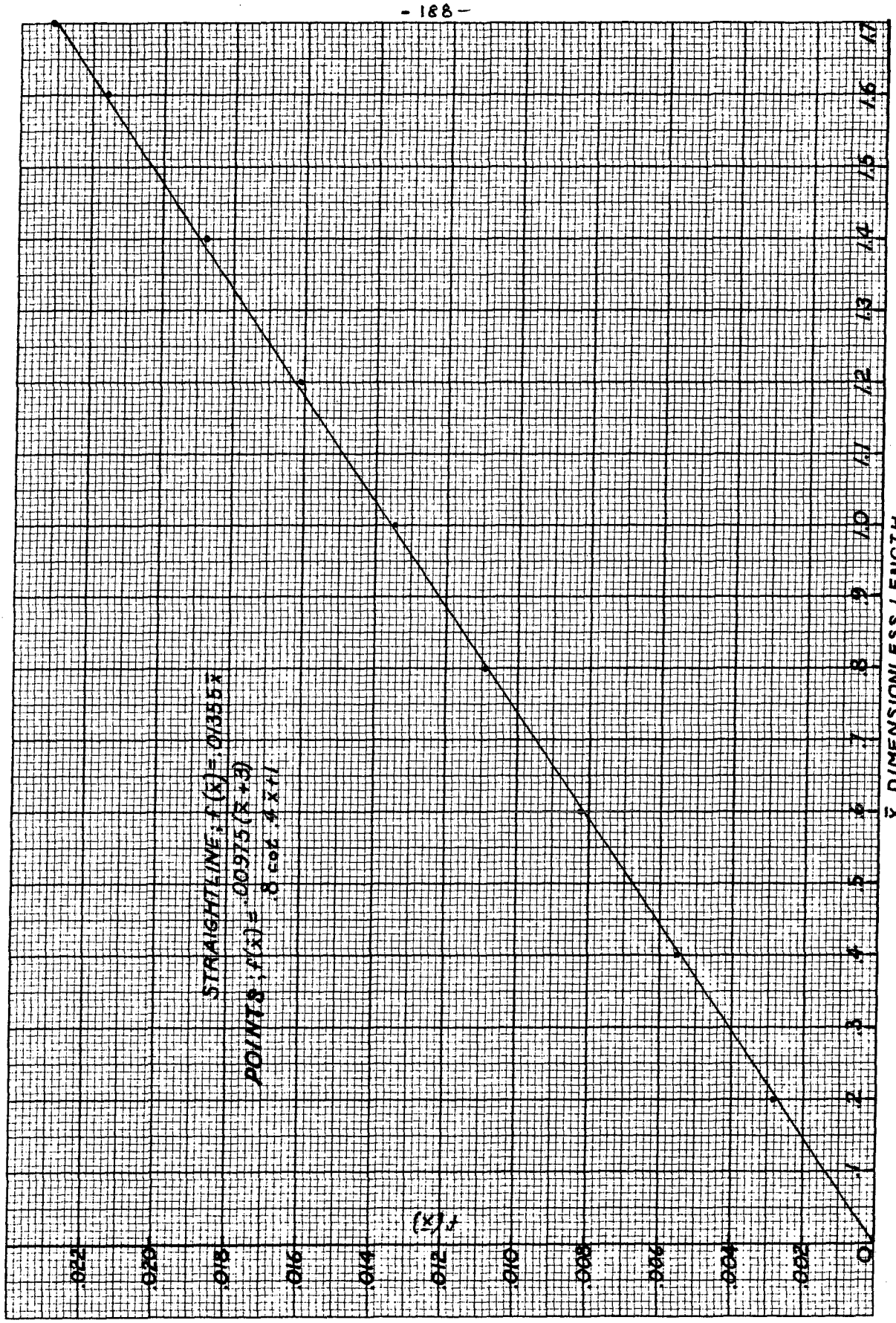

FIG. 4-1. PLOTS OF $f(\bar{x})$ TO CHECK EQUATION 4:43

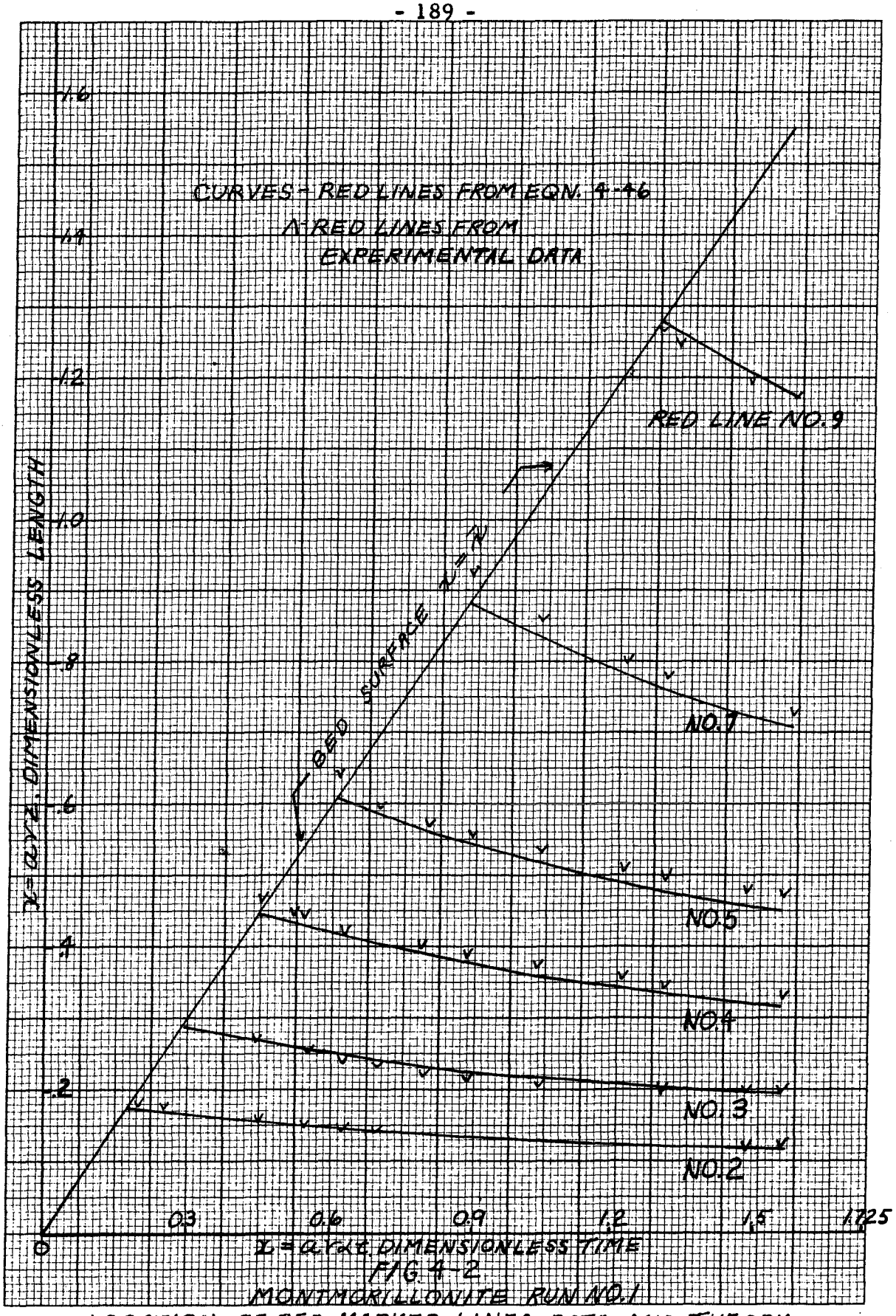

FIG. 4-2
MONTMORILLONITE RUN NO. 1
LOCATION OF RED MARKER LINES - DATA AND THEORY

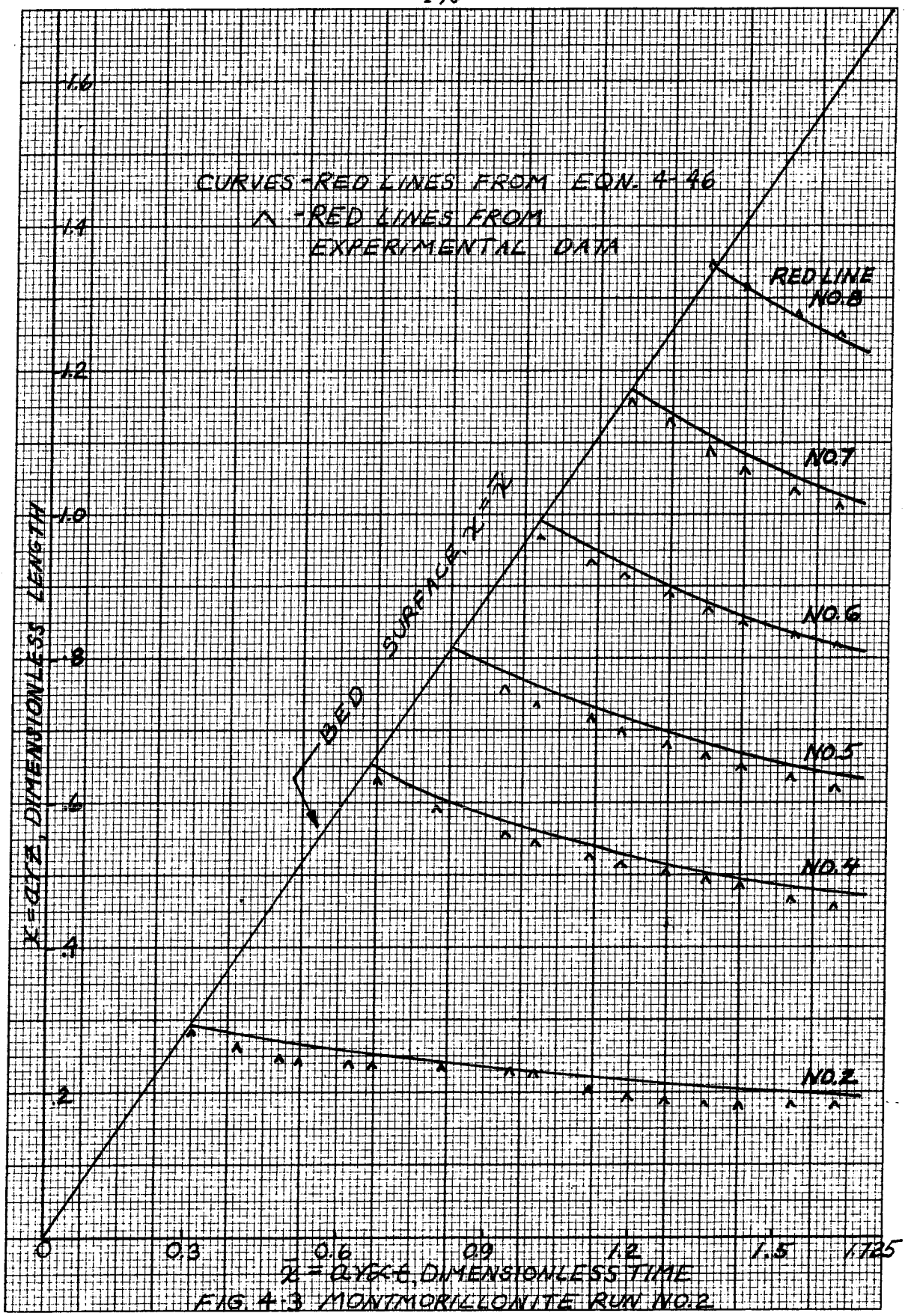

FIG. 4-3 MONTMORILLONITE RUN NO.2

LOCATION OF RED MARKER LINES - DATA AND THEORY

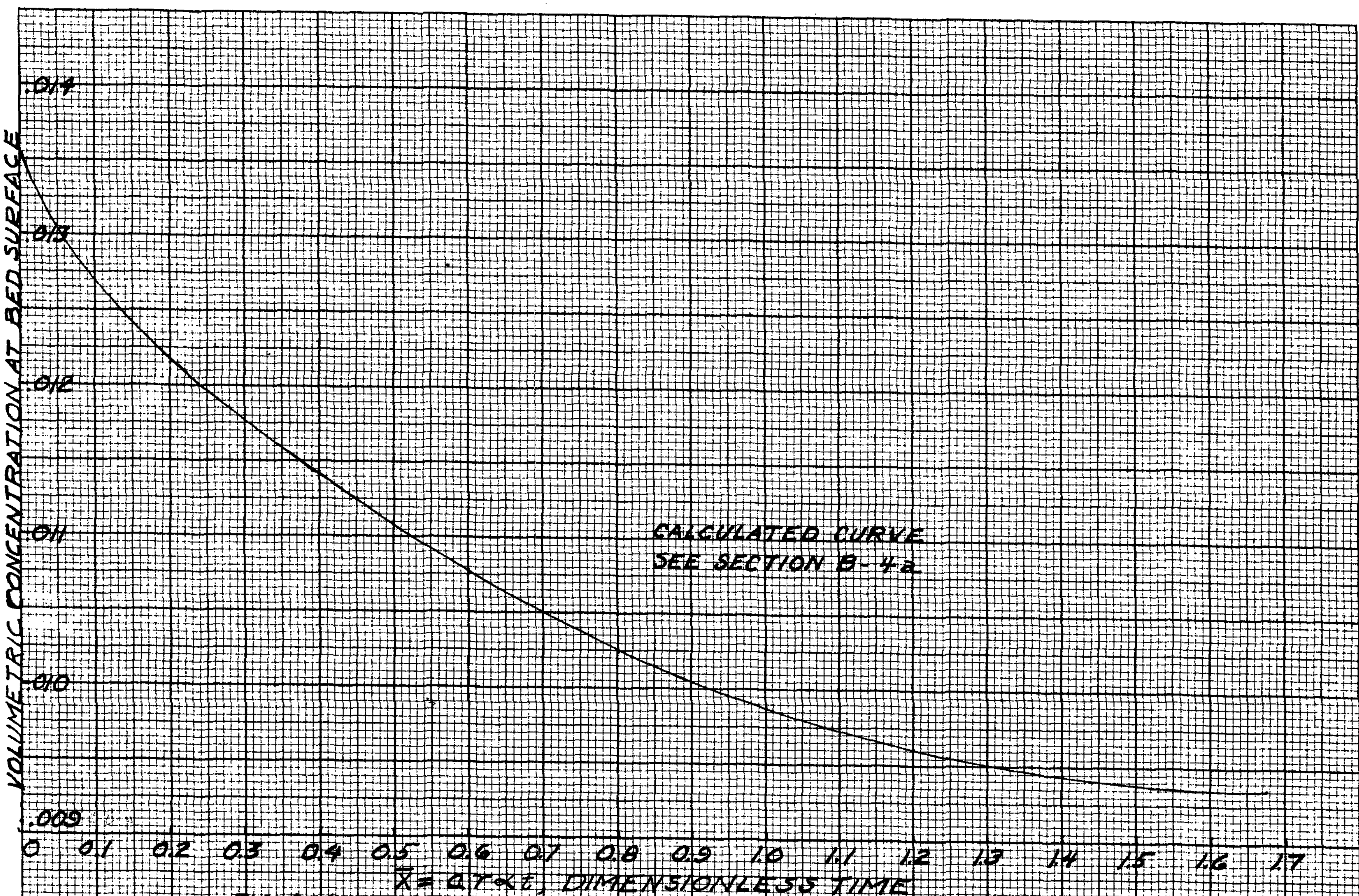

FIG 4-4 SURFACE CONCENTRATION DURING CLAY INPUT PERIOD

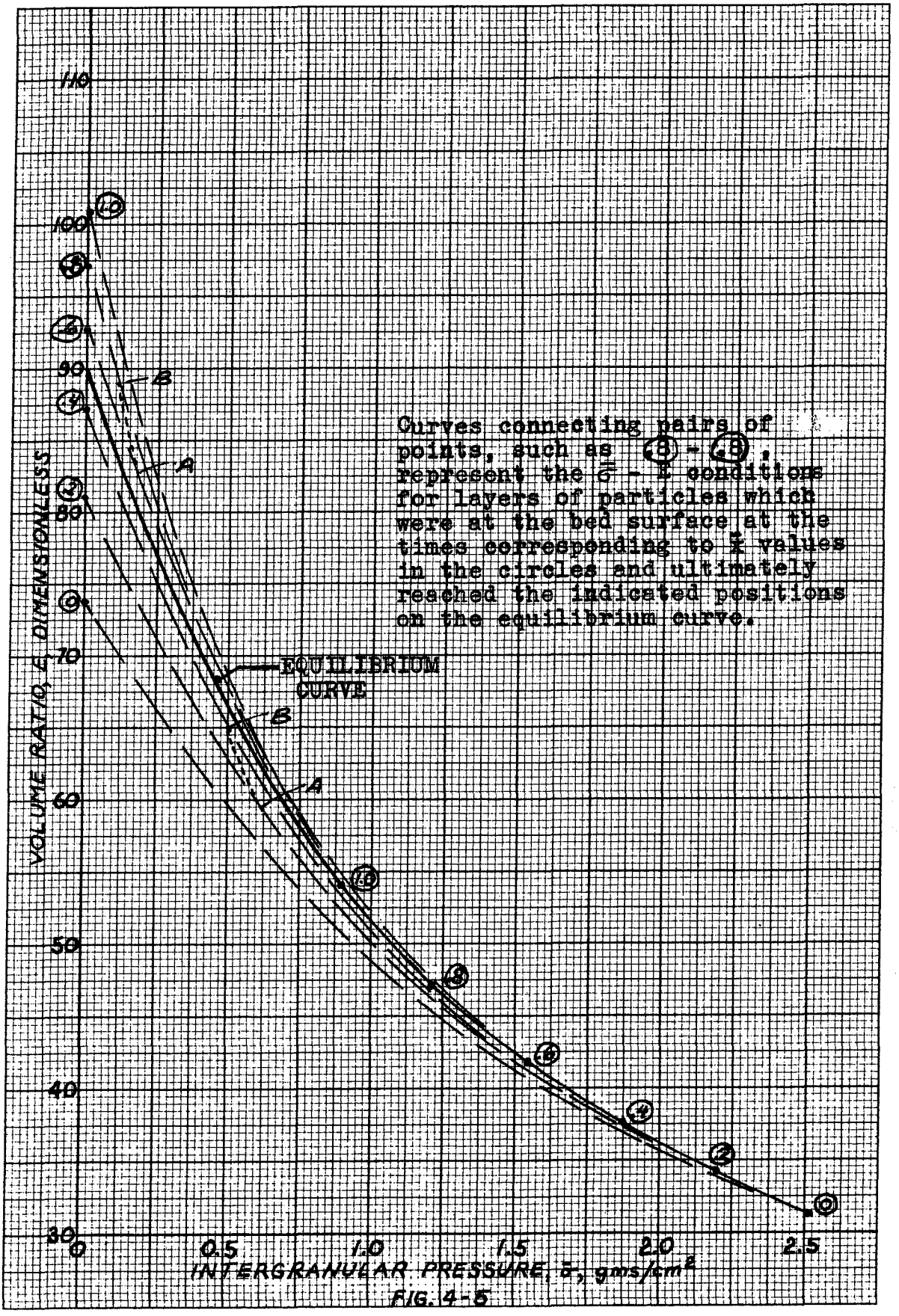

FIG. 4-5

σ̄ - E CURVES - MONTMORILLONITE EXPERIMENTS 1 AND 2

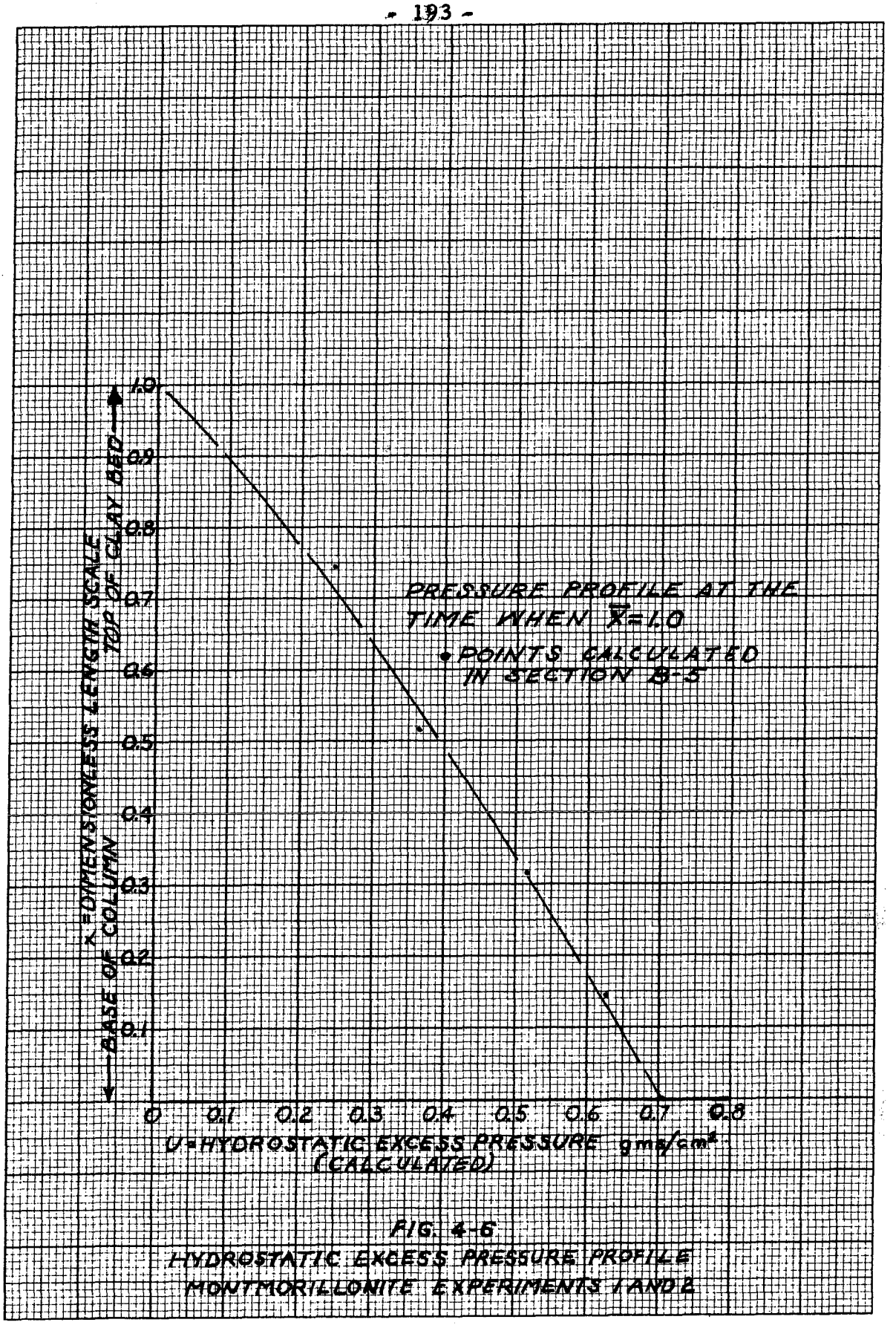

FIG. 4-6

HYDROSTATIC EXCESS PRESSURE PROFILE
MONTMORILLONITE EXPERIMENTS 1 AND 2

APPENDIX

Summary of Symbols

a = a constant in a_v = a F(E), cm^2/gm

a_v = $-\frac{dE}{d\bar{\sigma}}$ = coefficient of compressibility, cm^2/gm

A = various constants

c = $\frac{\gamma_s}{E}$ = weight concentration of soil, gms/cm^3

c_o = c when E = 1, a constant, gms/cm^2

c_v = $\frac{kE}{a_v \gamma_w}$ = coefficient of consolidation, cm^2/min

C = $\frac{c}{c_o} = \frac{1}{E}$, volume concentration of soil, dimensionless

C_a = an average C, dimensionless

C_s = a surface C, dimensionless

D = diameter of shear vanes, cm.

e = $\frac{V_v}{V_s}$ = void ratio, dimensionless

E = $\frac{V}{V_s}$ = volume ratio, dimensionless

F = a function of E, "

G = " " " " "

h = head drop in permeability test, cm of water

H = depth of slurry in agitator tank, cm

APPENDIX (Continued)

i	=	velocity of soil particles, cm/min
j	=	superficial velocity of pore fluid, cm/min
k	=	permeability, cm/min
K	=	a constant in $k = KG(E)$, cm/min
L	=	a constant
M	=	"
n	=	$\frac{V_v}{V}$ = porosity, dimensionless
N	=	a constant
p	=	an exponent in $F = C^p$
P	=	a constant
q	=	an exponent in $G = C^q$
R	=	conductivity, min^{-1}
s	=	shear stress in soil, gms/cm^2
t	=	time, minutes
T	=	$\frac{a \gamma^2 K}{\gamma_w} t$, a dimensionless time variable
u	=	hydrostatic excess pressure, gms/cm^2
v	=	evaporation rate, cm/min
V	=	total volume
V_s	=	volume of soil particles
V_v	=	volume of soil pores
W	=	weight of clay in slurry tank, gms

APPENDIX (Continued)

x = $a \gamma z$, a dimensionless length variable

$\bar{x}$ = $a \gamma \bar{z}$, " " "

y = $\frac{x}{\bar{x}}$, " " "

z = length variable, cm

$\bar{z}$ = z at soil surface, cm

α = a constant in $\bar{z} = \alpha t$, cm/min

β = $\frac{K \gamma}{\alpha \gamma_w}$ = a constant in $\tau = \beta \bar{x}$, dimensionless

γ_s = unit weight of soil particles, gms/cm^3

γ_w = " " " water, gms/cm^3

γ = $\gamma_s - \gamma_w$

δ = a constant

ε = the Naperian base

θ = a function of τ, dimensionless

ξ = length down from water table, cm

ρ = $\phi^{q+1} \frac{d\phi}{dx}$

σ = $\bar{\sigma} + u$, gms/cm^2

$\bar{\sigma}$ = intergranular stress, gms/cm^2

σ_o = σ at z = 0

APPENDIX (Continued)

$\sigma_t = \sigma + \gamma_w \xi_@$ = total stress, gms/cm^2

$\tau = \frac{a \gamma^2 K}{\gamma_w} t$, a dimensionless time variable

ϕ = a function of x, dimensionless

REFERENCES

Chapter I

1, 1 Terzaghi, K., "Erdbaumechanik auf Bodenphysikalischer Grundlage," Deuticke, Leipzig, (1925).

1, 2 Carslaw, H. S. and J. C. Jaeger, "Conduction of Heat in Solids," 2nd Ed., Oxford, (1959).

1, 3 Crank, J., "The Mathematics of Diffusion," Oxford, (1956).

1, 4 Muskat, M., "The Flow of Homogeneous Fluids Through Porous Media," J. W. Edwards, Ann Arbor, Michigan, (1946).

1, 5 Taylor, D. W., "Fundamentals of Soil Mechanics," Wiley, New York, (1948).

1, 6 Courant, R., K. Friedrichs, and H. Lewy, "Uber die partiellen Differenzengleichungen der mathematischen Physik," Mathematische Annalen, J. Springer, Berlin, Vol. 100, pp. 32-84, (1928).

1, 7 Helfferich, F. and M. S. Plesset, "Ion Exchange Kinetics. A Nonlinear Diffusion Problem," J. of Chem. Physics, Vol. 28, No. 3, pp. 418-424, March (1958); part II of same paper, J. of Chem. Physics, Vol. 29, No. 5, pp. 1064-1069, Nov. (1958).

1, 8 Richtmyer, R. D., "Difference Methods for Initial Valve Problems," Interscience, New York, (1957).

1, 9 U. S. Dept. of Int., Geological Survey, "Lake Mead Comprehensive Survey of 1948-49", Feb. (1954) in 3 volumes.

1, 10 Rouse, Hunter (editor), "Engineering Hydraulics," Wiley, New York, (1950.).

1, 11 Michon, X., "Etude du Tussement et de la Comsolidation des Boues," Memoire presente aux Troisiemes Journees de L'Hdraulique, 12-14 April 1954, La Houille Blanche, Grenoble, France.

1, 12 Moore, D. G. and George Shumway, "Sediment Thickness and Physical Properties: Pigeon Point Shelf, California," J. of Geophysical Res., Vol. 64, No. 3, pp. 367-374, March (1959.).

1, 13 Emery, K. O., "Continental Shelf Sediments of Southern California," Bull. Geol. Soc. Am., Vol. 63, pp. 1105-1108, (1952).

1, 14 Schiffman, R. L., "Consolidation of Soil Under Time-Dependent Loading and Varying Permeability," Proc. Hwy. Res. Bd., Vol. 37, No. 584, (1958).

1, 15 Abbott, M. B., "One-Dimensional Consolidation of Multi-Layered Soils," Geotechnique, Vol. X, No. 4, pp. 151-165. (19).

1, 16 Gibson, R. E., "The Progress of Consolidation in a Clay Layer Increasing in Thickness with Time," Geotechnique, Vol. VIII, No. 4, pp. 171-182. (19).

Chapter II

2, 1 Verwey, E. J. W., and J. Th. G. Overbeek, "Theory of the Stability of Lyophobic Colloids," Elsevier Pub. Co., New York, (1948).

2, 2 Lambe, T. W., "Soil Testing for Engineers," Wiley, New York, (1951).

2, 3 Mitchell, J. K., "Fundamental Aspects of Thixotropy in Soils," Jour. S. M. and Found. Div. SM3, Proc. ASCE, 86, 19, June, (1960).

2, 4 Skempton, A. W. "Vane Tests in the Alluvial Plain of the River Forth near Grangemouth," Geotechnique, 1, 2, 111, (1948).

Chapter III

3, 1 Scott, R. F., "New Method of Consolidation Coefficient Evaluation," Proc. ASCE, Jour. S.M. & F.E., Vol. 87, No. SM1, pp. 29-39, Feb. (1961).

Chapter IV

4, 1 Dwight, B. D., "Tables of Integrals and Other Mathematical Data," Macmillan, New York, (1957).